Brown University

Doctoral Thesis

Celestial Amplitudes, Cluster Adjacency, and Symbol Alphabets

Author:
Anders Øhrberg Schreiber

Supervisor:
Prof. Anastasia Volovich

A dissertaton submitted in partial fulfillment of the requirements for the degree of Doctor of Philosophy

in the

Department of Physics at Brown University

Providence, Rhode Island

February, 2021

This dissertation by Anders Øhrberg Schreiber is accepted in its present form by
the Department of Physics as satisfying the
dissertation requirement for the degree of
Doctor of Philosophy

Date: ....

Anastasia Volovich, Advisor

Recommended to the Graduate Council

Date: ....

Antal Jevicki, Reader

Date: ....

Chung-I Tan, Reader

Approved by the Graduate Council

Date: ....

Andrew G. Campbell

Dean of the Graduate School

"*All we have to decide is what to do with the time that is given to us.*"

— J.R.R. Tolkien, *The Fellowship of the Ring*

BROWN UNIVERSITY

Abstract

Anastasia Volovich

Department of Physics at Brown University

Doctor of Philosophy

Celestial Amplitudes, Cluster Adjacency, and Symbol Alphabets

by Anders Øhrberg Schreiber

In this thesis we present studies of scattering amplitudes on the celestial sphere at null infinity (celestial amplitudes), the cluster adjacency structure of scattering amplitudes in planar maximally supersymmetric Yang-Mills theory ($\mathcal{N} = 4$ SYM), and a method to derive symbol letters for loop amplitudes in $\mathcal{N} = 4$ SYM.

First, we show that n-particle celestial gluon tree amplitudes take the form of Aomoto-Gelfand hypergeometric functions and Gelfand A-hypergeometric functions. We then study conformal properties, conformal partial wave decomposition, and the optical theorem of four-particle celestial amplitudes in massless scalar ϕ^3 theory and Yang-Mills theory. Subsequently, we derive single- and multi-soft theorems for celestial amplitudes in Yang-Mills theory.

Second, we provide computational evidence that each rational Yangian invariant in $\mathcal{N} = 4$ SYM has poles that are cluster adjacent (belong to the same cluster in the $Gr(4, n)$ cluster algebra) through the Sklyanin bracket test. We also use this bracket test to study cluster adjacency of the symbol of one-loop NMHV amplitudes in $\mathcal{N} = 4$ SYM.

Finally, we suggest an algorithm for computing symbol alphabets from plabic graphs by solving matrix equations of the form $C \cdot Z = 0$ to associate functions on $Gr(m, n)$ to parameterizations of certain cells in $Gr(k, n)$ indexed by plabic graphs. For $m = 4$ and $n = 8$

we show that this association precisely reproduces the 18 algebraic symbol letters of the two-loop NMHV eight-particle amplitude from four plabic graphs.

Curriculum Vitae

Anders Øhrberg Schreiber

Contact and Date of Birth

Date of birth:	30 March, 1992
Country of Citizenship:	Denmark
Address:	Physics Department, Barus and Holley Building Brown University, 182 Hope Street, Providence, RI 02912.
Phone:	+1 401 480 3895
Email:	anders_schreiber@brown.edu

Research

Dec 2020 - Dec 2021	Postdoctoral Research Associate at University of Oxford, Postdoc at the Mathematical Institute under the grant: "Scattering Amplitudes and the Galois Theory of Periods".
Jun 2018 - Dec 2020	Research Assistantship at Brown University, Research assistant working under Prof. Anastasia Volovich on mathematical aspects of scattering amplitudes.

Education

Feb 2021	**Ph.D. in Physics**, Brown University
Aug 2016	**Master's Degree in Physics at the Niels Bohr Institute**, University of Copenhagen
Jan 2015	**Bachelor's Degree in Physics at the Niels Bohr Institute**, University of Copenhagen
May 2014	**Exchange Abroad Program**, University of California, Berkeley

Teaching

Sep 2016 - May 2018	Teaching assistant at Brown University, Taught introductory labs in Physics 0070, Physics 0040, and problem solving workshops in Physics 0070.
Sep 2014 - Jun 2016	Teaching assistant at The Niels Bohr Institute, Copenhagen Taught labs in Electrodynamics 2 and Quantum Mechanics 1 and taught exercise classes in Statistical Physics and Mathematics for Physicists 1 and 2.
Jun 2014 - Aug 2014	Physics Teacher at Herning Gymnasium, Herning Taught a high school physics B level class in the High School Supplementary Course program. Teaching involved lectures, experimental work, correcting problem sets and experimental reports, and examining students an oral final.

List of Publications

This thesis is based on the following publications:

Jul 2020	"Symbol Alphabets from Plabic Graphs", with Jorge Mago, Marcus Spradlin, and Anastasia Volovich, JHEP **10**, 128 (2020) [arXiv:2007.00646].
May 2020	"A Note on One-loop Cluster Adjacency in N = 4 SYM", with Jorge Mago, Marcus Spradlin, and Anastasia Volovich, Accepted for publication in JHEP [arXiv:2005.07177].
Jun 2019	"Yangian Invariants and Cluster Adjacency in N=4 Yang-Mills", with Jorge Mago, Marcus Spradlin, and Anastasia Volovich, JHEP **1910**, 099 (2019) [arXiv:1906.10682].
Apr 2019	"Celestial Amplitudes: Conformal Partial Waves and Soft Limits", with Dhritiman Nandan, Anastasia Volovich, and Michael Zlotnikov, JHEP **1910**, 018 (2019) [arXiv:1904.10940].
Nov 2017	"Tree-level gluon amplitudes on the celestial sphere", with Anastasia Volovich and Michael Zlotnikov, Phys. Lett. B **781**, 349 (2018) [arXiv:1711.08435].

Awards, Scholarships, and Fellowships

May 2020	Physics Merit Fellowship from Brown University, Department of Physics
May 2017	Excellence as a Graduate Teaching Assistant from Brown University, Department of Physics
May 2017	Samuel Miller Research Scholarship from the Sigma Alpha Mu Foundation

Schools and Talks

Sep 2020	Conference talk at the DESY Virtual Theory Forum 2020 Plabic Graphs and Symbol Alphabets in N=4 super-Yang-Mills Theory
Jan 2020	GGI Lectures on the Theory of Fundamental Interactions
Jan 2020	HET Seminar at NBI Cluster Adjacency in N=4 Super Yang-Mills Theory
Jul 2019	Poster at Amplitudes 2019 Scattering Amplitudes on the Celestial Sphere
Jun 2019	TASI 2019
Jan 2017	Nordic Winter School on Cosmology and Particle Physics 2017

Additional Skills

Languages: Danish, English, German.

Computer Literacy: MS Windows, MS Office, LaTeX, Python, Matlab, Mathematica

Acknowledgements

The journey of my PhD has been fantastic. I have faced many challenges, but a lot of people have been there to help and guide me through these. Firstly, I would like to thank my advisor Anastasia Volovich, who has been tremendously helpful in making me grow as a physicist. I am grateful for your patience, support, and guidance throughout my graduate studies. I would also like to thank the other professors in the high energy theory group including Stephon Alexander, Ji Ji Fan, Herb Fried, Jim Gates, Antal Jevicki, Savvas Koushiappas, David Lowe, Marcus Spradlin, and Chung-I Tan. You have all stimulated a rich and exciting research environment on the fifth floor of Barus and Holley and have made it a pleasure to work in your group. I would like to especially thank Antal Jevicki and Chung-I Tan for being on my thesis committee. Thank you also to the postdocs in the high energy theory group over the years, including Cheng Peng, Giulio Salvatori, David Ramirez, J.J. Stankowicz, and Akshay Yelleshpur Srikant. I have learned a lot from my discussions with all of you. Finally, I would like to thank Idalina Alarcon, Barbara Cole, Mary Ann Rotondo, Mary Ellen Woycik. You have all made my life in the physics department infinitely easier and I have enjoyed the many conversations we have had.

I would now like to thank all the other students in the high energy theory group, that I have had the pleasure to work alongside with during my PhD. Thank you all for being good friends and supporting me on my journey, Jatan Buch, Atreya Chatterjee, Tom Harrington, Yangrui Crystal Hu, Leah Jenks, Michael Toomey, Shing Chau John Leung, Luke Lippstreu, Sze Ning Hazel Mak, Igor Prlina, Lecheng Ren, Robert Sims, Stefan Stanojevic, Kenta Suzuki, Jorge Leonardo Mago Trejo, and Peter Tsang.

I have spent a large chunk of my free time in the Nelson Fitness Center throughout my PhD, where I have enjoyed training for powerlifting. I would like to thank all my fellow lifters in from the Nelson and in the Brown Barbell Club. All of you have lifted me up to be a better powerlifter.

I am so thankful for my lovely girlfriend Nicole Ozdowski. Thank you for being there for me and supporting me every day. Big thanks to my parents Per Schreiber, Tina Schreiber, my brother Jesper Schreiber, my grandparents Lizzie Pedersen, Bodil Schreiber, and Karl-Johan Schreiber who have been my biggest supporters from day one.

Finally, I would like to thank all the people I have not listed here. I have met so many people at Brown over the years and you have all had a positive impact on my life and my journey towards PhD. Thank you all!

Contents

Abstract **v**

Acknowledgements **xi**

1 Introduction **1**

1.1 Celestial Amplitudes and Holography 3

1.1.1 Conformal Primary Wavefunctions 3

1.1.2 Celestial Amplitudes 4

1.2 Cluster Algebras in planar $\mathcal{N} = 4$ super Yang-Mills Theory 6

1.2.1 Momentum Twistors and Dual Conformal Symmetry 6

1.2.2 Cluster Algebras and Cluster Adjacency 8

1.3 Symbols Alphabet and Plabic Graphs 10

1.3.1 Yangian Invariants and Leading Singularities 11

1.3.2 Plabic Graphs and Cluster Algebras 11

2 Tree-level Gluon Amplitudes on the Celestial Sphere **15**

2.1 Gluon amplitudes on the celestial sphere 17

2.2 n-point MHV 19

2.2.1 Integrating out one ω_i 19

2.2.2 Integrating out momentum conservation δ-functions 20

2.2.3 Integrating the remaining ω_i 22

2.2.4 6-point MHV 24

2.3 n-point NMHV 25

2.4 n-point N^{k}MHV 28

2.5 Generalized hypergeometric functions 31

3 Celestial Amplitudes: Conformal Partial Waves and Soft Limits 35

3.1 Scalar Four-Point Amplitude 37

3.2 Gluon Four-Point Amplitude 42

3.3 Soft limits 43

3.4 Conformal Partial Wave Decomposition 47

3.5 Inner Product Integral 49

4 Yangian Invariants and Cluster Adjacency in $\mathcal{N} = 4$ Yang-Mills 53

4.1 Cluster Coordinates and the Sklyanin Poisson Bracket 56

4.2 An Adjacency Test for Yangian Invariants 58

4.2.1 NMHV 60

4.2.2 N^{2}MHV 62

4.2.3 N^{3}MHV and Higher 63

4.3 Explicit Matrices for $k = 2$ 64

5 A Note on One-loop Cluster Adjacency in $\mathcal{N} = 4$ SYM 69

5.1 Cluster Adjacency and the Sklyanin Bracket 70

5.2 One-loop Amplitudes 73

5.2.1 BDS- and BDS-like Subtracted Amplitudes 73

5.2.2 NMHV Amplitudes 75

5.3 Cluster Adjacency of One-Loop NMHV Amplitudes 76

5.3.1 The Symbol and Steinmann Cluster Adjacency 76

5.3.2 Final Entry and Yangian Invariant Cluster Adjacency 76

5.4 Cluster Adjacency and Weak Separation 79

5.5 n-point NMHV Transcendental Functions 82

6 Symbol Alphabets from Plabic Graphs **85**

6.1 A Motivational Example 87

6.2 Six-Particle Cluster Variables 91

6.3 Towards Non-Cluster Variables 95

6.4 Algebraic Eight-Particle Symbol Letters 98

6.5 Discussion 101

6.6 Some Six-Particle Details 104

6.7 Notation for Algebraic Eight-Particle Symbol Letters 105

List of Figures

1.1 A cluster in the $Gr(4,6)$ cluster algebra. Boxed coordinates are frozen and do not change under mutations, while unboxed coordinates are mutable. 9

1.2 An example of a plabic graph of $Gr(2,6)$. 12

3.1 Four-Point Exchange Diagrams 37

5.1 Weak separation graph indicating that if both i and j are within any of the green regions (or on the green chords), then $\langle i-1, i, j-1, j\rangle$ is cluster adjacent to $\langle k(l\,l+1)(m\,m+1)(k-1\,k+1)\rangle$. 80

5.2 Weak separation graph indicating that if both i and j are within any of the green regions (or on the green chords), then $\langle i-1, i, j-1, j\rangle$ is cluster adjacent to $\langle k(l\,l+1)(m\,m+1)(p\,p+1)\rangle$. 81

6.1 The three types of (reduced, perfectly orientable, bipartite) plabic graphs corresponding to km-dimensional cells of $\mathrm{Gr}(k,n)_{\geq 0}$ for $k = 2$, $m = 4$ and $n = 6$ are shown in (a)–(c). The associated input and output clusters (see text) are shown in (d)–(f) and (g)–(i) respectively. Lines connecting two frozen nodes are usually omitted, but we include in (g)–(i) the dotted lines (having "black on the right" in the dual plabic graph) that encode (6.6), (6.27) and (6.29) (up to signs). 93

List of Tables

Dedicated to my family: Tina, Per, Jesper, Lizzie, Bodil, and Karl-Johan.

I love you all!

Chapter 1

Introduction

The study of elementary particles and their interactions have led to a paradigm shift in our understanding of the laws of nature in the past 100 years. From early discoveries of charged particles in cloud chambers to deep probing of the structure of hadrons in high powered particle accelerators, we today have an incredible understanding of how the universe works through the Standard Model of particle physics. The enormous success of the Standard Model of particle physics is hinged on our ability to calculate scattering cross sections, which we measure in particle scattering experiments like the Large Hadron Collider (LHC). The computation of scattering cross sections in turn depend on our ability to compute scattering amplitudes.

When we are taught quantum field theory in graduate school, we learn the method of Feynman diagrams [1] to compute scattering amplitudes. This method originally revolutionized the way one thinks about scattering in quantum field theories, as it gives a neat way to organize computations via simple diagrams. However, computations of scattering amplitudes via Feynman diagrams have rapidly scaling complexity with the number of particles involved in the scattering process. For example, if we consider 2-to-n gluon scattering at tree level in Yang-Mills theory, the following number of Feynman diagrams need to be calculated:

$$
\begin{aligned}
&g+g \to g+g: && 4 \text{ diagrams}\ ,\\
&g+g \to g+g+g: && 25 \text{ diagrams}\ ,\\
&g+g \to g+g+g+g: && 220 \text{ diagrams}\ .
\end{aligned}
$$

However, amplitudes often enjoy dramatic simplifications once all the diagrams are added up. A classic example of this is the Parke-Taylor formula [2] for maximally helicity violating (MHV) scattering of any number of particles. This reduction in complexity hints at hidden simplicity and potentially more efficient techniques for computing amplitudes.

To understand and develop new computational techniques, we need to understand the analytic structure of amplitudes. We therefore study amplitudes in various bases and variables, as this can highlight special properties. The choice of basis states of external particles can make various symmetry properties of amplitudes manifest. Certain kinematic variables offer simplifications, like in the Parke-Taylor formula, but also highlight deeper properties of the amplitudes like dual superconformal symmetry [3] and, when utilizing momentum twistors [4], cluster algebraic structure [5] in planar maximally supersymmetric Yang-Mills theory ($\mathcal{N}=4$ SYM) becomes apparent.

In the next three sections, we review the three main topics of this thesis: scattering amplitudes on the celestial sphere at null infinity of flat space, cluster adjacency in scattering amplitudes in $\mathcal{N}=4$ SYM, and the determination of symbol alphabets of loop amplitudes in $\mathcal{N}=4$ SYM via plabic graphs.

1.1 Celestial Amplitudes and Holography

In the last 23 years, theoretical physics has seen a paradigm shift with the introduction of the anti-de Sitter space/conformal field theory (AdS/CFT) holographic principle [6]. Here, observables of string theories in the bulk of the AdS are dual to observables of CFTs that live on the boundary of AdS. This principle has a strong/weak coupling duality, where for example observables in the bulk theory at weak coupling are dual to observables of the boundary CFT at strong coupling. This offers a powerful tool, as we can use perturbation theory at weak coupling to do computations and get results in theories at strong coupling via the duality. In flat Minkowski space, a similar connection was observed in [7], as it is possible to slice Minkowski space in four dimensions into slices of AdS_3 where one can apply the tools of AdS/CFT. This has recently lead to an application in scattering amplitudes in flat space [8], where it is possible to map plane-waves to the celestial sphere at null infinity via conformal primary wavefunctions [9].

1.1.1 Conformal Primary Wavefunctions

When we compute scattering amplitudes in flat space, the initial and final states are chosen in the basis of plane-waves: $e^{\pm ik\cdot X}$ (for scalars). The plane-wave basis makes translation symmetry manifest, while other features, like boosts, are obscured. A new basis, called conformal primary wavefunctions, was introduced in [9]. These wavefunctions connect plane-wave representations of particle wavefunctions, at a point in flat space X^μ, to a point on the celestial sphere at null infinity $(z, \bar{z})$ (in stereographic coordinates). For a massless scalar particle, the conformal primary wavefunction takes the form of a Mellin transform,

$$\phi^{\Delta,\pm}(X;z,\bar{z}) = \int_0^\infty d\omega\, \omega^{\Delta-1} e^{\pm i\omega q\cdot X}\,, \tag{1.1}$$

where Δ is a free parameter that will take the role of conformal dimension. By requiring ϕ to form an orthonormal basis with respect to the Klein-Gordon inner product, Δ is restricted to the principal series: $\Delta = 1 + i\lambda$. In the above formula, we have parameterized the momentum associated with the massless scalar as

$$k^\mu = \omega q^\mu(z,\bar{z}) = \omega(1+z\bar{z}, z+\bar{z}, -i(z-\bar{z}), 1-z\bar{z})\,, \tag{1.2}$$

where q^μ is a null vector. In four dimensions, Lorentz transformations act as two-dimensional conformal transformations on the celestial sphere [10], and under Lorentz transformations (1.1) transforms as

$$\phi^{\Delta,\pm}\left(\Lambda^\mu{}_\nu X^\nu; \frac{az+b}{cz+d}, \frac{\bar{a}\bar{z}+\bar{b}}{\bar{c}\bar{z}+\bar{d}}\right) = |cz+d|^{2\Delta}\phi^{\Delta,\pm}(X;z,\bar{z})\,, \tag{1.3}$$

which is exactly how scalar conformal primaries transform. The formula (1.1) extends to massless spinning particles, of integer spin, given by a Mellin transform of the associated polarization vector and plane-wave [9].

1.1.2 Celestial Amplitudes

Given a scattering amplitudes, we can change the basis to conformal primary wavefunctions by applying a Mellin transform to each external particle involved in the scattering process.

This defines the celestial amplitude [9]

$$\tilde{\mathcal{A}}_{J_1\cdots J_n}(\Delta_j, z_j, \bar{z}_j) = \prod_{j=1}^{n} \int_0^\infty d\omega_j\, \omega_j^{\Delta_j - 1} \mathcal{A}_{\ell_1\cdots\ell_n}\,, \tag{1.4}$$

where ℓ_j is helicity of particle j, and J_j is the spin of the associated conformal primary wavefunction, given by $J_j = \ell_j$. Note that the scattering amplitude, $\mathcal{A}$, here includes the overall momentum conservation delta function. The celestial amplitude transforms as a conformal correlator under $SL(2,\mathbb{C})$ Lorentz transformations,

$$\tilde{\mathcal{A}}_{J_1\cdots J_n}\left(\Delta_j, \frac{az+b}{cz+d}, \frac{\bar{a}\bar{z}+\bar{b}}{\bar{c}\bar{z}+\bar{d}}\right) = \prod_{j=1}^{n} \left[(cz_j+d)^{\Delta_j+J_j}(\bar{c}\bar{z}+\bar{d})^{\Delta_j-J_j}\right] \tilde{\mathcal{A}}_{J_1\cdots J_n}(\Delta_j, z_j, \bar{z}_j)\,. \tag{1.5}$$

Due to the conformal correlator nature of celestial amplitudes, it is possible that there exists a conformal field theory on the celestial sphere that generates scattering amplitudes in the form of celestial amplitudes. In Chapter 2 we will explore how to compute n-point celestial gluon amplitudes.

In Chapter 3 we will explore conformal properties of four-point massless scalar celestial amplitudes, conformal partial wave decomposition, and optical theorem. For four-point celestial gluon amplitudes we compute the conformal partial wave decomposition and study single- and multi-soft theorems.

1.2 Cluster Algebras in planar $\mathcal{N} = 4$ super Yang-Mills Theory

Theories with a large amount of symmetry often see fruitful developments from studying them in terms of different kinematic variables. We will study $\mathcal{N} = 4$ SYM, which enjoys superconformal symmetry in spacetime in addition to dual superconformal symmetry in dual momentum space [3]. When kinematics are parameterized in terms of momentum twistors [4], n-points on $\mathbb{P}^3$, dual conformal symmetry enhances the kinematic space to the Grassmannian $Gr(4, n)$ [5]. This space has a cluster algebraic structure which strongly constrains the analytic structure of amplitudes in the theory. At tree-level, amplitudes in $\mathcal{N} = 4$ SYM are rational functions, depending on dual superconformally invariant combinations of momentum twistors called Yangian invariants [11]. At loop-level, trancendental functions appear which, in the cases of our interest, can be described by iterated integrals called generalized polylogarithms. These have a total differential, given by a product of $d\log$'s, which can be mapped to a tensor product structure called the symbol [12]. The structure of both Yangian invariants and symbols is constrained by cluster adjacency, which we will describe below. Cluster adjacency has been used to perform computations of high loop amplitudes in the cluster bootstrap program [13].

1.2.1 Momentum Twistors and Dual Conformal Symmetry

Dual conformal symmetry [3] in $\mathcal{N} = 4$ SYM was discovered by studying scattering amplitudes in dual momentum space. We start with scattering amplitudes described by momenta

k_i^μ of massless particles. We define dual momenta, x_i^μ, as

$$k_i^\mu = x_i^\mu - x_{i+1}^\mu \,, \tag{1.6}$$

where the index i labels particles $i \in \{1, \ldots, n\}$ in an ordered fashion. Let us now define a second set of coordinates, called momentum twistors [4]. We can define these through incidence relations. Since we are considering massless particles, the definition of dual momenta combined with the spinor-helicity formalism (see [14] for a review) allows us to write (1.6) as

$$\langle i|_{\dot{a}} x_i^{\dot{a}a} = \langle i|_{\dot{a}} x_{i+1}^{\dot{a}a} \equiv [\mu_i|^a \,. \tag{1.7}$$

We can pair the momentum twistor components, $[\mu_i|^a$, with the spinor-helicity angle bracket to form a joint spinor that we will collectively refer to as a momentum twistor:

$$Z_i^I = (|i\rangle^{\dot{a}}, [\mu_i|^a) \,, \tag{1.8}$$

where $I = (\dot{a}, a)$ is an $SU(2,2)$ index. As the momentum twistor is defined from two points in dual momentum space, this definition maps any two null separated points in dual momentum space to a point in momentum twistor space. With a bit of algebra, we can write point in dual momentum in terms of the momentum twistor variables:

$$x_i^{\dot{a}a} = \frac{|i\rangle^{\dot{a}}[\mu_{i-1}|^a - |i-1\rangle^{\dot{a}}[\mu_i|^a}{\langle i-1\, i\rangle} \,. \tag{1.9}$$

Due to the construction of the momentum twistor variables via (1.7), all coordinates in the momentum twistor Z_i^I scales uniformly under little group transformations. Thus for n-particle scattering, the kinematic space is n-points on $\mathbb{P}^3$, also known as twistor space [15, 16]. Furthermore, dual conformal transformations act as $GL(4)$ transformations on momentum twistors, thus enhancing the momentum twistors from living in $\mathbb{P}^3$ to $Gr(4,n)$. Dual conformal generators act linearly on functions of momentum twistors, and we can construct a dual conformally invariant quantity from the $SU(2,2)$ Levi-Civita symbol,

$$\langle ijkl\rangle = \epsilon_{IJKL} Z_i^I Z_j^J Z_k^K Z_l^L \,, \tag{1.10}$$

which will be the central objects that we construct scattering amplitudes from.

1.2.2 Cluster Algebras and Cluster Adjacency

Cluster algebras [17, 18, 19, 20] can be represented by quivers with cluster coordinates (each quiver corresponding to a single cluster) equipped with a mutation rule. Starting with an initial cluster, we can mutate on individual cluster coordinates and obtain different clusters. As an example, consider a cluster in the $Gr(4,6)$ cluster algebra, Figure 1.1. Here we have frozen coordinates (in boxes), that we are not allowed to mutate, and non-frozen coordinates (unboxed) that we can mutate on. The mutation rule is defined by an adjacency matrix,

$$b_{ij} = (\#\text{ arrows } i \to j) - (\#\text{ arrows } j \to i)\,, \tag{1.11}$$

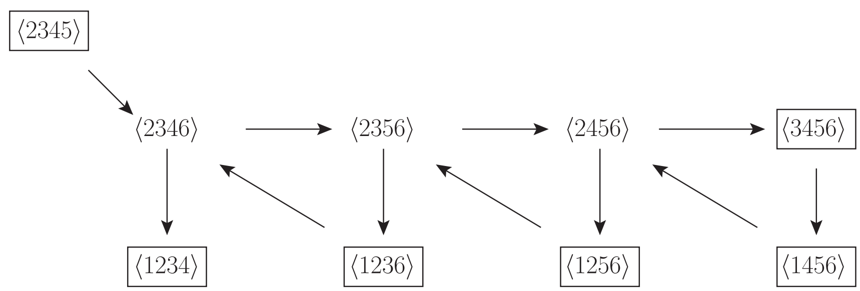

FIGURE 1.1: A cluster in the $Gr(4,6)$ cluster algebra. Boxed coordinates are frozen and do not change under mutations, while unboxed coordinates are mutable.

such that when we mutate on a cluster coordinate a_k, we obtain a new coordinate a_k' given by

$$a_k a_k' = \prod_{i|b_{ik}>0} a_i^{b_{ik}} + \prod_{i|b_{ik}<0} a_i^{-b_{ik}} . \tag{1.12}$$

To complete the mutation, we flip all arrows in the quiver connected to a_k'. This way we can generate all clusters in the cluster algebra if it is of finite type. We say that a cluster algebra is of infinite type, if it contains an infinite number of clusters. $Gr(4,n)$ cluster algebras [21] are of finite type when $n = 6, 7$ and of infinite type when $n \geq 8$.

The notion of cluster adjacency plays an important role in the analytic structure of scattering amplitudes. Two cluster coordinates are said to be cluster adjacent if and only they can be found in a common cluster together. As an example, from Figure 1.1, we see that $\{\langle 2346\rangle, \langle 2356\rangle, \langle 2456\rangle\}$ are all cluster adjacent. In Chapter 4 we study how cluster adjacency constrains the pole structure Yangian invariants in $\mathcal{N} = 4$ SYM. In Chapter 5, we explore how cluster adjacency constrains the symbol in one-loop NMHV amplitudes.

1.3 Symbols Alphabet and Plabic Graphs

An outstanding problem in the computation of scattering amplitudes of $\mathcal{N} = 4$ SYM is the determination of symbol alphabets of amplitudes. When amplitudes are computed say via the cluster bootstrap method, the symbol alphabet is an important input, but it is only known in certain cases either via cluster algebras [5] or direct computation [22, 23, 24]. From cluster algebras, we are limited to cases where the cluster algebra is of finite type ($n = 6, 7$). Is there an alternative way to predict the symbol alphabet of amplitudes in $\mathcal{N} = 4$ SYM? One approach is using Landau analysis [25, 26], but here we will discuss a separate approach involving plabic graphs that index Grassmannian cells. Formulas involving integrals over Grassmannian spaces are commonplace in $\mathcal{N} = 4$ SYM [27, 28]. Yangian invariants and leading singularities are computed as integrals over Grassmannian cells indexed by plabic graphs [29, 30]. These integral formulas are localized on solutions to matrix equations of the form $C \cdot Z = 0$, where C is a $k \times n$ matrix representation of the auxiliary Grassmannian space $Gr(k, n)$ and Z is the collection of $4 \times n$ momentum twistors. As these equations, together with the integral formulas, determine the structure of Yangian invariants and leading singularities, it is interesting to ask if we can derive complete symbol alphabets of amplitudes by collecting coordinates appearing in the solutions to $C \cdot Z = 0$.

1.3.1 Yangian Invariants and Leading Singularities

We can represent Yangian invariants in $\mathcal{N} = 4$ SYM as integrals over an auxiliary Grassmannian space [27, 28],

$$Y(\{Z|\eta\}) = \int \prod_{i=1}^{4k} d\log f_i \prod_{I=1}^{4} \prod_{\alpha=1}^{k} \delta(\sum_{a=1}^{n} C_{\alpha a}(Z|\eta)_{aI}), \tag{1.13}$$

where f_i are variables parameterizing the $k \times n$ matrix C. The integration is localized on solutions to the matrix equations $C_{\alpha a}(Z|\eta)_{aI} \equiv C \cdot Z = 0$ for $a = 1, \ldots, n$, $I = 1, \ldots, 4$, and $\alpha = 1, \ldots, k$. Here k corresponds to the level of helicity violation of an $N^k MHV$ amplitude. For a n, we can consider the finite set of all $Gr(k,n)$ cells, each with an associated matrix C, such that they exactly localize the integration (1.13). Thus for each $Gr(k,n)$ cell there is a corresponding Yangian invariant, where variables appearing in the Yangian invariant are dictated by the solutions to $C \cdot Z = 0$.

1.3.2 Plabic Graphs and Cluster Algebras

Cells of $Gr(k,n)$ Grassmannians can be indexed by decorated permutations [29], i.e. permutations σ of length n with $\sigma(a)$ if $a < \sigma(a)$ and $\sigma(a)+n$ if $\sigma(a) < a$. Furthermore, k refers to the number of entries in a permutation with $\sigma(a) < a$. Such decorated permutations can be represented by plabic graphs - planar bicolored graphs [29].

Example: Consider the plabic graph in Figure 1.2, which has an associated decorated permutation $\{3,4,5,6,7,8\}$. To read off the permutation, we start at any external point, move through the graph, turn to the first left path if we meet a white vertex, while we turn to the first right path if we meet a black vertex.

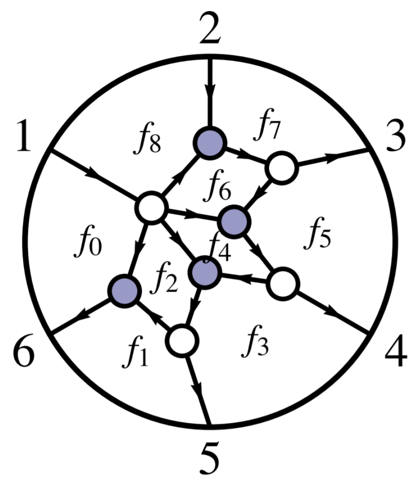

FIGURE 1.2: An example of a plabic graph of $Gr(2,6)$.

We can read off the C-matrix, parameterizing the associated cell in $Gr(k,n)$, from the plabic graph. We start with a matrix that has the identity in the columns corresponding to sources in the plabic graph. Each entry in the remaining columns is given by the formula

$$c_{ij} = (-1)^s \sum_{p:i\mapsto j} \prod_{\alpha\in\hat{p}} f_\alpha \,, \tag{1.14}$$

where s is the number of sources strictly between i and j, the sum runs over all allowed paths p from i to j (allowed paths must traverse each edge only in the direction of its arrow), and the product runs over all faces α to the right of the path p, denoted by $\hat{p}$. On top of this, the face variables f_i over-count the degrees of freedom in a plabic graph by one, and satisfy the relation

$$\prod_i f_i = 1 \,. \tag{1.15}$$

With the construction (1.14), we will study solutions to the matrix equations $C \cdot Z = 0$.

In Chapter 6, we will see how this method can be used to generate all $Gr(4,n)$ cluster coordinates when $n = 6,7$ (which are known to be the $n = 6,7$ symbols alphabets), but also algebraic coordinates, that are known to appear in scattering amplitudes, but are not cluster coordinates.

Chapter 2

Tree-level Gluon Amplitudes on the Celestial Sphere

This chapter is based on the publication [31].

The holographic description of bulk physics in terms of a theory living on the boundary has been concretely realised by the AdS/CFT correspondence for spacetimes with global negative curvature. It remains an important outstanding problem to understand suitable formulations of holography for flat spacetime, a goal that has elicited a considerable amount of work from several complementary approaches [32].

Recently, Pasterski, Shao and Strominger [8] studied the scattering of particles in four-dimensional Minkowski space and formulated a prescription that maps these amplitudes to the celestial sphere at infinity. The Lorentz symmetry of four-dimensional Minkowski space acts as the conformal group $SL(2,\mathbb{C})$ on the celestial sphere. It has been shown explicitly that the near-extremal three-point amplitude in massive cubic scalar field theory has the correct structure to be identified as a three-point correlation function of a conformal field theory living on the celestial sphere [8]. The factorization singularities of more general scattering amplitudes in this CFT perspective have been further studied in [33]. The map uses conformal primary wave functions which have been constructed for various fields in arbitrary dimensions in [9]. In [34] it was shown that the change of basis from plane waves to the conformal primary wave functions is implemented by a Mellin transform, which was computed explicitly for three and four-point tree-level gluon amplitudes. The optical theorem in the conformal basis and scattering in three dimensions were studied in [35]. One-loop and two-loop four-point amplitudes have also been considered in [36].

In this note we use the prescription [34] to investigate the structure of CFT correlators corresponding to arbitrary n-point gluon tree-level scattering amplitudes, thus generalizing their three- and four-point MHV results. Gluon amplitudes can be represented in many different ways that exhibit different, complementary aspects of their rich mathematical structure. It is natural to suspect that they may also take a particularly interesting form when written as correlators on the celestial sphere. We find that Mellin transforms of n-point MHV gluon amplitudes are given by Aomoto-Gelfand generalized hypergeometric functions on the Grassmannian $Gr(4, n)$ (2.24). For non-MHV amplitudes the analytic structure of the resulting functions is more complicated, and they are given by Gelfand A-hypergeometric functions (2.33) and its generalizations. It will be very interesting to explore further the structure of these functions, and possibly make connections to other representations of tree-level amplitudes [37] which we leave for future work.

2.1 Gluon amplitudes on the celestial sphere

We work with tree-level n-point scattering amplitudes of massless particles $\mathcal{A}_{\ell_1\cdots\ell_n}(k_j^\mu)$ which are functions of external momenta k_j^μ and helicities $\ell_j = \pm 1$, where $j = 1, \ldots, n$. We want to map these scattering amplitudes to the celestial sphere. To that end we can parametrize the massless external momenta k_j^μ as

$$k_j^\mu = \epsilon_j \omega_j q_j^\mu \equiv \epsilon_j \omega_j (1 + |z_j|^2, z_j + \bar{z}_j, -i(z_j - \bar{z}_j), 1 - |z_j|^2), \tag{2.1}$$

where $z_j, \bar{z}_j$ are the usual complex cordinates on the celestial sphere, ϵ_j encodes a particle as incoming ($\epsilon_j = -1$) or outgoing ($\epsilon_j = +1$), and ω_j is the angular frequency associated with the energy of the particle [34]. Therefore, the amplitude $\mathcal{A}_{\ell_1\cdots\ell_n}(\omega_j, z_j, \bar{z}_j)$ is a function of ω_j, z_j and $\bar{z}_j$ under the parametrization (2.1).

Usually, we write any massless scattering amplitude in terms of spinor-helicity angle- and square-brackets representing Weyl-spinors (see [14] for a review). The spinor-helicity variables are related to external momenta k_j^μ, so that in turn we can express them in terms of variables on the celestial sphere via [34]:

$$[ij] = 2\sqrt{\omega_i \omega_j}\bar{z}_{ij} \, , \qquad \langle ij \rangle = -2\epsilon_i \epsilon_j \sqrt{\omega_i \omega_j} z_{ij} \, , \tag{2.2}$$

where $z_{ij} = z_i - z_j$ and $\bar{z}_{ij} = \bar{z}_i - \bar{z}_j$.

In [9, 34] it was proposed that any massless scattering amplitude is mapped to the celestial sphere via a Mellin transform:

$$\tilde{\mathcal{A}}_{J_1\cdots J_n}(\lambda_j, z_j, \bar{z}_j) = \prod_{j=1}^{n} \int_0^\infty d\omega_j\, \omega_j^{i\lambda_j}\, \mathcal{A}_{\ell_1\cdots\ell_n}(\omega_j, z_j, \bar{z}_j)\,. \tag{2.3}$$

The Mellin transform maps a plane wave solution for a helicity ℓ_j field in momentum space to a corresponding conformal primary wave function on the boundary with spin J_j, where helicity ℓ_j and spin J_j are mapped onto each other, and the operator dimension takes values in the principal continuous series representation $\Delta_j = 1+i\lambda_j$ [9]. Therefore, $\tilde{\mathcal{A}}_{J_1\cdots J_n}(\lambda_j, z_j, \bar{z}_j)$ has the structure of a conformal correlator on the celestial sphere, where the symmetry group of diffeomorphisms is the conformal group $SL(2,\mathbb{C})$.

Explicitly, under conformal transformations, we have the following behavior:

$$\omega_j \to \omega_j' = |cz_j + d|^2 \omega_j \quad , \quad z_j \to z_j' = \frac{az_j + b}{cz_j + d} \quad , \quad \bar{z}_j \to \bar{z}_j' = \frac{\bar{a}\bar{z}_j + \bar{b}}{\bar{c}\bar{z}_j + \bar{d}}, \tag{2.4}$$

where $a, b, c, d \in \mathbb{C}$ and $ad - bc = 1$. The transformation for $z_j, \bar{z}_j$ is familiar from the usual action of $SL(2,\mathbb{C})$ on the complex coordinates on a sphere. Concerning ω_j, recall that q_j^μ transforms as $q_j^\mu \to |cz_j + d|^{-2} \Lambda^\mu{}_\nu q_j^\nu$ [9], where $\Lambda^\mu{}_\nu$ is a Lorentz transformation in Minkowski space corresponding to the celestial sphere conformal transformation. Thus, ω_j must transform as in (2.4) to ensure that k_j^μ transforms as a Lorentz vector: $k_j^\mu \to \Lambda^\mu{}_\nu k_j^\nu$.

The conformal covariance of $\tilde{\mathcal{A}}_{J_1\cdots J_n}(\lambda_j, z_j, \bar{z}_j)$ on the celestial sphere demands:

$$\tilde{\mathcal{A}}_{J_1\cdots J_n}\left(\lambda_j, \frac{az_j + b}{cz_j + d}, \frac{\bar{a}\bar{z}_j + \bar{b}}{\bar{c}\bar{z}_j + \bar{d}}\right) = \prod_{j=1}^{n} \left[(cz_j + d)^{\Delta_j + J_j} (\bar{c}\bar{z}_j + \bar{d})^{\Delta_j - J_j} \right] \tilde{\mathcal{A}}_{J_1\cdots J_n}(\lambda_j, z_j, \bar{z}_j)\,, \tag{2.5}$$

as expected for a correlator of operators with weights Δ_j and spins J_j.

2.2 n-point MHV

The cases of 3- and 4-point gluon amplitudes have been considered in [34]. Here we will map $n \geq 5$-point MHV gluon amplitudes to the celestial sphere.

2.2.1 Integrating out one ω_i

Starting from (2.3), we can anchor the integration to one of our variables ω_i by making a change of variables for all $l \neq i$

$$\omega_l \to \frac{\omega_i}{s_i}\omega_l, \tag{2.6}$$

where s_i is a constant factor that cancels the conformal scaling of ω_i in (2.4), so that the ratio $\frac{\omega_i}{s_i}$ is conformally invariant. One choice which is always possible in Minkowski signature is

$$s_i = \frac{|z_{i-1\ i+1}|}{|z_{i-1\ i}|\,|z_{i\ i+1}|}. \tag{2.7}$$

Since gluon scattering amplitudes scale homogeneously under uniform rescalings, collecting all the factors in front, we have

$$\tilde{\mathcal{A}}_{J_1\cdots J_n}(\lambda_j, z_j, \bar{z}_j) = \int_0^\infty \frac{d\omega_i}{\omega_i}\left(\frac{\omega_i}{s_i}\right)^{\sum_{j=1}^n i\lambda_j} s_i^{1+i\lambda_i}\left(\prod_{\substack{a=1\\ a\neq i}}^n \int_0^\infty d\omega_a\, \omega_a^{i\lambda_a}\right)\mathcal{A}_{\ell_1\cdots\ell_n}(s_i, \omega_l, z_j, \bar{z}_j)\,, \tag{2.8}$$

where we used that the scaling power of dressed gluon amplitudes is $\mathcal{A}_n(\Lambda\omega_i) \to \Lambda^{-n}\mathcal{A}_n(\omega_i)$. We recognize that the integral over ω_i is the Mellin transform of 1, which is given by

$$\int_0^\infty \frac{d\omega_i}{\omega_i}\left(\frac{\omega_i}{s_i}\right)^{iz} = 2\pi\delta(z). \tag{2.9}$$

With this we simplify the transformation prescription (2.3) to

$$\tilde{\mathcal{A}}_{J_1\cdots J_n}(\lambda_j, z_j, \bar{z}_j) = 2\pi\delta\left(\sum_{j=1}^n \lambda_j\right) s_i^{1+i\lambda_i}\left(\prod_{\substack{a=1\\a\neq i}}^n \int_0^\infty d\omega_a\, \omega_a^{i\lambda_a}\right)\mathcal{A}_{\ell_1\cdots\ell_n}(s_i, \omega_l, z_j\bar{z}_j)\,. \tag{2.10}$$

2.2.2 Integrating out momentum conservation δ-functions

For simplicity, we choose the anchor variable above to be ω_1 and use $\omega_{n-3}, \ldots, \omega_n$ to localize the momentum conservation δ-functions in the amplitude. These δ-functions can then be equivalently rewritten as follows, compensating the transformation by a Jacobian:

$$\delta^4(\epsilon_1 s_1 q_1 + \sum_{i=2}^n \epsilon_i\omega_i q_i) = \frac{4}{U}\prod_{j=n-3}^n s_j\delta\left(\omega_j - \omega_j^*\right)\mathbf{1}_{>0}(\omega_j^*), \tag{2.11}$$

where ω_j^* are solutions to the initial set of linear equations:

$$\omega_j^\star = -s_j\left(\frac{U_{1,j}}{U} + \sum_{i=2}^{n-4}\frac{\omega_i}{s_i}\frac{U_{i,j}}{U}\right). \tag{2.12}$$

The U_{ij} and U are minor determinants by Cramer's rule:

$$U_{i,j} = \det(M^{\{n-3,\ldots,j\to i,\ldots,n\}}), \quad U = \det(M^{\{n-3,\ldots,n\}}), \tag{2.13}$$

where $j \to i$ means that index j is replaced by index i. $M^{\{a,b,c,d\}}$ denotes the 4×4 matrix

$$M^{\{a,b,c,d\}} = \left(p_a\, p_b\, p_c\, p_d\right). \tag{2.14}$$

For the purpose of determinant calculation, the column vectors $p_i^\mu = \epsilon_i s_i q_i^\mu$ can be written in a manifestly conformally invariant form:

$$\begin{aligned} &p_1^\mu(z,\bar z) = \epsilon_1(1,0,0,-1) \;\;,\;\; p_2^\mu(z,\bar z) = \epsilon_2(1,0,0,1) \;\;,\;\; p_3^\mu(z,\bar z) = \epsilon_3(2,2,0,0)\,, \\ &p_i^\mu(z,\bar z) = \epsilon_i \frac{1}{|u_i|}\left(1+|u_i|^2, u_i+\bar u_i, -i(u_i-\bar u_i), 1-|u_i|^2\right) \quad \text{for} \quad i = 4,5,...,n\,, \end{aligned} \tag{2.15}$$

in terms of conformal invariant cross-ratios

$$u_i = \frac{z_{31} z_{i2}}{z_{32} z_{i1}} \quad \text{and} \quad \bar u_i = \frac{\bar z_{31} \bar z_{i2}}{\bar z_{32} \bar z_{i1}} \quad \text{for} \quad i = 4,5,...,n\,, \tag{2.16}$$

but if, and only if, we also specify the explicit choice

$$s_1 = \frac{|z_{3,2}|}{|z_{3,1}|\,|z_{1,2}|}\,, \quad s_2 = \frac{|z_{3,1}|}{|z_{3,2}|\,|z_{2,1}|}\,, \quad \text{and} \quad s_i = \frac{|z_{1,2}|}{|z_{1,i}|\,|z_{i,2}|} \quad \text{for} \quad i = 3,...,n. \tag{2.17}$$

The indicator functions $\prod_{i=n-3}^{n} \mathbf{1}_{>0}(\omega_i^*)$ appear due to the integration range in all ω being along the positive real line, such that the δ-functions can only be localized in this region.

Furthermore, in order for all the remaining integration variables ω_j with $j = 2,...,n-4$ to be defined on the whole integration range, the indicator functions $\prod_{i=n-3}^{n} \mathbf{1}_{>0}(\omega_i^*)$ have to demand $\frac{U_{i,j}}{U} < 0$ for all $i = 1,\dots,n-4$ and $j = n-3,...,n$, so that we can write them as $\prod_{i,j} \mathbf{1}_{<0}(\frac{U_{i,j}}{U})$.

2.2.3 Integrating the remaining ω_i

In this section we apply (2.10) to the usual n-point MHV Parke-Taylor amplitude [2] in spinor-helicity formalism for $n \geq 5$ rewritten via (3.27):

$$\mathcal{A}_{--+\ldots+}(s_1,\omega_j,z_j,\bar{z}_j) = \frac{z_{12}^3 s_1 \omega_2 \delta^4(\epsilon_1 s_1 q_1 + \sum_{i=2}^n \epsilon_i \omega_i q_i)}{(-2)^{n-4} z_{23} z_{34} \ldots z_{n1} \omega_3 \omega_4 \ldots \omega_n}. \tag{2.18}$$

Making use of the solutions (2.11) and performing four of the integrations in (2.10), we have:

$$\tilde{\mathcal{A}}_{--+\ldots+}(\lambda_i,z_i,\bar{z}_i) = 2\pi \frac{\delta(\sum_{j=1}^n \lambda_j) z_{12}^3 \, s_1^{i\lambda_1+2}}{(-2)^{n-4} U z_{23} z_{34} \ldots z_{n1}} \prod_{a=2}^{n-4} \int_0^\infty d\omega_a \, \omega_a^{i\lambda_a} \frac{\omega_2 \prod_{b=n-3}^n s_b \omega_b^{*\,i\lambda_{n-3}}}{\omega_3 \omega_4 \ldots \omega_n^*} \prod_{i,j} \mathbf{1}_{<0}\left(\frac{U_{i,j}}{U}\right). \tag{2.19}$$

For convenience, we transform the remaining integration variables as:

$$\omega_i = s_i \frac{U_{1,n}}{U_{i,n}} \frac{u_{i-1}}{1 - \sum_{j=1}^{n-5} u_j} \quad , \quad i = 2,3,\ldots,n-4\,, \tag{2.20}$$

which leads to

$$\tilde{\mathcal{A}}_{--+\ldots+}(\lambda_i,z_i,\bar{z}_i) \sim \frac{z_{12}^3 s_1^{i\lambda_1+2} s_2^{i\lambda_2+2} s_3^{i\lambda_3} \ldots s_n^{i\lambda_n}}{z_{23} z_{34} \ldots z_{n1} U_{1,n}} \delta\left(\sum_{j=1}^n \lambda_j\right) \hat{\varphi}(\{\alpha\},x) \prod_{i,j} \mathbf{1}_{<0}\left(\frac{U_{i,j}}{U}\right). \tag{2.21}$$

Note that the overall factor in (2.21) accounts for proper transformation weight of the resulting correlator under conformal transformations (2.5).

Here we recognize a hypergeometric function $\hat{\varphi}(\{\alpha\},x)$ of type $(n-4,n)$, as defined in section 3.8.1 of [38] and described in appendix 2.5. In particular, here we have:

$$\begin{aligned} \hat{\varphi}(\{\alpha\},x) \equiv & \int_{\substack{u_1\geq 0,\ldots,u_{n-5}\geq 0\\ 1-\sum_a u_a\geq 0}} \prod_{j=1}^{n} P_j(u)^{\alpha_j}\, d\varphi \quad , \quad d\varphi = \frac{dP_2}{P_2}\wedge\ldots\wedge\frac{dP_{n-4}}{P_{n-4}}\,, \\ P_j(u) = & x_{0j} + x_{1j}u_1 + \ldots + x_{n-5\,j}u_{n-5} \quad , \quad 1\leq j\leq n\,. \end{aligned} \tag{2.22}$$

The parameters in (2.22) corresponding to (2.21) read:[1]

$$\begin{aligned} \alpha_1 = & 1\,,\ \alpha_2 = 2+i\lambda_2\,,\ \alpha_3 = i\lambda_3\,,\ \ldots,\ \alpha_{n-4} = i\lambda_{n-4}\,,\ \alpha_{n-3} = i\lambda_{n-3}-1\,,\ \ldots,\ \alpha_{n-1} = i\lambda_{n-1}-1, \\ \alpha_n = & 1+i\lambda_1\,,\ x_{0\,i} = \frac{U_{1,i}}{U_{1,n}}\,,\ x_{j-1\,i} = \frac{U_{j,i}}{U_{j,n}} - \frac{U_{1,i}}{U_{1,n}}\,,\ x_{0n} = -\frac{U}{U_{1,n}}\,,\ x_{j-1\,n} = \frac{U}{U_{1,n}}\,,\ x_{01} = 1\,,\ x_{j-1\,j} = -\frac{U}{U_{j,n}}\,, \end{aligned} \tag{2.23}$$

for $i = n-3, n-2, n-1$ and $j = 2,3,\ldots,n-4$, and all other $x_{ab} = 0$.

These kinds of functions are also known as Aomoto-Gelfand hypergeometric functions on the Grassmannian $Gr(n-4,n)$.

Making use of eq. (3.24) and (3.25) from [38], we can write down a dual representation of the same function, which yields a hypergeometric function of type $(4,n)$:

$$\begin{aligned} \hat{\varphi}(\{\alpha\},x) \equiv & \frac{c_2}{c_1}\int_{\substack{u_1\geq 0,\ldots,u_3\geq 0\\ 1-\sum_a u_a\geq 0}} \prod_{j=1}^{n} P_j(u)^{\alpha_j}\, d\varphi \quad , \quad d\varphi = \frac{dP_{n-3}}{P_{n-3}}\wedge\ldots\wedge\frac{dP_{n-1}}{P_{n-1}}\,, \\ P_j(u) = & x_{0j} + x_{1j}u_1 + x_{2j}u_2 + x_{3j}u_3 \quad , \quad 1\leq j\leq n\,. \end{aligned} \tag{2.24}$$

[1] For $n=5$, the normally different cases $\alpha_2 = 2+i\lambda_2$ and $\alpha_{n-3} = i\lambda_{n-3}-1$ are reduced to a single $\alpha_2 = 1+i\lambda_2$. In this case there also are no integrations so that the result becomes a simple product of factors.

In this case, the parameters of (2.24) corresponding to (2.21) read:

$$\begin{gathered}\alpha_1 = 1\,,\ \alpha_2 = -2 - i\lambda_2\,,\ \alpha_3 = -i\lambda_3\,, \dots,\ \alpha_{n-4} = -i\lambda_{n-4}\,,\ \alpha_{n-3} = 1 - i\lambda_{n-3}\,, \dots,\ \alpha_{n-1} = 1 - i\lambda_{n-1},\\ \alpha_n = -\, i\lambda_n\,,\ x_{0j} = \frac{U_{j,n}}{U_{1,n}}\,,\ x_{ij} = \frac{U_{j,n-4+i}}{U_{1,n-4+i}} - \frac{U_{j,n}}{U_{1,n}}\,,\ x_{0n} = -\frac{U}{U_{1,n}}\,,\ x_{in} = \frac{U}{U_{1,n}}\,,\ x_{01} = 1\,,\\ x_{1\,n-3} = \frac{-U}{U_{1,n-3}}\,,\ x_{2\,n-2} = \frac{-U}{U_{1,n-2}}\,,\ x_{3\,n-1} = \frac{-U}{U_{1,n-1}}\,,\ \frac{c_2}{c_1} = \frac{\Gamma(2+i\lambda_1)\Gamma(2+i\lambda_2)\prod_{j=3}^{n-4}\Gamma(i\lambda_j)}{\Gamma(1-i\lambda_1)\prod_{i=1}^{3}\Gamma(1-i\lambda_{n-i})}.\end{gathered} \tag{2.25}$$

for $i = 1, 2, 3$ and $j = 2, 3, ..., n-4$, and all other $x_{ab} = 0$.

The hypergeometric functions $\hat{\varphi}(\{\alpha\}, x)$ form a basis of solutions to a Pfaffian form equation which defines a Gauss-Manin connection as described in section 3.8 of [38]. This Pfaffian form equation can be interpreted as a generalized Knizhnik-Zamolodchikov equation satisfied by our correlators [40, 39]. Similar generalized hypergeometric functions appeared in [41] in the context of $\mathcal{N} = 4$ Yang-Mills scattering amplitudes and the deformed Grassmannian.

2.2.4 6-point MHV

In the special case of six gluons there is only one integral in (2.22), such that the function reduces to the simpler case of Lauricella function $\hat{\varphi}_D$:

$$\begin{aligned}\hat{\varphi}_D(\{\alpha\}, x) = &\left(\frac{-U}{U_{2,6}}\right)^{\mathrm{i}\lambda_1+1}\left(\frac{-U}{U_{1,6}}\right)^{\mathrm{i}\lambda_2+2}\left(\frac{U_{2,3}}{U_{2,6}}\right)^{\mathrm{i}\lambda_3-1}\left(\frac{U_{2,4}}{U_{2,6}}\right)^{\mathrm{i}\lambda_4-1}\left(\frac{U_{2,5}}{U_{2,6}}\right)^{\mathrm{i}\lambda_5-1}\times\\ &\times\int_0^1 dt\, t^{\alpha-1}(1-t)^{\gamma-\alpha-1}\prod_{i=1}^{3}(1-x_i t)^{-\beta_i},\end{aligned} \tag{2.26}$$

with parameters and arguments given by

$$\alpha = 2 + i\lambda_2,\ \gamma = 4 + i\lambda_1 + i\lambda_2,\ \beta_i = 1 - i\lambda_{i+2},\ x_i = 1 - \frac{U_{1,i+2}U_{2,6}}{U_{1,6}U_{2,i+2}} \ \text{ for }\ i = 1, 2, 3. \tag{2.27}$$

Note that x_{0j} arguments have been factored out of the integrand to achieve this form.

2.3 n-point NMHV

In this section we will map the n-point NMHV split helicity amplitude $\mathcal{A}_{---++\cdots+}$ to the celestial sphere via (2.10). The spinor-helicity expression for $\mathcal{A}_{---++\cdots+}$ can be found e.g. in [42]

$$\mathcal{A}_{---++\cdots+} = \frac{1}{F_{3,1}} \sum_{j=4}^{n-1} \frac{\langle 1|P_{2,j}P_{j+1,2}|3\rangle^3}{P_{2,j}^2 P_{j+1,2}^2} \frac{\langle j+1\ j\rangle}{[2|P_{2,j}|j+1\rangle\langle j|P_{j+1,2}|2]} \equiv \sum_{j=4}^{n-1} \{M_j\} \tag{2.28}$$

where $F_{i,j} \equiv \langle i\ i+1\rangle\langle i+1\ i+2\rangle\cdots\langle j-1\ j\rangle$ and $P_{x,y} \equiv \sum_{k=x}^{y} |k\rangle[k|$ where $x < y$ cyclically.

We will work with $\{M_4\}$ for the purpose of our calculations. Using momentum conservation and writing $\{M_4\}$ in terms of spinor-helicity variables, we find

$$\begin{aligned}\{M_4\} =& \frac{1}{\langle 34\rangle\langle 45\rangle\cdots\langle n-1\ n\rangle\langle n1\rangle} \frac{(\langle 12\rangle[24]\langle 43\rangle + \langle 13\rangle[34]\langle 43\rangle)^3}{(\langle 23\rangle[23] + \langle 24\rangle[24] + \langle 34\rangle[34])\langle 34\rangle[34]} \times \\ &\times \frac{\langle 54\rangle}{([23]\langle 35\rangle + [24]\langle 45\rangle)(\langle 43\rangle[32])}.\end{aligned} \tag{2.29}$$

Writing this in terms of celestial sphere variables via (3.27), we find

$$\{M_4\} = \frac{\frac{\omega_1\omega_4(\epsilon_2 z_{12}\bar{z}_{24}\omega_2 + \epsilon_3 z_{13}\bar{z}_{34}\omega_3)^3}{2^{n-4} z_{56}z_{67}\cdots z_{n-1,n}z_{n1}\bar{z}_{23}\bar{z}_{34}\prod_{j=2,j\neq 4}^{n}\omega_j}}{(\epsilon_3 z_{35}\bar{z}_{23}\omega_3 + \epsilon_4 z_{45}\bar{z}_{24}\omega_4)\left(\epsilon_2\omega_2\left(\epsilon_3|z_{23}|^2\omega_3 + \epsilon_4|z_{24}|^2\omega_4\right) + \epsilon_3\epsilon_4|z_{34}|^2\omega_3\omega_4\right)}. \tag{2.30}$$

The following map of the above formula to the celestial sphere will only be strictly valid for $n \geq 8$. We will comment on changes at 6- and 7-points in the next section. We use the map (2.10), anchor the calculation about ω_1, make use of solutions (2.11) and perform a change of variables

$$\omega_i = s_i \frac{u_{i-1}}{1 - \sum_{j=1}^{n-5} u_j}, \quad i = 2, \dots, n-4, \tag{2.31}$$

to find the resulting term in the n-point NMHV correlator

$$\{\tilde{M_4}\} \sim \delta\left(\sum_{j=1}^{n} \lambda_j\right) \frac{\prod_{i=1}^{n} s_i^{i\lambda_i}}{\bar{z}_{12}\bar{z}_{23}\bar{z}_{13}z_{45}z_{56}\cdots z_{n-1,n}z_{4,n}} \frac{\bar{z}_{12}\bar{z}_{13}z_{45}z_{4,n}s_1^2 s_4^2}{\bar{z}_{34}z_{n1}U} \hat{\mathcal{F}}(\alpha,x) \prod_{i,j} \mathbf{1}_{<0}(\frac{U_{i,j}}{U}), \tag{2.32}$$

with the function $\hat{\mathcal{F}}(\alpha, x)$ being a Gelfand A-hypergeometric function as defined in Appendix 2.5. In this case it explicitly reads:

$$\begin{aligned} \hat{\mathcal{F}}(\{\alpha\}, x) = \int_{\substack{u_1 \geq 0, \dots u_{n-5} \geq 0 \\ 1-u_1-\dots-u_{n-5} \geq 0}} \prod_{a=1}^{n-5} \frac{du_a}{u_a} \prod_{j=1}^{n-5} u_j^{i\lambda_{j+1}} u_3^2 (u_1u_2x_{10} + u_1u_3x_{20} + u_2u_3x_{30})^{-1} \\ \times \prod_{i=1}^{7} (x_{0i} + u_1x_{1i} + \dots + u_{n-5}x_{n-5,i})^{\alpha_i}, \end{aligned} \tag{2.33}$$

where parameters are given by

$$\alpha_1 = 3,\ \alpha_2 = -1,\ \alpha_3 = i\lambda_1 + 1,\ \alpha_4 = i\lambda_{n-3} - 1,\ \alpha_5 = i\lambda_{n-2} - 1,\ \alpha_6 = i\lambda_{n-1} - 1,\ \alpha_7 = i\lambda_n - 1, \tag{2.34}$$

and function arguments are given by

$$
\begin{aligned}
&x_{10} = \epsilon_2\epsilon_3|z_{23}|^2 s_2 s_3,\ x_{20} = \epsilon_2\epsilon_4|z_{24}|^2 s_2 s_4,\ x_{30} = \epsilon_3\epsilon_4|z_{34}|^2 s_3 s_4,\\
&x_{11} = \epsilon_2 z_{12}\bar{z}_{24} s_2,\ x_{21} = \epsilon_3 z_{13}\bar{z}_{34} s_3,\ x_{22} = \epsilon_3 z_{35}\bar{z}_{23} s_3,\ x_{32} = \epsilon_4 z_{45}\bar{z}_{24} s_4,\\
&x_{03} = 1,\ x_{j3} = -1,\ j = 1,\dots,n-5,\ x_{04} = \frac{U_{1,n-3}}{U}, \quad x_{j4} = \frac{U_{j,n-3} - U_{1,n-3}}{U},\ j = 1,\dots,n-5,\\
&x_{05} = \frac{U_{1,n-2}}{U}, \quad x_{j5} = \frac{U_{j,n-2} - U_{1,n-2}}{U},\ j = 1,\dots,n-5,\\
&x_{06} = \frac{U_{1,n-1}}{U}, \quad x_{j6} = \frac{U_{j,n-1} - U_{1,n-1}}{U},\ j = 1,\dots,n-5,\\
&x_{07} = \frac{U_{1,n}}{U}, \quad x_{j7} = \frac{U_{j,n} - U_{1,n}}{U},\ j = 1,\dots,n-5.
\end{aligned}
\tag{2.35}
$$

Note that the first fraction in (2.32) accounts for the correct transformaton weight of the correlator under conformal tranformation (2.5).

6- and 7-point NMHV

In the cases of 6- and 7-point the results in the previous section change somewhat, due to the presence of ω_3 and ω_4 in the denominator of (2.30). These variables are fixed by momentum conservation δ-functions in the lower point cases, such that the parameters and function arguments of the resulting Gelfand A-hypergeometric functions change.

For the 6-point case, we find that the resulting correlator part $\{\tilde{M}_4\}$ is proportional to a Gelfand A-hypergeometric function as defined in Appendix 2.5:

$$
\hat{\mathcal{F}}(\{\alpha\}, x) = \int_{\substack{u_1 \geq 0 \\ 1-u_1 \geq 0}} \frac{du_1}{u_1}\, u_1^{i\lambda_2}(x_{00} + u_1 x_{10} + u_1^2 x_{20})^{-1}(1-u_1)^{i\lambda_1+1}\prod_{i=2}^{7}(x_{0i} + u_1 x_{1i})^{\alpha_i} \tag{2.36}
$$

where parameters are given by

$$\alpha_2 = i\lambda_3 - 1,\ \alpha_3 = i\lambda_4 + 1,\ \alpha_4 = i\lambda_5 - 1,\ \alpha_5 = i\lambda_6 - 1,\ \alpha_6 = 3,\ \alpha_7 = -1, \tag{2.37}$$

and function arguments x_{ij} depend on $\epsilon_i, z_i, \bar{z}_i$ and U_{ij}. Performing a partial fraction decomposition on the quadratic denominator in (2.36), we can reduce the result to a sum of two Lauricella functions.

In the 7-point case, we find that the resulting correlator part $\{\tilde{M_4}\}$ is proportional to a Gelfand A-hypergeometric function as defined in Appendix 2.5:

$$\begin{aligned}\hat{\mathcal{F}}(\{\alpha\}, x) = &\int_{\substack{u_1\geq 0, u_2 \geq 0\\ 1-u_1-u_2\geq 0}} \frac{du_1}{u_1}\frac{du_2}{u_2}\, u_1^{i\lambda_2} u_2^{i\lambda_3} (u_1 x_{10} + u_2 x_{20} + u_1 u_2 x_{30} + u_1^2 x_{40} + u_2^2 x_{50})^{-1} \\ &\times \prod_{i=1}^{7} (x_{0i} + u_1 x_{1i} + u_2 x_{2i})^{\alpha_i},\end{aligned} \tag{2.38}$$

where parameters are given by

$$\alpha_1 = i\lambda_1 + 1,\ \alpha_2 = i\lambda_4 + 1,\ \alpha_3 = i\lambda_5 - 1,\ \alpha_4 = i\lambda_6 - 1,\ \alpha_5 = i\lambda_7 - 1,\ \alpha_6 = 3,\ \alpha_7 = -1, \tag{2.39}$$

and function arguments x_{ij} again depend on $\epsilon_i, z_i, \bar{z}_i$ and U_{ij}.

2.4 n-point N^{k}MHV

In this section we discuss the schematic structure of N^{k}MHV amplitudes with higher k under the Mellin transform (2.10).

N^{2}MHV amplitude

In the 8-point N^{2}MHV split helicity case, $\mathcal{A}_{----++++}$, we consider one of the six terms of the amplitude found in e.g. [42] on page 6 as an example:

$$\frac{1}{F_{4,1}\bar{F}_{2,3}}\frac{\langle 1|P_{2,6}P_{7,2}P_{3,5}P_{6,3}|4\rangle^3}{P_{2,6}^2P_{7,2}^2P_{3,5}^2P_{6,3}^2}\frac{\langle 76\rangle[23]\langle 65\rangle}{[2|P_{2,6}|7\rangle\langle 6|P_{7,2}|2][3|P_{3,5}|6\rangle\langle 5|P_{6,3}|3]}, \tag{2.40}$$

where $\bar{F}_{i,j}$ is the complex conjugate of $F_{i,j}$. Performing the same sequence of steps as in the previous sections, we find a resulting Gelfand A-hypergeometric function of the form

$$\hat{\mathcal{F}}(\{\alpha\},x) = \int_{\substack{u_1\geq 0,u_2\geq 0,u_3\geq 0\\ 1-u_1-u_2-u_3\geq 0}} \frac{du_1}{u_1}\frac{du_2}{u_2}\frac{du_3}{u_3}\, u_1^{\alpha_1}u_2^{\alpha_2}u_3^{\alpha_3}\mathcal{P}_{\{4\}}^3\prod_{i=4}^{13}(x_{0i}+u_1x_{1i}+u_2x_{2i}+u_3x_{3i})^{\alpha_i}$$

$$\times\prod_{j=14}^{17}(x_{0j}+u_1x_{1j}+u_2x_{2j}+u_3x_{3j}+u_1u_2x_{4j}+u_1u_3x_{5j}+u_2u_3x_{6j}+u_1^2x_{7j}+u_2^2x_{8j}+u_3^2x_{9j})^{\alpha_j}, \tag{2.41}$$

for some parameters α_i, where $\mathcal{P}_{\{4\}}$ is a degree four polynomial in u_i, and function arguments x_{ij} again depend on $\epsilon_i, z_i, \bar{z}_i$ and U_{ij}.

N^{k}MHV amplitude

More generally a split helicity N^{k}MHV amplitude $\mathcal{A}_{-\cdots-+\cdots+}$ involves a sum over the terms described in eq. (3.1), (3.2) of [42]. Terms corresponding in complexity to $\{\tilde{M}_4\}$ discussed in the previous section are always present, with constant Laurent polynomial powers at any

k. However, for higher k, the most complicated contributing summands result in hypergeometric integrals schematically given by

$$\hat{\mathcal{F}}(\{\alpha\},x) = \int_{\substack{u_1,\ldots,u_{n-4}\geq 0 \\ 1-u_2-\cdots-u_{n-4}\geq 0}} \prod_{l=2}^{n-4} \frac{du_l}{u_l} u_l^{\alpha_l} \left(1 - \sum_{j=2}^{n-4} u_j\right)^{\alpha_1} \mathcal{P}^3_{\{2k\}} \left(\prod_i (\mathcal{P}^i_{\{1\}})^{\alpha_i}\right)\left(\prod_j (\mathcal{P}^j_{\{2\}})^{\alpha_j}\right) \tag{2.42}$$

where α_i are parameters and $\mathcal{P}_{\{d\}}$ is a degree d polynomial in u_a. Here we explicitly see an increase in power of the Laurent polynomials with increasing k in N^{k}MHV. The examples above feature the Gelfand A-hypergeometric function $\hat{\mathcal{F}}$. The increase in Laurent polynomial degree is traced back to the presence of Mandelstam invariants $P^2_{i,j}$ for degree two polynomials, as well as the factors $\langle a|P_{i,j}P_{k,l}...P_{r,t}|b\rangle$ for higher degree polynomials. The length of chains of the $P_{i,j}$ depends on n and k, such that multivariate Laurent polynomials of any positive degree are present at sufficiently high n, k.

Similar generalized hypergeometric functions, or, equivalently, generalized Euler integrals are found in the case of string scattering amplitudes [43, 44]. It will be interesting to explore this connection further.

2.5 Generalized hypergeometric functions

The Aomoto-Gelfand hypergeometric functions of type $(n+1, m+1)$ relevant in this work can be defined as in section 3.5.1 of [38]:

$$\hat{\varphi}(\{\alpha\}, x) \equiv \int_{\substack{u_1 \geq 0, \ldots, u_n \geq 0 \\ 1 - \sum_a u_a \geq 0}} \prod_{j=0}^{m} P_j(u)^{\alpha_j} \, d\varphi \,, \tag{2.43}$$

$$d\varphi = \frac{dP_{j_1}}{P_{j_1}} \wedge \ldots \wedge \frac{dP_{j_n}}{P_{j_n}} \quad , \quad 0 \leq j_1 < \ldots < j_n \leq m \,, \tag{2.44}$$

$$P_j(u) = x_{0j} + x_{1j} u_1 + \ldots + x_{nj} u_n \quad , \quad 1 \leq j \leq m \,, \tag{2.45}$$

where here the parameters α_i collectively describe all the powers for the factors in the integrand. When all α_i are zero, the function reduces to the Aomoto polylogarithm.

The arguments x_{ij} of the hypergeometric function of type $(m+1, n+1)$ in (2.45) can be arranged in a matrix:

$$\bar{X} = \begin{pmatrix} x_{00} & \ldots & x_{0m} \\ x_{10} & \ldots & x_{1m} \\ \vdots & \ddots & \vdots \\ x_{n0} & \ldots & x_{nm} \end{pmatrix} . \tag{2.46}$$

Each column in this matrix defines a hyperplane in $\mathbb{C}^n$ that appears in the hypergeometric integral as $(x_{0j} + \sum_{i=1}^{n} x_{ij} u_i)^{\alpha_i}$. Furthermore, $(n+1) \times (n+1)$ minor determinants of the matrix can be regarded as Plücker coordinates on the Grassmannian $Gr(n+1, m+1)$ over the space of arguments x_{ij}.

Sometimes it is convenient to transform the argument arrangement (2.46) to the following gauge fixed form

$$\begin{pmatrix} 1 & 0 & \dots & 0 & 1 & 1 & \dots & 1 \\ 0 & 1 & \dots & 0 & -1 & -x_{11} & \dots & -x_{1\,m-n-1} \\ \vdots & & \ddots & & -1 & \vdots & \vdots & \vdots \\ 0 & 0 & \dots & 1 & -1 & -x_{n1} & \dots & -x_{n\,m-n-1} \end{pmatrix}. \tag{2.47}$$

In this case the hypergeometric function can then be written in the following two equivalent ways, eq. (3.24) of [38]:

$$\begin{aligned} F((\alpha_i),(\beta_j),\gamma;x) =& c_1 \int_{\substack{u_1\geq 0,\dots,u_n\geq 0 \\ 1-\sum_a u_a\geq 0}} d^n u \prod_{i=1}^{n} u_i^{\alpha_i-1}\cdot(1-\sum_{l=1}^{n} u_l)^{\gamma-\sum_i\alpha_i-1}\prod_{j=1}^{m-n-1}(1-\sum_{i=1}^{n} x_{ij}u_i)^{-\beta_j}, \\ c_1 =& \Gamma(\gamma)/\Gamma(\gamma-\sum_{i=1}^{n}\alpha_i)\cdot\prod_{i=1}^{n}\Gamma(\alpha_i), \end{aligned} \tag{2.48}$$

and the dual representation in eq. (3.25) of [38]:

$$\begin{aligned} F((\alpha_i),(\beta_j),\gamma;x) =& c_2 \int_{\substack{u_1\geq 0,\dots,u_{m-n-1}\geq 0 \\ 1-\sum_a u_a\geq 0}} d^{m-n-1} u \prod_{i=1}^{m-n-1} u_i^{\beta_i-1}\cdot(1-\sum_{l=1}^{m-n-1} u_l)^{\gamma-\sum_i\beta_i-1}\prod_{j=1}^{n}(1-\sum_{i=1}^{m-n-1} x_{ji}u_i)^{-\alpha_j}, \\ c_2 =& \Gamma(\gamma)/\Gamma(\gamma-\sum_{i=1}^{m-n-1}\beta_i)\cdot\prod_{i=1}^{m-n-1}\Gamma(\beta_i), \end{aligned} \tag{2.49}$$

where the parameters are assumed to satisfy the conditions

$$\begin{aligned} &\alpha_i\notin\mathbb{Z},\ 1\leq i\leq n,\ \beta_j\notin\mathbb{Z},\ 1\leq j\leq m-n-1, \\ &\gamma-\sum_{i=1}^{n}\alpha_i\notin\mathbb{Z},\ \gamma-\sum_{j=1}^{m-n-1}\beta_j\notin\mathbb{Z}. \end{aligned} \tag{2.50}$$

The hypergeometric functions (2.43) comprise a basis of solutions to the defining set of differential equations

$$\begin{aligned}
&(1) \quad \sum_{i=0}^{n} x_{ij} \frac{\partial \hat{\varphi}}{\partial x_{ij}} = \alpha_j \hat{\varphi}\,, && 0 \le j \le m, \\
&(2) \quad \sum_{j=0}^{m} x_{ij} \frac{\partial \hat{\varphi}}{\partial x_{ij}} = -(1+\alpha_i) \hat{\varphi}\,, && 0 \le i \le n, \\
&(3) \quad \frac{\partial^2 \hat{\varphi}}{\partial x_{ij} \partial x_{pq}} = \frac{\partial^2 \hat{\varphi}}{\partial x_{iq} \partial x_{pj}}, && 0 \le i, p \le n, \quad 0 \le j, q \le m.
\end{aligned} \tag{2.51}$$

In cases where factors of the integrand are non-linear in the integration variables, the functions can be generalized further to Gelfand A-hypergeometric functions [45, 46] defined as:

$$\hat{\mathcal{F}}(\{\alpha\}, x) = \int_{\substack{u_1 \ge 0, \ldots, u_k \ge 0 \\ 1 - \sum_a u_a \ge 0}} \prod_i \mathcal{P}_i(u_1, \ldots, u_k)^{\alpha_i} u_1^{\alpha_1} \ldots u_k^{\alpha_k} du_1 \ldots du_k, \tag{2.52}$$

where α_i are complex parameters and $\mathcal{P}_i$ now are Laurent polynomials in $u_1, \ldots, u_k$.

Chapter 3

Celestial Amplitudes: Conformal Partial Waves and Soft Limits

This chapter is based on the publication [47].

Pasterski, Shao, and Strominger (PSS) have proposed a map between $\mathcal{S}$-matrix elements in four-dimensional Minkowski spacetime and correlation functions in two-dimensional conformal field theory (CFT) living on the celestial sphere [8, 34]. Celestial CFT is interesting both for understanding the long elusive holographic description of flat spacetime [48] as well as for exploring the mathematical structures of amplitudes. In recent years many remarkable properties of amplitudes have been uncovered via twistor space, momentum twistor space, scattering equations, etc.(see [49] for review), hence it is quite plausible that exploring properties of celestial amplitudes may also lead to new insights.

A key idea behind the PSS proposal was to transform the plane wave basis to a manifestly conformally covariant basis called the conformal primary wavefunction basis. This basis was constructed explicitly by Pasterski and Shao [9] for particles of various spins in diverse dimensions. The celestial sphere is the null infinity of four-dimensional Minkowski spacetime.

The double cover of the four-dimensional Lorentz group is identified with the $SL(2,\mathbb{C})$ conformal group of the celestial sphere. Two-dimensional correlators on the celestial sphere will be referred to as celestial amplitudes from here on.

The celestial amplitudes of *massless* particles are given by Mellin transforms of the corresponding four-dimensional amplitudes

$$\tilde{\mathcal{A}}_n(z_j,\bar{z}_j) = \int_0^\infty \prod_{l=1}^n d\omega_l\, \omega_l^{\Delta_l-1}\mathcal{A}_n(k_l)\,, \tag{3.1}$$

where $\Delta_l = 1 + i\lambda_l$, with $\lambda_l \in \mathbb{R}$ [9], are conformal dimensions taking values in the principal continuous series, in order to ensure the orthogonality and completeness of the conformal primary wavefunction basis. Further details are given below.

In the spirit of recent developments in understanding scattering amplitudes from the on-shell perspective by studying symmetries, analytic properties, and unitarity, many recent studies have delved into similar aspects of celestial amplitudes. The structure of factorization of singularities of celestial amplitudes was investigated in [33]; three- and four-point gluon amplitudes were computed in [34] and arbitrary tree-level ones in [31]. Celestial four-point string amplitudes have been discussed in [50]. Unitarity via the manifestation of the optical theorem on celestial amplitudes has been observed recently [36, 35] and the generators of Poincaré and conformal groups in the celestial representation were constructed in [51].

This paper is organized as follows. In section 3.1 we compute massless scalar four-point celestial amplitudes and study its properties such as conformal partial wave decomposition, crossing relations, and optical theorem. In section 3.2 we derive conformal partial wave decomposition for four-point gluon celestial amplitude, and in section 3.3 single and double

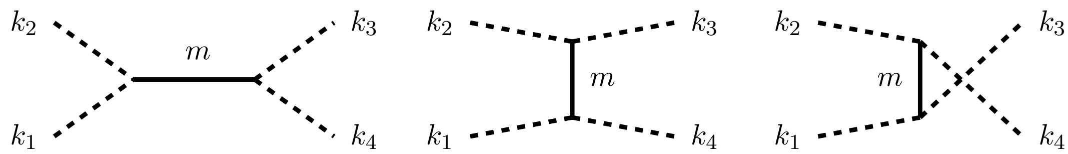

FIGURE 3.1: Four-Point Exchange Diagrams

soft limits for all gluon celestial amplitudes. The conformal partial wave decomposition formalism is summarized in appendix 3.4 and details about inner product integrals, required in the main text, are evaluated in appendix 3.5.

Note added: During this work, we became aware of related work by Pate, Raclariu, and Strominger [52] which has some overlap with section 4 of our paper.

3.1 Scalar Four-Point Amplitude

In this section we study a tree level four-point amplitude of massless scalars mediated by exchange of a massive scalar depicted on Figure 3.1[1].

The corresponding celestial amplitude (3.1) is

$$\tilde{\mathcal{A}}_4(z_j,\bar{z}_j) = g^2 \int_0^\infty \prod_{j=1}^4 d\omega_j\, \omega_j^{\Delta_j-1} \delta^{(4)}\left(\sum_{i=1}^4 k_i\right)\left(\frac{1}{(k_1+k_2)^2+m^2}+\frac{1}{(k_1+k_3)^2+m^2}+\frac{1}{(k_1+k_4)^2+m^2}\right), \tag{3.2}$$

where $z_j, \bar{z}_j$ are coordinates on the celestial sphere and ω_j are the energies. Defining $\epsilon_j = -1$ $(+1)$ for incoming (outgoing) particles, we can parameterize the momenta k_j^μ as

$$k_j^\mu = \epsilon_j \omega_j \left(1+|z_j|^2, z_j+\bar{z}_j, i\bar{z}_j - i z_j, 1-|z_j|^2\right). \tag{3.3}$$

[1] The same amplitude in three dimensions was studied in [35].

Under conformal transformations, by construction [9], the four-point celestial amplitude behaves as a four-point CFT correlation function of operators with conformal weights

$$(h_j, \bar{h}_j) = \frac{1}{2}(\Delta_j + J_j, \Delta_j - J_j)\,, \tag{3.4}$$

where J_j are spins. We can split the four-point celestial amplitude into a conformally invariant function of only the cross-ratios $\tilde{A}_4(z,\bar{z})$ and a universal prefactor

$$\tilde{\mathcal{A}}_4(z_j,\bar{z}_j) = \frac{\left(\frac{z_{24}}{z_{14}}\right)^{h_{12}}\left(\frac{z_{14}}{z_{13}}\right)^{h_{34}}}{z_{12}^{h_1+h_2} z_{34}^{h_3+h_4}} \frac{\left(\frac{\bar{z}_{24}}{\bar{z}_{14}}\right)^{\bar{h}_{12}}\left(\frac{\bar{z}_{14}}{\bar{z}_{13}}\right)^{\bar{h}_{34}}}{\bar{z}_{12}^{\bar{h}_1+\bar{h}_2} \bar{z}_{34}^{\bar{h}_3+\bar{h}_4}} \tilde{A}_4(z,\bar{z})\,, \tag{3.5}$$

where we define $h_{ij} = h_i - h_j$, $\bar{h}_{ij} = \bar{h}_i - \bar{h}_j$ and cross-ratios

$$z = \frac{z_{12}z_{34}}{z_{13}z_{24}}\,, \quad \bar{z} = \frac{\bar{z}_{12}\bar{z}_{34}}{\bar{z}_{13}\bar{z}_{24}} \quad \text{with} \quad z_{ij} = z_i - z_j\,, \quad \bar{z}_{ij} = \bar{z}_i - \bar{z}_j\,. \tag{3.6}$$

Let's fix the external points in (3.2) as $z_1 = 0, z_2 = z, z_3 = 1, z_4 = 1/\tau$ with $\tau \to 0$, and compute

$$\tilde{A}_4(z) \equiv |z|^{\Delta_1+\Delta_2} \lim_{\tau\to 0} \tau^{-2\Delta_4} \tilde{\mathcal{A}}_4(0,z,1,1/\tau)\,. \tag{3.7}$$

We will consider the case where particles 1 and 2 are incoming while 3 and 4 are outgoing, so $\epsilon_1 = \epsilon_2 = -\epsilon_3 = -\epsilon_4 = -1$ and denote it as $12 \leftrightarrow 34$. The s-channel diagram on figure 3.1 is

$$\tilde{A}_{4,s}^{12\leftrightarrow 34}(z) \sim g^2 |z|^{\Delta_1+\Delta_2} \lim_{\tau\to 0} \tau^{-2\Delta_4} \int_0^\infty \prod_{i=1}^4 d\omega_i\, \omega_i^{\Delta_i - 1} \delta^{(4)}\left(\sum_{j=1}^4 k_j\right) \frac{1}{m^2 - 4\omega_1\omega_2|z|^2}\,. \tag{3.8}$$

The momentum conservation delta functions can be rewritten as:

$$\delta^{(4)}\left(\sum_{j=1}^{4} k_j\right) = \frac{4\tau^2}{\omega_1}\delta(i\bar{z} - iz)\prod_{i=2}^{4}\delta(\omega_i - \omega_i^*)\,, \tag{3.9}$$

where

$$\omega_2^* = \frac{\omega_1}{z-1} \quad , \quad \omega_3^* = \frac{z\omega_1}{z-1} \quad , \quad \omega_4^* = z\omega_1\tau^2\,. \tag{3.10}$$

The delta function only has solutions when all the ω_i^* are positive, so $z > 1$.

Then (3.8) reduces to a single integral

$$\begin{aligned}\tilde{A}_{4,s}^{12\leftrightarrow 34}(z) &\sim g^2\delta(i\bar{z} - iz)z^{\Delta_1+\Delta_2}\lim_{\tau\to 0}\tau^{2-2\Delta_4}\int_0^\infty d\omega_1\omega_1^{\Delta_1-2}\prod_{i=2}^{4}(\omega_i^*)^{\Delta_i-1}\frac{1}{m^2 - \frac{4z^2}{z-1}\omega_1^2}\\ &= \frac{g^2\,(im/2)^{2\alpha-2}}{\sin(\pi\alpha)}\delta(i\bar{z} - iz)\,z^2\,(z-1)^{h_{12}-h_{34}}\,.\end{aligned} \tag{3.11}$$

Adding the s-, t-, and u-channel contributions, we obtain our final result

$$\tilde{A}_4^{12\leftrightarrow 34}(z) \sim g^2\frac{(m/2)^{2\alpha-2}}{\sin(\pi\alpha)}\delta(i\bar{z} - iz)\,z^2\,(z-1)^{h_{12}-h_{34}}\left(e^{\pi i\alpha} + \left(\frac{z}{z-1}\right)^{\alpha} + z^{\alpha}\right), \tag{3.12}$$

where

$$\alpha = \sum_{i=1}^{4} h_i - 2\,. \tag{3.13}$$

Let us discuss some properties of this expression.

• First, it is straightforward to verify that the Poincaré generators on the celestial sphere, constructed in [51],

$$
\begin{aligned}
&L_{1,i} = (1 - z_i^2)\partial_{z_i} - 2z_i h_i\,, &&L_{2,i} = (1 + z_i^2)\partial_{z_i} + 2z_i h_i\,, &&L_{3,i} = 2(z_i\partial_{z_i} + h_i)\,,\\
&\bar{L}_{1,i} = (1 - \bar{z}_i^2)\partial_{\bar{z}_i} - 2\bar{z}_i \bar{h}_i\,, &&\bar{L}_{2,i} = (1 + \bar{z}_i^2)\partial_{\bar{z}_i} + 2\bar{z}_i \bar{h}_i\,, &&\bar{L}_{3,i} = 2(\bar{z}_i\partial_{\bar{z}_i} + \bar{h}_i)\,,\\
&P_{0,i} = (1 + |z_i|^2)e^{(\partial_{h_i}+\partial_{\bar{h}_i})/2}\,, &&P_{1,i} = (z_i + \bar{z}_i)e^{(\partial_{h_i}+\partial_{\bar{h}_i})/2}\,, &&\\
&P_{2,i} = -i(z_i - \bar{z}_i)e^{(\partial_{h_i}+\partial_{\bar{h}_i})/2}\,, &&P_{3,i} = (1 - |z_i|^2)e^{(\partial_{h_i}+\partial_{\bar{h}_i})/2} &&
\end{aligned}
\tag{3.14}
$$

annihilate the celestial amplitude on the support of the delta function $\delta(i\bar{z} - iz)$.

• Second, we can show that $\tilde{A}_4$ satisfies the crossing relations

$$
\tilde{A}_4^{13\leftrightarrow 24}(1-z) = \left(\frac{1-z}{z}\right)^{2(h_2+h_3)} \tilde{A}_4^{13\leftrightarrow 24}(z)\,, \qquad 0 < z < 1\,, \tag{3.15}
$$

as well as

$$
\begin{aligned}
\tilde{A}_4^{13\leftrightarrow 24}(z) &= z^{2(h_1+h_4)}\tilde{A}_4^{12\leftrightarrow 34}(1/z)\\
&= (1-z)^{2(h_{12}-h_{34})}\tilde{A}_4^{14\leftrightarrow 23}\left(\frac{z}{z-1}\right)
\end{aligned}\,, \qquad 0 < z < 1\,. \tag{3.16}
$$

The relations (3.15) and (3.16) generalize similar relations in [35].

• Third, the conformal partial wave decomposition of s-channel celestial amplitude (3.11)[2] is computed in the appendix 3.4, 3.5 and takes the following form

$$
\tilde{A}_{4,s}^{12\leftrightarrow 34}(z) \sim \frac{g^2\,(im/2)^{2\alpha-2}}{2\sin(\pi\alpha)} \int_{\mathcal{C}} \frac{d\Delta}{4\pi^2}\, \frac{\Gamma\left(1-\frac{\Delta}{2}-h_{12}\right)\Gamma\left(\frac{\Delta}{2}-h_{12}\right)\Gamma\left(1-\frac{\Delta}{2}-h_{34}\right)\Gamma\left(\frac{\Delta}{2}-h_{34}\right)}{\Gamma(1-\Delta)\Gamma(\Delta-1)}\,\Psi_{h_i}^{\Delta}(z,\bar{z})\,, \tag{3.17}
$$

[2]The other two channels can be obtained in similar manner.

where $\Psi^{\Delta}_{h_i}(z,\bar{z})$ is given in (3.45) restricted to the internal scalar case with $J=0$ and the contour $\mathcal{C}$ runs from $1-i\infty$ to $1+i\infty$.

The gamma functions in (3.17) unambiguously specify all pole sequences in conformal dimensions. Closing the contour to the right or left of the complex axis in Δ, we find simple poles at Δ and their shadows at $\tilde{\Delta}$ given by

$$\frac{\Delta}{2}=1-h_{12}+n \quad , \quad \frac{\Delta}{2}=1-h_{34}+n \quad , \quad \frac{\tilde{\Delta}}{2}=h_{12}-n \quad , \quad \frac{\tilde{\Delta}}{2}=h_{34}-n\,, \tag{3.18}$$

with $n=0,1,2,3,\ldots$.

• Finally, let's explicitly check the celestial optical theorem derived by Shao and Lam in [35], which relates the imaginary part of the four-point celestial amplitude to the product of two three-point celestial amplitudes with the appropriate integration measure. Taking imaginary part of (3.17) we obtain

$$\mathrm{Im}\left[\tilde{A}^{12\leftrightarrow34}_{4,s}(z)\right]\sim\int_{\mathcal{C}}d\Delta\,\mu(\Delta)C(h_1,h_2;\Delta)C(h_3,h_4;2-\Delta)\boldsymbol{\Psi}^{\Delta}_{h_i}(z,\bar{z})\,, \tag{3.19}$$

up to some overall constants independent of h_i. Here $C(h_i,h_j;\Delta)$ is the coefficient of the three-point function given by [35]

$$C(h_i,h_j;\Delta)=g\frac{(m^2)^{h_i+h_j-2}}{4^{h_i+h_j}}\frac{\Gamma\left(h_{ij}+\frac{\Delta}{2}\right)\Gamma\left(\frac{\Delta}{2}-h_{ij}\right)}{\Gamma(\Delta)}\,, \tag{3.20}$$

$\mu(\Delta)$ is the integration measure

$$\mu(\Delta)=\frac{\Gamma(\Delta)\Gamma(2-\Delta)}{4\pi^3\Gamma(\Delta-1)\Gamma(1-\Delta)}\,, \tag{3.21}$$

and $\boldsymbol{\Psi}^{\Delta}_{h_i}(z,\bar z)$ is

$$\boldsymbol{\Psi}^{\Delta}_{h_i}(z,\bar z) \equiv \frac{\Gamma\left(1-\frac{\Delta}{2}-h_{12}\right)\Gamma\left(\frac{\Delta}{2}-h_{34}\right)}{\Gamma\left(\frac{\Delta}{2}+h_{12}\right)\Gamma\left(1-\frac{\Delta}{2}+h_{34}\right)}\Psi^{\Delta}_{h_i}(z,\bar z)\,. \tag{3.22}$$

3.2 Gluon Four-Point Amplitude

In this section we study the massless four-point gluon celestial amplitude, which has been computed in [34], and is given by

$$\tilde{A}^{12\leftrightarrow 34}_{--++}(z) \sim \delta(i\bar z - iz)|z|^3|1-z|^{h_{12}-h_{34}-1}\,, \quad z>1\,, \tag{3.23}$$

where the conformal ratios $z,\bar z$ are defined in (3.6).

Evaluating the integral in appendix 3.5, we find the conformal partial wave expansion is given by the following simple result[3]

$$\tilde{A}^{12\leftrightarrow 34}_{--++}(z) \sim 2i{\sum_{J=0}^{\infty}}' \int_{\mathcal{C}} \frac{dh}{4\pi^2}\,\Psi^{h,\bar h}_{h_i,\bar h_i}\frac{\pi\,(1-2h)(2h-1-2J)}{(h_{34}-h_{12})\sin(\pi(h_{12}-h_{34}))}\left(\frac{\Gamma(h-h_{12})\Gamma(1+J-h_{34}-h)}{\Gamma(h+h_{12})\Gamma(1+J+h_{34}-h)}+(h_{12}\leftrightarrow h_{34})\right), \tag{3.24}$$

where $\sum'$ means that the $J=0$ term contributes with weight $1/2$.

There is no truncation of the spins J in this case, so primary operators of all integer spins contribute to the OPE expansion of the external gluon operators, in contrast with the previously considered scalar case.

[3]When considering $J<0$, take $h\leftrightarrow\bar h$ in the expansion coefficient.

Poles Δ and shadow poles $\tilde{\Delta}$ are located at

$$\frac{\Delta - J}{2} = 1 - h_{12} + n \quad , \quad \frac{\Delta - J}{2} = 1 - h_{34} + n \quad , \quad \frac{\tilde{\Delta} + J}{2} = h_{12} - n \quad , \quad \frac{\tilde{\Delta} + J}{2} = h_{34} - n \,, \tag{3.25}$$

with $n = 0, 1, 2, 3, \dots$. These poles are integer spaced as expected.

3.3 Soft limits

Single soft limits

In this section we study the analog of soft limits for celestial amplitudes. The universal soft behavior of color-ordered gluon scattering amplitudes, corresponding to $\omega_k \to 0$, is well-known [53] and takes the form

$$\begin{aligned} \lim_{\omega_k \to 0} \mathcal{A}_n^{\ell_k = +1} &= \frac{\langle k-1\, k+1 \rangle}{\langle k-1\, k \rangle \langle k\, k+1 \rangle} \mathcal{A}_{n-1} \,, \\ \lim_{\omega_k \to 0} \mathcal{A}_n^{\ell_k = -1} &= \frac{[k-1\, k+1]}{[k-1\, k][k\, k+1]} \mathcal{A}_{n-1} \,, \end{aligned} \tag{3.26}$$

where ℓ_k is the helicity of particle k.

The spinor-helicity variables are related to the celestial sphere variables via [34]

$$[ij] = 2\sqrt{\omega_i \omega_j}\, \bar{z}_{ij} \,, \qquad \langle ij \rangle = -2\epsilon_i \epsilon_j \sqrt{\omega_i \omega_j}\, z_{ij} \,. \tag{3.27}$$

Conformal primary wavefunctions become soft (pure gauge) when $\Delta_k \to 1$ (or $\lambda_k \to 0$) [9, 54]. In this limit we can utilize the delta function representation[4]

$$\delta(x) = \frac{1}{2} \lim_{\lambda \to 0} i\lambda \, |x|^{i\lambda - 1} \,, \tag{3.28}$$

such that (3.1) becomes

$$\lim_{\lambda_k \to 0} \tilde{\mathcal{A}}_n(z_j, \bar{z}_j) = \frac{1}{i\lambda_k} \prod_{j=1, j\neq k}^{n} \int_0^\infty d\omega_j \, \omega_j^{i\lambda_j} \int_0^\infty d\omega_k \, 2\,\delta(\omega_k)\, \omega_k \, \mathcal{A}_n(\omega_j; z_j, \bar{z}_j) \,. \tag{3.29}$$

We see that the $\lambda_k \to 0$ limit localizes the integral at $\omega_k = 0$ and we obtain

$$\lim_{\lambda_k \to 0} \tilde{\mathcal{A}}_n^{J_k=+1} = \frac{1}{i\lambda_k} \frac{z_{k-1\,k+1}}{z_{k-1\,k} z_{k\,k+1}} \tilde{\mathcal{A}}_{n-1} \,, \tag{3.30}$$

$$\lim_{\lambda_k \to 0} \tilde{\mathcal{A}}_n^{J_k=-1} = \frac{1}{i\lambda_k} \frac{\bar{z}_{k-1\,k+1}}{\bar{z}_{k-1\,k} \bar{z}_{k\,k+1}} \tilde{\mathcal{A}}_{n-1} \,. \tag{3.31}$$

An alternative derivation of these relations was given in [55].

Double soft limits

For consecutive soft limits, one can apply (3.30) or (3.31) multiple times and the consecutive soft factors are simply products of single soft factors.

[4] See `http://mathworld.wolfram.com/DeltaFunction.html`

For simultaneous double soft limits, energies of particles are simultaneously scaled by δ, so $\omega_k \to \delta\omega_k$ and $\omega_l \to \delta\omega_l$ with $\delta \to 0$, which for example yields [56, 57]

$$\lim_{\delta\to 0} \mathcal{A}_n(\delta\omega_1, \delta\omega_2, \omega_j; z_k, \bar{z}_k) = \frac{1}{\langle n|1+2|3]} \left(\frac{[13]^3\langle n3\rangle}{[12][23]s_{123}} + \frac{\langle n2\rangle^3[n3]}{\langle n1\rangle\langle 12\rangle s_{n12}} \right) \mathcal{A}_{n-2}(\omega_j; z_j, \bar{z}_j)\,, \tag{3.32}$$

for $\ell_1 = +1$, $\ell_2 = -1$, $j = 3, \ldots, n$, and $k = 1, \ldots, n$. Here $s_{ijl} = (k_i + k_j + k_l)^2$. More generally we will write

$$\lim_{\delta\to 0} \mathcal{A}_n(\delta\omega_k, \delta\omega_l, \omega_j; z_i, \bar{z}_i) = \mathrm{DS}(k^{\ell_k}, l^{\ell_l}) \mathcal{A}_{n-2}(\omega_j; z_j, \bar{z}_j)\,, \tag{3.33}$$

where $\mathrm{DS}(k^{\ell_k}, l^{\ell_l})$ is the simultaneous double soft factor.

For celestial amplitudes, the analog of the simultaneous double soft limit is to take two λ's, scale them by ϵ, $\lambda_k \to \epsilon\lambda_k$ and $\lambda_l \to \epsilon\lambda_l$, and take the $\epsilon \to 0$ limit. To implement this practically in (3.1), we change variables for the associated ω's

$$\omega_k = r\cos(\theta), \quad \omega_l = r\sin(\theta), \quad 0 \le r < \infty, \quad 0 \le \theta \le \frac{\pi}{2}\,. \tag{3.34}$$

The mapping (3.1) becomes

$$\begin{aligned} \tilde{\mathcal{A}}_n(z_j, \bar{z}_j) = \prod_{j=1, j\neq k,l}^{n} \int_0^\infty d\omega_j\, \omega_j^{i\lambda_j} \int_0^\infty dr \int_0^{\pi/2} d\theta\, r^{(i\lambda_k + i\lambda_l)\epsilon - 1} \\ \times (\cos(\theta))^{i\lambda_k\epsilon} (\sin(\theta))^{i\lambda_l\epsilon} r^2 \mathcal{A}_n(\omega_j; z_j, \bar{z}_j)\,. \end{aligned} \tag{3.35}$$

We can use (3.28) to obtain a delta function in r, which enforces the simultaneous double soft limit for the scattering amplitude as in (3.32). The result is

$$\lim_{\epsilon\to 0}\tilde{\mathcal{A}}_n(\lambda_k\epsilon,\lambda_l\epsilon)=\tilde{\mathrm{DS}}(k^{J_k},l^{J_l})\tilde{\mathcal{A}}_{n-2}\,, \tag{3.36}$$

where $\tilde{\mathrm{DS}}(k^{J_k},l^{J_l})$ is the simultaneous double soft factor on the celestial sphere,

$$\tilde{\mathrm{DS}}(k^{J_k},l^{J_l})=\frac{1}{(i\lambda_k+i\lambda_l)\epsilon}\left[2\int_0^{\pi/2}d\theta\,(\cos(\theta))^{i\lambda_k\epsilon}(\sin(\theta))^{i\lambda_l\epsilon}\left[r^2\mathrm{DS}(k^{\ell_k},l^{\ell_l})\right]_{r=0}\right]_{\epsilon\to 0}. \tag{3.37}$$

As an example, consider the simultaneous double soft factor in (3.32). We can use (3.27) to translate it into celestial sphere coordinates and plug into (3.37) to obtain

$$\tilde{\mathrm{DS}}(1^{+1},2^{-1})\sim\frac{1}{2(i\lambda_1+i\lambda_2)\epsilon^2}\frac{1}{z_{n1}\bar{z}_{23}}\left(\frac{1}{i\lambda_1}\frac{\bar{z}_{n3}z_{2n}}{z_{12}\bar{z}_{2n}}+\frac{1}{i\lambda_2}\frac{z_{3n}\bar{z}_{31}}{\bar{z}_{12}z_{31}}\right). \tag{3.38}$$

Explicitly let us check (3.36) by considering the six-point NMHV split helicity amplitude [42]

$$\begin{aligned}\mathcal{A}_{+++---}&=\delta^{(4)}\left(\sum_{i=1}^{6}k_i\right)\frac{1}{4\omega_1\cdots\omega_6}\\&\times\left[\frac{\frac{\omega_1^2\omega_4^2(\omega_3z_{34}\bar{z}_{13}-\omega_2z_{24}\bar{z}_{12})^3}{(\omega_3\omega_4z_{34}\bar{z}_{34}-\omega_2\omega_4z_{24}\bar{z}_{24}-\omega_2\omega_3z_{23}\bar{z}_{23})}}{z_{23}z_{34}\bar{z}_{56}\bar{z}_{61}\left(\omega_4z_{24}\bar{z}_{54}-\omega_3z_{23}\bar{z}_{35}\right)}+\frac{\frac{\omega_3^2\omega_6^2(\omega_4z_{46}\bar{z}_{34}+\omega_5z_{56}\bar{z}_{35})^3}{(\omega_3\omega_4z_{34}\bar{z}_{34}+\omega_3\omega_5z_{35}\bar{z}_{35}+\omega_4\omega_5z_{45}\bar{z}_{45})}}{z_{12}z_{16}\bar{z}_{34}\bar{z}_{45}\left(\omega_3z_{23}\bar{z}_{35}+\omega_4z_{24}\bar{z}_{45}\right)}\right],\end{aligned} \tag{3.39}$$

and map it via (3.1). Taking the simultaneous double soft limit of particles 3 and 4, as prescribed in (3.36), we find

$$\lim_{\epsilon\to 0}\tilde{\mathcal{A}}_{+++---}(\lambda_3\epsilon,\lambda_4\epsilon) = \frac{1}{2(i\lambda_3+i\lambda_4)\epsilon^2}\frac{1}{z_{23}\bar{z}_{45}}\left(\frac{1}{i\lambda_3}\frac{\bar{z}_{25}z_{41}}{z_{34}\bar{z}_{42}}+\frac{1}{i\lambda_4}\frac{z_{52}\bar{z}_{53}}{\bar{z}_{34}z_{53}}\right)\tilde{\mathcal{A}}_{++--}\,, \tag{3.40}$$

where the four-point correlator is given by mapping the appropriate MHV amplitude via (3.1)

$$\tilde{\mathcal{A}}_{++--} = 4i\delta(\lambda_1+\lambda_2+\lambda_5+\lambda_6)\frac{z_{56}^3\,\delta(i\bar{z}'-iz')}{z_{12}z_{25}^2z_{16}^2\bar{z}_{25}\bar{z}_{61}}\left(\frac{z_{15}\bar{z}_{61}}{z_{25}\bar{z}_{26}}\right)^{i\lambda_2-1}\left(\frac{z_{12}\bar{z}_{16}}{z_{25}\bar{z}_{56}}\right)^{i\lambda_5+1}\left(\frac{z_{15}\bar{z}_{12}}{z_{56}\bar{z}_{26}}\right)^{i\lambda_6+1}, \tag{3.41}$$

where $z'=\frac{z_{12}z_{56}}{z_{25}z_{61}}$ and $\bar{z}'=\frac{\bar{z}_{12}\bar{z}_{56}}{\bar{z}_{25}\bar{z}_{61}}$. The conformal soft factor found in (3.40) matches our general result by taking the double soft factor [56, 57]

$$\frac{1}{\langle 2|3+4|5]}\left(\frac{[35]^3\langle 25\rangle}{[34][45]s_{345}}+\frac{\langle 24\rangle^3[25]}{\langle 23\rangle\langle 34\rangle s_{234}}\right), \tag{3.42}$$

and mapping it via (3.37).

It is straightforward to generalize (3.36) to m particles taken simultaneously soft, by introducing m-dimensional spherical coordinates as in (3.34) and scale m λ's by ϵ.

3.4 Conformal Partial Wave Decomposition

In the CFT four-point function defined as (3.5), we can expand the conformally invariant part $\tilde{A}_4(z,\bar{z})$ on the basis of conformal partial waves $\Psi^{h,\bar{h}}_{h_i,\bar{h}_i}(z,\bar{z})$. As can be shown along the lines of [58, 60, 59], the expansion takes the following form

$$\tilde{A}_4(z,\bar{z}) = i\sum_{J=0}^{\infty}{}' \int_{\mathcal{C}} d\Delta\, \Psi^{h,\bar{h}}_{h_i,\bar{h}_i}(z,\bar{z}) \frac{(1-2h)(2\bar{h}-1)}{(2\pi)^2} \langle \tilde{A}_4(z,\bar{z}), \Psi^{h,\bar{h}}_{h_i,\bar{h}_i}(z,\bar{z}) \rangle\,, \tag{3.43}$$

where $h-\bar{h}=J$, $h+\bar{h}=\Delta=1+i\lambda$. The contour $\mathcal{C}$ runs from $1-i\infty$ to $1+i\infty$. The integration and summation is over all dimensions and spins of exchanged primary operators in the theory. $\sum'$ means that the $J=0$ summand contributes with a weight of $1/2$. The inner product is defined by

$$\langle G(z,\bar{z}), F(z,\bar{z}) \rangle \equiv \int \frac{dz d\bar{z}}{(z\bar{z})^2} G(z,\bar{z}) \overline{F(z,\bar{z})}\,. \tag{3.44}$$

The conformal partial waves $\Psi^{h,\bar{h}}_{h_i,\bar{h}_i}(z,\bar{z})$ have been computed in [61, 62, 63] and are given by

$$\Psi^{h,\bar{h}}_{h_i,\bar{h}_i}(z,\bar{z}) = c_1' F_+(z,\bar{z}) + c_2' F_-(z,\bar{z})\,, \tag{3.45}$$

with

$$\begin{aligned}
F_+(z,\bar{z}) =& \frac{1}{z^{h_{34}}\bar{z}^{\bar{h}_{34}}}\, {}_2F_1\left(\begin{matrix}1-h+h_{34}, h+h_{34}\\ 1+h_{12}+h_{34}\end{matrix}; \frac{1}{z}\right) {}_2F_1\left(\begin{matrix}1-\bar{h}+\bar{h}_{34}, \bar{h}+\bar{h}_{34}\\ 1+\bar{h}_{12}+\bar{h}_{34}\end{matrix}; \frac{1}{\bar{z}}\right), \\
F_-(z,\bar{z}) =& z^{h_{12}}\bar{z}^{\bar{h}_{12}}\, {}_2F_1\left(\begin{matrix}1-h-h_{12}, h-h_{12}\\ 1-h_{12}-h_{34}\end{matrix}; \frac{1}{z}\right) {}_2F_1\left(\begin{matrix}1-\bar{h}-\bar{h}_{12}, \bar{h}-\bar{h}_{12}\\ 1-\bar{h}_{12}-\bar{h}_{34}\end{matrix}; \frac{1}{\bar{z}}\right), \\
c_1' =& (-1)^{h-\bar{h}+h_{12}-\bar{h}_{12}} \frac{\Gamma(-h_{12}-h_{34})}{\Gamma\left(1+\bar{h}_{12}+\bar{h}_{34}\right)} \frac{\Gamma(1-h+h_{12})\Gamma(h+h_{34})\Gamma\left(\bar{h}+\bar{h}_{12}\right)\Gamma\left(1-\bar{h}+\bar{h}_{34}\right)}{\Gamma(1-h-h_{12})\Gamma(h-h_{34})\Gamma\left(\bar{h}-\bar{h}_{12}\right)\Gamma\left(1-\bar{h}-\bar{h}_{34}\right)}, \\
c_2' =& (-1)^{h-\bar{h}+h_{34}-\bar{h}_{34}} \frac{\Gamma(h_{12}+h_{34})}{\Gamma\left(1-\bar{h}_{12}-\bar{h}_{34}\right)}\,.
\end{aligned} \tag{3.46}$$

Here we made use of hypergeometric identities discussed in [62] to rewrite the result in a form which is suited for the region $z, \bar{z} > 1$.

Conformal partial waves are orthogonal with respect to the inner product (3.44)

$$\langle \Psi^{h,\bar{h}}_{h_i,\bar{h}_i}(z,\bar{z}), \Psi^{h',\bar{h}'}_{h_i,\bar{h}_i}(z,\bar{z}) \rangle = \frac{(2\pi)^2}{(1-2h)(2\bar{h}-1)} \delta_{J,J'} \delta(\lambda - \lambda') \,. \tag{3.47}$$

The basis functions (3.45) span a complete basis for bosonic fields on each of the ranges

$$(J \in \mathbb{Z} \;,\; \lambda \in \mathbb{R}^+ \mid J \in \mathbb{Z}^+ \;,\; \lambda \in \mathbb{R} \mid J \in \mathbb{Z} \;,\; \lambda \in \mathbb{R}^- \mid J \in \mathbb{Z}^- \;,\; \lambda \in \mathbb{R}) \,. \tag{3.48}$$

We can perform the Δ integration in (3.43) by collecting residues of poles located to the left or to the right of the complex axis. One can use e.g. the integral representation of the conformal partial wave (3.45) (given by eq. (7) in [63]) to make sure that the half-circle integration at infinity vanishes.

3.5 Inner Product Integral

In this appendix we evaluate the inner product

$$\langle \tilde{A}_4(z,\bar{z}), \Psi^{h,\bar{h}}_{h_i,\bar{h}_i}(z,\bar{z}) \rangle \equiv \int \frac{dz d\bar{z}}{(z\bar{z})^2} \delta(i\bar{z} - iz) \, |z|^{2+\sigma} \, |z-1|^{h_{12}-h_{34}-\sigma} \, \overline{\Psi^{h,\bar{h}}_{h_i,\bar{h}_i}(z,\bar{z})} \,, \tag{3.49}$$

for $\sigma = 0$ and $\sigma = 1$, where $\Psi^{h,\bar{h}}_{h_i,\bar{h}_i}(z,\bar{z})$ is given by (3.45)[5].

[5] Note that in both of our examples we have $\bar{h}_{ij} = h_{ij}$, and the complex conjugation prescription $h \to 1-\bar{h}$, $\bar{h} \to 1-h$, $h_{ij} \to -h_{ij}$ and $z \leftrightarrow \bar{z}$

First we change integration variables to $z = x + iy$, $\bar{z} = x - iy$ and localize the delta function on $y = 0$. Subsequently, we write the hypergeometric functions from (3.45) in the following Mellin-Barnes representation:

$$ {}_2F_1(a,b;c;z) = \frac{\Gamma(c)}{\Gamma(a)\Gamma(b)\Gamma(c-a)\Gamma(c-b)} \int_C \frac{ds}{2\pi i}(1-z)^s \Gamma(-s)\Gamma(c-a-b-s)\Gamma(a+s)\Gamma(b+s)\,, \tag{3.50} $$

where $(1-z) \in \mathbb{C}\backslash\mathbb{R}_-$ and the contour C goes from minus to plus complex infinity while separating pole sequences in $\Gamma(-s)\Gamma(c-a-b-s)$ from pole sequences in $\Gamma(a+s)\Gamma(b+s)$.

The $x > 1$ integral then gives a beta function which we express in terms of gamma functions. At this point, similarly to section 3.4 in [64], the gamma function arguments in the integrand arrange themselves exactly such that one of the Mellin-Barnes integrals (3.50) can be evaluated by second Barnes lemma.[6] The final inverse Mellin transform integral is then done by closing the integration contour to the left, or to the right of the complex axis. Performing the sum over all residues of poles wrapped by the contour in this process we obtain

$$ \begin{aligned} \langle \tilde{A}_4(z,\bar{z}), \Psi^{h,\bar{h}}_{h_i,\bar{h}_i}(z,\bar{z})\rangle \;=\; & \pi^2 (-1)^{h-\bar{h}} \csc\left(\pi\left(h_{12}-h_{34}\right)\right) \csc\left(\pi\left(h_{12}+h_{34}\right)\right) \Gamma(1-\sigma) \qquad (3.51) \\ & \left[\left(\frac{\Gamma\left(1-\sigma+h_{12}-h_{34}\right)\, {}_4F_3\left({1-\sigma, 1-\bar{h}+h_{12}, \bar{h}+h_{12}, 1-\sigma+h_{12}-h_{34} \atop 2-h-\sigma+h_{12}, h-\sigma+h_{12}+1, h_{12}-h_{34}+1} ; 1 \right)}{\Gamma\left(h_{12}-h_{34}+1\right)\Gamma\left(1-\bar{h}+h_{34}\right)\Gamma\left(\bar{h}+h_{34}\right)\Gamma\left(2-h-\sigma+h_{12}\right)\Gamma\left(h-\sigma+h_{12}+1\right)} - (h_{12} \leftrightarrow h_{34}) \right) \right. \\ & \left. + \frac{\left(\frac{\Gamma(1-\bar{h}-h_{12})\Gamma(\bar{h}-h_{12})\Gamma(1-\sigma-h_{12}+h_{34})}{\Gamma(1-h_{12}+h_{34})\Gamma(2-h-\sigma-h_{12})\Gamma(h-\sigma-h_{12}+1)}\, {}_4F_3\left({1-\sigma, 1-\bar{h}-h_{12}, \bar{h}-h_{12}, 1-\sigma-h_{12}+h_{34} \atop 2-h-\sigma-h_{12}, h-\sigma-h_{12}+1, 1-h_{12}+h_{34}} ; 1 \right) - (h_{12} \leftrightarrow h_{34}) \right)}{\Gamma\left(1-h+h_{12}\right)\Gamma\left(h+h_{12}\right)\Gamma\left(1-h+h_{34}\right)\Gamma\left(h+h_{34}\right)} \right], \end{aligned} $$

[6] We assume the integrals to be regulated appropriately such that these formal manipulations hold.

where we used identities such as $\sin(x+\pi\bar{h})\sin(y+\pi\bar{h}) = \sin(x+\pi h)\sin(y+\pi h)$ for integer J, and $\sin(\pi x) = \pi/(\Gamma(x)\Gamma(1-x))$ to write (3.51) in a shorter form.

Evaluation for $\sigma = 0$

When $\sigma = 0$, one upper and one lower parameter in the ${}_4F_3$ hypergeometric functions become equal and cancel, so that the functions reduce to ${}_3F_2$. Interestingly, an even greater simplification occurs as

$$ {}_3F_2\left(\begin{matrix} 1, a-c+1, a+c \\ a-b+2, a+b+1 \end{matrix}; 1\right) = \frac{\frac{\Gamma(a-b+2)\Gamma(a+b+1)}{\Gamma(a-c+1)\Gamma(a+c)} - (a-b+1)(a+b)}{(b-c)(b+c-1)} . \tag{3.52} $$

Then, making use of various sine- and gamma function identities as mentioned above, it turns out that the result is proportional to

$$ \frac{\sin(2\pi J)}{2\pi J} = \begin{cases} 1 \ ; J = 0 \\ 0 \ ; J \neq 0 \end{cases} . \tag{3.53} $$

Therefore, the only non-vanishing inner product in this case comes from the scalar conformal partial wave $\Psi^{\Delta}_{h_i} \equiv \Psi^{h,\bar{h}}_{h_i,\bar{h}_i}\Big|_{J=0}$, which simplifies to

$$ \langle \tilde{A}_4(z,\bar{z}), \Psi^{\Delta}_{h_i}(z,\bar{z})\rangle = \frac{\Gamma\left(1-\frac{\Delta}{2}-h_{12}\right)\Gamma\left(\frac{\Delta}{2}-h_{12}\right)\Gamma\left(1-\frac{\Delta}{2}-h_{34}\right)\Gamma\left(\frac{\Delta}{2}-h_{34}\right)}{\Gamma(2-\Delta)\Gamma(\Delta)} . \tag{3.54} $$

Evaluation for $\sigma = 1$

As we take $\sigma \to 1$ the overall factor $\Gamma(1-\sigma)$ diverges. However, the rest of the terms conspire to cancel this pole, so that the limit $\sigma \to 1$ is finite. The simplification of the result in all generality is quite tedious, here we instead discuss a less rigorous but quick way to arrive at the end result.

The cases for the first few values of $J = 0, 1, \ldots$ can be simplified directly e.g. in Mathematica. We recognize that the result is always proportional to $\csc(\pi(h_{12} - h_{34}))/(h_{12} - h_{34})$. To quickly arrive at the full result, start with (3.51) and divide out the overall factor $\csc(\pi(h_{12} - h_{34}))/(h_{12} - h_{34})$. By the previous observation we see that the rest is finite in $h_{12} - h_{34} \to 0$. Sending $h_{34} \to h_{12}$ under a small $1 - \sigma$ deformation, the hypergeometric functions become equal to 1 for $\sigma \to 1$ and the remaining terms simplify. To recover the full h_{12}, h_{34} dependence it then suffices to match these terms e.g. to the specific example in the case $J = 1$, which then for all $J \geq 0$ leads to

$$\langle \tilde{A}_4(z,\bar{z}), \Psi^{h,\bar{h}}_{h_i,\bar{h}_i}(z,\bar{z})\rangle = \frac{\pi \csc(\pi(h_{12} - h_{34}))}{(h_{34} - h_{12})} \left(\frac{\Gamma(h - h_{12})\Gamma(1 - h_{34} - \bar{h})}{\Gamma(h + h_{12})\Gamma(1 + h_{34} - \bar{h})} + (h_{12} \leftrightarrow h_{34}) \right). \tag{3.55}$$

To obtain the result for $J < 0$ substitute $h \leftrightarrow \bar{h}$.

Chapter 4

Yangian Invariants and Cluster Adjacency in $\mathcal{N} = 4$ Yang-Mills

This chapter is based on the publication [65].

In recent years cluster algebras have shed interesting light on the mathematical properties of scattering amplitudes in planar $\mathcal{N} = 4$ supersymmetric Yang-Mills (SYM) theory [5]. Cluster algebraic structure manifests itself in several distinct ways, notably including the appearance of certain $\mathrm{Gr}(4, n)$ cluster coordinates in the symbol alphabets [5, 66, 67, 68], cobrackets [5, 69, 70, 71, 72], and integrands [30] of n-particle amplitudes.

There has been a recent revival of interest in the cluster structure of SYM amplitudes following the observation [73] that certain amplitudes exhibit a property called *cluster adjacency*. Cluster coordinates are grouped into sets called clusters, with two coordinates being called adjacent if there exists a cluster containing both. The central problem of the "cluster adjacency" literature is to identify (and, hopefully, to explain!) correlations between sets of pairs (or larger groupings) of cluster coordinates, and the manner in which those pairs are observed to appear together in various amplitudes.

For example, for loop amplitudes, all evidence available to date [81, 22, 131, 75, 76, 77, 78, 80, 79, 82, 89, 83] supports the hypothesis that two cluster coordinates appear in adjacent symbol entries only if they are cluster adjacent. In [89] it was shown that this type of cluster adjacency implies the Steinmann relations [84, 85, 86]. For tree amplitudes a somewhat analogous version of cluster adjacency was proposed in [81], where it was checked in several cases, and conjectured in general, that every Yangian invariant in the BCFW expansion of tree-level amplitudes in SYM theory has poles given by cluster coordinates that are all contained in a common cluster.

In this paper we provide further evidence for this and the even stronger conjecture that cluster adjacency holds for every rational Yangian invariant in SYM theory, even those that do not appear in any representation of tree amplitudes.

In Sec. 2 we review the main tool of our analysis, the Sklyanin Poisson bracket [87, 88] which can be used to diagnose whether two cluster coordinates on $\mathrm{Gr}(4,n)$ are adjacent, which we will call the *bracket test* [89]. In Sec. 3 we review the Yangian invariants of SYM theory and explain how (in principle) to use the bracket test to provide evidence that N^kMHV Yangian invariants satisfy cluster adjacency. We carry out this check for all $k \leq 2$ invariants and many $k = 3$ invariants.

Before proceeding we make a few comments clarifying the ways in which our tests are weaker than the analysis of [81], and the ways in which they are stronger:

1. It could have happened that only certain repreresentations of tree-level amplitudes (depending, perhaps, on the choice of shifts during intermediate steps of BCFW recursion) satisfy cluster adjacency, but as already noted, our results suggest that every

rational Yangian invariant satisfies cluster adjacency. If true, this suggests that the connection between cluster adjacency and Yangian invariants admits a mathematical explanation independent of the physics of scattering amplitudes.

2. For any fixed k there are finitely many functionally independent N^kMHV Yangian invariants. If it is known that these all satisfy cluster adjacency, it immediately follows that the n-particle N^kMHV amplitude satisfies cluster adjacency for all n. Our results therefore extend the analysis of [81] in both k and n.

3. However, unlike in [81], we make no attempt to check whether each of the polynomial factors we encounter is actually a $\mathrm{Gr}(4,n)$ cluster coordinate. Indeed for $n > 7$ there is no known algorithm for determining, in finite time, whether or not a given homogeneous polynomial in Plücker coordinates is a cluster coordinate. The bracket does not help here; it is trivial to write down pairs of polynomials that pass the bracket test but are not cluster coordinates.

4. In the examples checked in [81] it was noted that each term in a BCFW expansion of an amplitude had the property that there exists a cluster of $\mathrm{Gr}(4,n)$ that simultaneously contains all of the cluster coordinates appearing in the denominator of that term. Our test is much weaker in that it can only establish pairwise cluster adjacency. For example, if we encounter a term with three polynomial factors p_1, p_2 and p_3, our test provides evidence that there is some cluster containing p_1 and p_2, and also some cluster containing p_2 and p_3, and also some cluster containing p_1 and p_3, but the bracket cannot provide any evidence for or against the existence of a cluster simultaneously containing all three.

4.1 Cluster Coordinates and the Sklyanin Poisson Bracket

The objects of study in this paper will be certain rational functions on the kinematic space of n cyclically ordered massless particles, of the type that appear in tree-level gluon scattering amplitudes. A point in this kinematic space is conveniently parameterized by a collection of n *momentum twistors* [4] $Z_1^I, \ldots, Z_n^I$, each of which can be regarded as a four-component ($I \in \{1, \ldots, 4\}$) homogeneous coordinate on $\mathbb{P}^3$.

In these variables dual conformal symmetry [3] is realized by $SL(4, \mathbb{C})$ transformations. For a given collection of n momentum twistors, the $\binom{n}{4}$ *Plücker coordinates* are the $SL(4, \mathbb{C})$-invariant quantities

$$\langle i\, j\, k\, l \rangle \equiv \epsilon_{IJKL} Z_i^I Z_j^J Z_k^K Z_l^L \,. \tag{4.1}$$

The $\mathrm{Gr}(4, n)$ Grassmannian cluster algebra, whose structure has been found to underlie at least certain amplitudes in SYM theory, is a commutative algebra with generators called *cluster coordinates*. Every cluster coordinate is a polynomial in Plückers that is homogeneous under a projective rescaling of each momentum twistor separately, for example

$$\langle 1\,2\,6\,7 \rangle \langle 2\,3\,4\,5 \rangle - \langle 1\,2\,4\,5 \rangle \langle 2\,3\,6\,7 \rangle \,. \tag{4.2}$$

Every Plücker coordinate is, on its own, a cluster coordinate. For $n < 8$ the number of cluster coordinates is finite and they can easily be enumerated, but for $n > 7$ the number of cluster coordinates is infinite.

The cluster coordinates of $\mathrm{Gr}(4, n)$ are grouped into non-disjoint sets of cardinality $4n-15$

called *clusters*. Two cluster coordinates are said to be *cluster adjacent* if there exists a cluster containing both. The n Plücker coordinates $\langle 1\,2\,3\,4\rangle$, $\langle 2\,3\,4\,5\rangle$, $\cdots$, $\langle n\,1\,2\,3\rangle$ containing four cyclically adjacent momentum twistors play a special role; these are called *frozen* coordinates and are elements of every cluster. Therefore, each frozen coordinate is adjacent to every cluster coordinate.

Two Plücker coordinates are cluster adjacent if and only if they satisfy the so-called *weak separation criterion* [90]. In order to address the central problem posed in the Introduction, it is desirable to have an efficient algorithm for testing whether two more general cluster coordinates are cluster adjacent. As proposed in [89], the Sklyanin Poisson bracket [87, 88] $\{\,,\}$ can serve because of the expectation (not yet completely proven, as far as we are aware) that two cluster coordinates a_1, a_2 are adjacent if and only if $\{\log a_1, \log a_2\} \in \frac{1}{2}\mathbb{Z}$.

In the next section we use the Sklyanin Poisson bracket to test the cluster adjacency properties of Yangian invariants. To that end let us briefly review, following [89] (see also [91]) how it can be computed. First, any generic $4 \times n$ momentum twistor matrix Z_i^I can be brought into the gauge-fixed form

$$Z_i^I = \begin{pmatrix} 1 & 0 & 0 & 0 & {y^1}_5 & \cdots & {y^1}_n \\ 0 & 1 & 0 & 0 & {y^2}_5 & \cdots & {y^2}_n \\ 0 & 0 & 1 & 0 & {y^3}_5 & \cdots & {y^3}_n \\ 0 & 0 & 0 & 1 & {y^4}_5 & \cdots & {y^4}_n \end{pmatrix} \tag{4.3}$$

by a suitable $GL(4,\mathbb{C})$ transformation. The Sklyanin Poisson bracket of the y's is defined as

$$\{y^I{}_a, y^J{}_b\} = \frac{1}{2}(\text{sign}(J-I) - \text{sign}(b-a))y^J{}_a y^I{}_b\,. \tag{4.4}$$

Finally, the Sklyanin Poisson bracket of two arbitrary functions f, g of momentum twistors can be computed by plugging in the parameterization (4.3) and then using the chain rule

$$\{f(y), g(y)\} = \sum_{a,b=1}^{n}\sum_{I,J=1}^{4}\frac{\partial f}{\partial y^I{}_a}\frac{\partial g}{\partial y^J{}_b}\{y^I{}_a, y^J{}_b\}\,. \tag{4.5}$$

4.2 An Adjacency Test for Yangian Invariants

The conformal [92] and dual conformal symmetry of scattering amplitudes in SYM theory combine to generate a Yangian [11] symmetry. *Yangian invariants* [3, 93, 94, 96, 95, 28, 98, 30, 97] are the basic building blocks in terms of which amplitudes can be constructed. We say that a Yangian invariant is *rational* if it is a rational function of momentum twistors; equivalently, it has intersection number $\Gamma = 1$ in the terminology of [30, 99]. Any n-particle tree-level amplitude in SYM theory can be written as the n-particle Parke-Taylor-Nair superamplitude [2, 100] times a linear combination of rational Yangian invariants (see for example [101]). In general the linear combination is not unique since Yangian invariants satisfy numerous linear relations.

Yangian invariants are actually superfunctions: an n-particle invariant is a polynomial of uniform degree $4k$ in $4kn$ Grassmann variables χ_i^A, where k is the N^{k}MHV degree. For a rational Yangian invariant Y, the coefficient of each distinct term in its expansion in χ's can be uniquely factored into a ratio of products of polynomials in Plücker coordinates, with each polynomial having uniform weight in each momentum twistor separately. Let $\{p_i\}$ denote the union of all such polynomials that appear in the denominator of the expansion of Y. Then we say that Y *passes the bracket test* if

$$\Omega_{ij} \equiv \{\log p_i, \log p_j\} \in \frac{1}{2}\mathbb{Z} \quad \forall i, j\,. \tag{4.6}$$

As explained in [30], n-particle Yangian invariants can be classified in terms of permutations on n elements. Since the bracket test is invariant[1] under the $\mathbb{Z}_n$ cyclic group that shifts the momentum twistors $Z_i \to Z_{i+1\,\mathrm{mod}\,n}$, we only need to consider one member from each cyclic equivalence class. The number of cyclic classes of rational N^{k}MHV Yangian invariants with nontrivial dependence on n momentum twistors was tabulated for various k and n in Table 3 of [30]. We record these numbers here, correcting typos in the $(3, 15)$ and $(4, 20)$ entries:

$k \backslash n$	5	6	7	8	9	10	11	12	13	14	15	16	17	18	19	20	**Total**
1	1	0	0	0	0	0	0	0	0	0	0	0	0	0	0	0	**1**
2	0	1	2	5	4	1	0	0	0	0	0	0	0	0	0	0	**13**
3	0	0	1	6	54	177	298	274	134	30	3	0	0	0	0	0	**977**
4	0	0	0	1	13	263	1988	7862	18532	28204	28377	18925	8034	2047	270	17	**114533**

When they appear in scattering amplitudes, Yangian invariants typically have trivial dependence on several of the particles. For example the five-particle NMHV Yangian invariant $Y^{(1)}(Z_1, Z_2, Z_3, Z_4, Z_5)$ could appear in a nine-particle NMHV amplitude as $Y^{(1)}(Z_2, Z_4, Z_5, Z_7, Z_8)$, among other possibilities. Fortunately, because of the simple

[1] Certainly the *value* of the Sklyanin Poisson bracket is not in general cyclic invariant, since evaluating it requires making a gauge choice which breaks cyclic symmetry, such as in (4.3), but the binary statement of whether some pair does or does not have half-integer valued bracket is cyclic invariant.

$\text{sign}(b-a)$ dependence on column number in the definition (4.4), the bracket test is insensitive to trivial dependence on additional momentum twistors[2].

Therefore for any fixed k, but arbitrary n, we can provide evidence for the cluster adjacency of every rational n-particle N^{k}MHV Yangian invariant by applying the bracket test described above (4.6) to each one of the (finitely many) rational Yangian invariants. In the next few subsections we present the results of our analysis, beginning with the trivial but illustrative case of $k = 1$.

4.2.1 NMHV

The unique $k = 1$ Yangian invariant is the well-known *five-bracket* [93] (originally presented as an "R-invariant" in [3])

$$Y^{(1)} = [1,2,3,4,5] \equiv \frac{\delta^{(4)}(\langle 1\,2\,3\,4\rangle \chi_5^A + \text{cyclic})}{\langle 1\,2\,3\,4\rangle\langle 2\,3\,4\,5\rangle\langle 3\,4\,5\,1\rangle\langle 4\,5\,1\,2\rangle\langle 5\,1\,2\,3\rangle} \tag{4.7}$$

whose denominator contains the five factors

$$\{p_1, \ldots, p_5\} = \{\langle 1\,2\,3\,4\rangle, \langle 2\,3\,4\,5\rangle, \langle 3\,4\,5\,1\rangle, \langle 4\,5\,1\,2\rangle, \langle 5\,1\,2\,3\rangle\}\,, \tag{4.8}$$

each of which is simply a Plücker coordinate. Evaluating these in the gauge (4.3) gives

$$\{p_1, \ldots, p_5\} = \{1, -y^1{}_5, -y^2{}_5, -y^3{}_5, -y^4{}_5\} \tag{4.9}$$

[2] As in footnote 1, the actual value of the Sklyanin Poisson bracket will in general change if the particle relabeling affects any of the first four gauge-fixed columns of Z.

and evaluating the bracket (4.6) in this basis using (4.4) gives

$$\Omega_{ij}^{(1)} = \{\log p_i, \log p_j\} = \begin{pmatrix} 0 & 0 & 0 & 0 & 0 \\ 0 & 0 & \frac{1}{2} & \frac{1}{2} & \frac{1}{2} \\ 0 & -\frac{1}{2} & 0 & \frac{1}{2} & \frac{1}{2} \\ 0 & -\frac{1}{2} & -\frac{1}{2} & 0 & \frac{1}{2} \\ 0 & -\frac{1}{2} & -\frac{1}{2} & -\frac{1}{2} & 0 \end{pmatrix}. \tag{4.10}$$

Since each entry is half-integer, the five-bracket (4.7) passes the bracket test.

We wrote out the steps in detail in order to illustrate the general procedure, although in this trivial case the conclusion was foregone: for $n = 5$ each Plücker coordinate in (4.7) is frozen, so each is automatically cluster adjacent to each of the others. It is however interesting to note that if we uplift (4.7) by introducing trivial dependence on additional particles, this simple argument no longer applies. For example, $[1,3,5,7,9]$ still passes the bracket test even though it does not involve any frozen coordinates. The fact that the five-bracket $[i,j,k,l,m]$ passes the bracket test for any choice of indices can be understood in terms of the *weak separation* criterion [90] for determining when two Plücker coordinates are cluster adjacent. The connection between the weak separation criterion and all Yangian invariants with $n = 5k$ will be explored in [102].

4.2.2 N^{2}MHV

The 13 rational Yangian invariants with $k=2$ are listed in Table 1 of [30] (we disregard the ninth entry in the table, which is algebraic but not rational[3]). They are given by

$$
\begin{aligned}
Y_1^{(2)} &= [1,2,(23)\cap(456),(234)\cap(56),6][2,3,4,5,6] \\
Y_2^{(2)} &= [1,2,(34)\cap(567),(345)\cap(67),7][3,4,5,6,7] \\
Y_3^{(2)} &= [1,2,3,(345)\cap(67),7][3,4,5,6,7] \\
Y_4^{(2)} &= [1,2,3,(456)\cap(78),8][4,5,6,7,8] \\
Y_5^{(2)} &= [1,2,3,4,8][4,5,6,7,8] \\
Y_6^{(2)} &= [1,2,3,(45)\cap(678),8][4,5,6,7,8] \\
Y_7^{(2)} &= [1,2,3,(45)\cap(678),(456)\cap(78)][4,5,6,7,8] \\
Y_8^{(2)} &= [1,2,3,4,(456)\cap(78)][4,5,6,7,8] \\
Y_9^{(2)} &= [1,2,3,4,9][5,6,7,8,9] \\
Y_{10}^{(2)} &= [1,2,3,4,(567)\cap(89)][5,6,7,8,9] \\
Y_{11}^{(2)} &= [1,2,3,4,(56)\cap(789)][5,6,7,8,9] \\
Y_{12}^{(2)} &= \varphi\times[1,2,3,(45)\cap(789),(46)\cap(789)][(45)\cap(123),(46)\cap(123),7,8,9] \\
Y_{13}^{(2)} &= [1,2,3,4,5][6,7,8,9,10]
\end{aligned}
\tag{4.11}
$$

[3] As mentioned in [81], it would be very interesting if some suitably generalized version of cluster adjacency could be found which applies to algebraic functions of momentum twistors.

where

$$(ij) \cap (klm) = Z_i \langle j\, k\, l\, m\rangle - Z_j \langle i\, k\, l\, m\rangle \tag{4.12}$$

denotes the point of intersection between the line (ij) and the plane (klm) in momentum twistor space. The Yangian invariant $Y_{12}^{(2)}$ has the prefactor

$$\varphi = \frac{\langle 4\,5\,(123) \cap (789)\rangle \langle 4\,6\,(123) \cap (789)\rangle}{\langle 1\,2\,3\,4\rangle \langle 4\,7\,8\,9\rangle \langle 5\,6\,(123) \cap (789)\rangle}\,, \tag{4.13}$$

where

$$(ijk) \cap (lmn) = (ij)\langle k\, l\, m\, n\rangle + (jk)\langle i\, l\, m\, n\rangle + (ki)\langle j\, l\, m\, n\rangle \tag{4.14}$$

denotes the line of intersection between the planes (ijk) and (lmn).

Following the same procedure outlined in the previous subsection, for each Yangian invariant $Y_a^{(2)}$ listed in (4.11) we enumerate all polynomial factors its denominator contains, and then compute the associated bracket matrix $\Omega_a^{(2)}$. Explicit results for these matrices are given in appendix 4.3. We find that each matrix is half-integer valued, and therefore conclude that all rational $k = 2$ Yangian invariants satisfy the bracket test.

4.2.3 N^{3}MHV and Higher

For $k > 2$ it is too cumbersome, and not particularly enlightening, to write explicit formulas for each of the 977 rational Yangian invariants. We can use [99] to compute a symbolic formula for each Yangian invariant Y in terms of the parameterization (4.3). Then we read off the list of all polynomials in the $y^I{}_a$'s that appear in the denominator of Y and compute the bracket matrix (4.6). We have carried out this test for all 238 rational N^3MHV invariants with $n \leq 10$ (and many invariants with $n > 10$), and find that each one passes the bracket test. Although it is straightforward in principle to continue checking higher n (and k) invariants, it becomes computationally prohibitive.

4.3 Explicit Matrices for $k = 2$

Using the notation given in (4.11), we present here for each rational N^2MHV Yangian invariant the bracket matrix of its polynomial factors:

$$\Omega_1^{(2)} = \begin{pmatrix} 0 & 0 & 1 & 1 & 0 & 0 & 0 & \frac{1}{2} & -\frac{1}{2} & -1 \\ 0 & 0 & 0 & 0 & -\frac{1}{2} & 0 & -\frac{1}{2} & \frac{1}{2} & -\frac{1}{2} & -1 \\ -1 & 0 & 0 & -1 & -\frac{3}{2} & 0 & -\frac{1}{2} & -\frac{1}{2} & -\frac{1}{2} & -1 \\ -1 & 0 & 1 & 0 & -\frac{3}{2} & 0 & -\frac{1}{2} & 0 & -1 & -1 \\ 0 & \frac{1}{2} & \frac{3}{2} & \frac{3}{2} & 0 & \frac{1}{2} & 0 & \frac{1}{2} & -\frac{1}{2} & -1 \\ 0 & 0 & 0 & 0 & -\frac{1}{2} & 0 & -\frac{1}{2} & 0 & 0 & 0 \\ 0 & \frac{1}{2} & \frac{1}{2} & \frac{1}{2} & 0 & \frac{1}{2} & 0 & 0 & 0 & 0 \\ -\frac{1}{2} & -\frac{1}{2} & \frac{1}{2} & 0 & -\frac{1}{2} & 0 & 0 & 0 & -\frac{1}{2} & -\frac{1}{2} \\ \frac{1}{2} & \frac{1}{2} & \frac{1}{2} & 1 & \frac{1}{2} & 0 & 0 & \frac{1}{2} & 0 & -\frac{1}{2} \\ 1 & 1 & 1 & 1 & 1 & 0 & 0 & \frac{1}{2} & \frac{1}{2} & 0 \end{pmatrix}$$

$$\Omega_2^{(2)} = \begin{pmatrix} 0 & 0 & 1 & 0 & 0 & 0 & 0 & -1 & -\frac{1}{2} & -\frac{1}{2} \\ 0 & 0 & 0 & -\frac{1}{2} & -\frac{1}{2} & 0 & -\frac{1}{2} & -\frac{1}{2} & -\frac{1}{2} & -\frac{1}{2} \\ -1 & 0 & 0 & -\frac{3}{2} & -\frac{3}{2} & 0 & -\frac{1}{2} & -\frac{3}{2} & -\frac{1}{2} & -\frac{1}{2} \\ 0 & \frac{1}{2} & \frac{3}{2} & 0 & -\frac{1}{2} & \frac{1}{2} & 0 & -1 & -\frac{1}{2} & -\frac{1}{2} \\ 0 & \frac{1}{2} & \frac{3}{2} & \frac{1}{2} & 0 & \frac{1}{2} & 0 & -1 & -\frac{1}{2} & -\frac{1}{2} \\ 0 & 0 & 0 & -\frac{1}{2} & -\frac{1}{2} & 0 & -\frac{1}{2} & -\frac{1}{2} & 0 & 0 \\ 0 & \frac{1}{2} & \frac{1}{2} & 0 & 0 & \frac{1}{2} & 0 & -\frac{1}{2} & 0 & 0 \\ 1 & \frac{1}{2} & \frac{3}{2} & 1 & 1 & \frac{1}{2} & \frac{1}{2} & 0 & 0 & 0 \\ \frac{1}{2} & \frac{1}{2} & \frac{1}{2} & \frac{1}{2} & \frac{1}{2} & 0 & 0 & 0 & 0 & -\frac{1}{2} \\ \frac{1}{2} & \frac{1}{2} & \frac{1}{2} & \frac{1}{2} & \frac{1}{2} & 0 & 0 & 0 & \frac{1}{2} & 0 \end{pmatrix}$$

$$\Omega_3^{(2)} = \begin{pmatrix} 0 & 0 & \frac{1}{2} & 0 & 0 & 0 & 0 & -1 & 0 & -\frac{1}{2} \\ 0 & 0 & -\frac{1}{2} & -\frac{1}{2} & -\frac{1}{2} & 0 & -\frac{1}{2} & -\frac{1}{2} & 0 & -\frac{1}{2} \\ -\frac{1}{2} & \frac{1}{2} & 0 & -1 & -1 & 0 & -\frac{1}{2} & -\frac{3}{2} & -\frac{1}{2} & -\frac{1}{2} \\ 0 & \frac{1}{2} & 1 & 0 & -\frac{1}{2} & \frac{1}{2} & 0 & -1 & 0 & -\frac{1}{2} \\ 0 & \frac{1}{2} & 1 & \frac{1}{2} & 0 & \frac{1}{2} & 0 & -1 & 0 & -\frac{1}{2} \\ 0 & 0 & 0 & -\frac{1}{2} & -\frac{1}{2} & 0 & -\frac{1}{2} & -\frac{1}{2} & 0 & 0 \\ 0 & \frac{1}{2} & \frac{1}{2} & 0 & 0 & \frac{1}{2} & 0 & -\frac{1}{2} & 0 & 0 \\ 1 & \frac{1}{2} & \frac{3}{2} & 1 & 1 & \frac{1}{2} & \frac{1}{2} & 0 & 0 & 0 \\ 0 & 0 & \frac{1}{2} & 0 & 0 & 0 & 0 & 0 & 0 & -\frac{1}{2} \\ \frac{1}{2} & \frac{1}{2} & \frac{1}{2} & \frac{1}{2} & \frac{1}{2} & 0 & 0 & 0 & \frac{1}{2} & 0 \end{pmatrix}$$

$$\Omega_4^{(2)} = \begin{pmatrix} 0 & 0 & 0 & 0 & 0 & 0 & 0 & -1 & -1 & 0 \\ 0 & 0 & -\frac{1}{2} & -\frac{1}{2} & -\frac{1}{2} & 0 & -\frac{1}{2} & -\frac{1}{2} & -\frac{1}{2} & 0 \\ 0 & \frac{1}{2} & 0 & -\frac{1}{2} & -\frac{1}{2} & \frac{1}{2} & 0 & -1 & -1 & 0 \\ 0 & \frac{1}{2} & \frac{1}{2} & 0 & -\frac{1}{2} & \frac{1}{2} & 0 & -1 & -1 & 0 \\ 0 & \frac{1}{2} & \frac{1}{2} & \frac{1}{2} & 0 & \frac{1}{2} & 0 & -1 & -1 & 0 \\ 0 & 0 & -\frac{1}{2} & -\frac{1}{2} & -\frac{1}{2} & 0 & -\frac{1}{2} & -\frac{1}{2} & -\frac{1}{2} & 0 \\ 0 & \frac{1}{2} & 0 & 0 & 0 & \frac{1}{2} & 0 & -\frac{1}{2} & -\frac{1}{2} & 0 \\ 1 & \frac{1}{2} & 1 & 1 & 1 & \frac{1}{2} & \frac{1}{2} & 0 & -\frac{1}{2} & 0 \\ 1 & \frac{1}{2} & 1 & 1 & 1 & \frac{1}{2} & \frac{1}{2} & \frac{1}{2} & 0 & 0 \\ 0 & 0 & 0 & 0 & 0 & 0 & 0 & 0 & 0 & 0 \end{pmatrix}$$

$$\Omega_5^{(2)} = \begin{pmatrix} 0 & 0 & 0 & 0 & 0 & 0 & 0 & 0 & 0 & 0 \\ 0 & 0 & -\frac{1}{2} & -\frac{1}{2} & -\frac{1}{2} & 0 & -\frac{1}{2} & -\frac{1}{2} & -\frac{1}{2} & 0 \\ 0 & \frac{1}{2} & 0 & -\frac{1}{2} & -\frac{1}{2} & \frac{1}{2} & 0 & 0 & 0 & 0 \\ 0 & \frac{1}{2} & \frac{1}{2} & 0 & -\frac{1}{2} & \frac{1}{2} & 0 & 0 & 0 & 0 \\ 0 & \frac{1}{2} & \frac{1}{2} & \frac{1}{2} & 0 & \frac{1}{2} & 0 & 0 & 0 & 0 \\ 0 & 0 & -\frac{1}{2} & -\frac{1}{2} & -\frac{1}{2} & 0 & -\frac{1}{2} & -\frac{1}{2} & -\frac{1}{2} & 0 \\ 0 & \frac{1}{2} & 0 & 0 & 0 & \frac{1}{2} & 0 & -\frac{1}{2} & -\frac{1}{2} & 0 \\ 0 & \frac{1}{2} & 0 & 0 & 0 & \frac{1}{2} & \frac{1}{2} & 0 & -\frac{1}{2} & 0 \\ 0 & \frac{1}{2} & 0 & 0 & 0 & \frac{1}{2} & \frac{1}{2} & \frac{1}{2} & 0 & 0 \\ 0 & 0 & 0 & 0 & 0 & 0 & 0 & 0 & 0 & 0 \end{pmatrix} \quad \Omega_6^{(2)} = \begin{pmatrix} 0 & 0 & 0 & 0 & 0 & 0 & 0 & 0 & -1 & 0 \\ 0 & 0 & -\frac{1}{2} & -\frac{1}{2} & -\frac{1}{2} & 0 & -\frac{1}{2} & -\frac{1}{2} & -\frac{1}{2} & 0 \\ 0 & \frac{1}{2} & 0 & -\frac{1}{2} & -\frac{1}{2} & \frac{1}{2} & 0 & 0 & -1 & 0 \\ 0 & \frac{1}{2} & \frac{1}{2} & 0 & -\frac{1}{2} & \frac{1}{2} & 0 & 0 & -1 & 0 \\ 0 & \frac{1}{2} & \frac{1}{2} & \frac{1}{2} & 0 & \frac{1}{2} & 0 & 0 & -1 & 0 \\ 0 & 0 & -\frac{1}{2} & -\frac{1}{2} & -\frac{1}{2} & 0 & -\frac{1}{2} & -\frac{1}{2} & -\frac{1}{2} & 0 \\ 0 & \frac{1}{2} & 0 & 0 & 0 & \frac{1}{2} & 0 & -\frac{1}{2} & -\frac{1}{2} & 0 \\ 0 & \frac{1}{2} & 0 & 0 & 0 & \frac{1}{2} & \frac{1}{2} & 0 & -\frac{1}{2} & 0 \\ 1 & \frac{1}{2} & 1 & 1 & 1 & \frac{1}{2} & \frac{1}{2} & \frac{1}{2} & 0 & 0 \\ 0 & 0 & 0 & 0 & 0 & 0 & 0 & 0 & 0 & 0 \end{pmatrix}$$

$$\Omega_7^{(2)} = \begin{pmatrix} 0 & 0 & 0 & 0 & 0 & 0 & 0 & 0 & -1 & 0 \\ 0 & 0 & -1 & -1 & -1 & 0 & 0 & -1 & -1 & 0 \\ 0 & 1 & 0 & -\frac{1}{2} & -\frac{1}{2} & \frac{1}{2} & \frac{1}{2} & -\frac{1}{2} & -\frac{3}{2} & 0 \\ 0 & 1 & \frac{1}{2} & 0 & -\frac{1}{2} & \frac{1}{2} & \frac{1}{2} & -\frac{1}{2} & -\frac{3}{2} & 0 \\ 0 & 1 & \frac{1}{2} & \frac{1}{2} & 0 & \frac{1}{2} & \frac{1}{2} & -\frac{1}{2} & -\frac{3}{2} & 0 \\ 0 & 0 & -\frac{1}{2} & -\frac{1}{2} & -\frac{1}{2} & 0 & -\frac{1}{2} & -\frac{1}{2} & -\frac{1}{2} & 0 \\ 0 & 0 & -\frac{1}{2} & -\frac{1}{2} & -\frac{1}{2} & \frac{1}{2} & 0 & -\frac{1}{2} & -\frac{1}{2} & 0 \\ 0 & 1 & \frac{1}{2} & \frac{1}{2} & \frac{1}{2} & \frac{1}{2} & \frac{1}{2} & 0 & -\frac{1}{2} & 0 \\ 1 & 1 & \frac{3}{2} & \frac{3}{2} & \frac{3}{2} & \frac{1}{2} & \frac{1}{2} & \frac{1}{2} & 0 & 0 \\ 0 & 0 & 0 & 0 & 0 & 0 & 0 & 0 & 0 & 0 \end{pmatrix} \quad \Omega_8^{(2)} = \begin{pmatrix} 0 & 0 & 0 & 0 & 0 & 0 & 0 & 0 & 0 & 0 \\ 0 & 0 & -1 & -1 & -1 & 0 & 0 & -1 & -1 & 0 \\ 0 & 1 & 0 & -\frac{1}{2} & -\frac{1}{2} & \frac{1}{2} & \frac{1}{2} & -\frac{1}{2} & -\frac{1}{2} & 0 \\ 0 & 1 & \frac{1}{2} & 0 & -\frac{1}{2} & \frac{1}{2} & \frac{1}{2} & -\frac{1}{2} & -\frac{1}{2} & 0 \\ 0 & 1 & \frac{1}{2} & \frac{1}{2} & 0 & \frac{1}{2} & \frac{1}{2} & -\frac{1}{2} & -\frac{1}{2} & 0 \\ 0 & 0 & -\frac{1}{2} & -\frac{1}{2} & -\frac{1}{2} & 0 & -\frac{1}{2} & -\frac{1}{2} & -\frac{1}{2} & 0 \\ 0 & 0 & -\frac{1}{2} & -\frac{1}{2} & -\frac{1}{2} & \frac{1}{2} & 0 & -\frac{1}{2} & -\frac{1}{2} & 0 \\ 0 & 1 & \frac{1}{2} & \frac{1}{2} & \frac{1}{2} & \frac{1}{2} & \frac{1}{2} & 0 & -\frac{1}{2} & 0 \\ 0 & 1 & \frac{1}{2} & \frac{1}{2} & \frac{1}{2} & \frac{1}{2} & \frac{1}{2} & \frac{1}{2} & 0 & 0 \\ 0 & 0 & 0 & 0 & 0 & 0 & 0 & 0 & 0 & 0 \end{pmatrix}$$

$$\Omega_9^{(2)} = \begin{pmatrix} 0 & 0 & 0 & 0 & 0 & 0 & 0 & 0 & 0 & 0 \\ 0 & 0 & -\frac{1}{2} & -\frac{1}{2} & -\frac{1}{2} & \frac{1}{2} & 0 & 0 & 0 & 0 \\ 0 & \frac{1}{2} & 0 & -\frac{1}{2} & -\frac{1}{2} & \frac{1}{2} & 0 & 0 & 0 & 0 \\ 0 & \frac{1}{2} & \frac{1}{2} & 0 & -\frac{1}{2} & \frac{1}{2} & 0 & 0 & 0 & 0 \\ 0 & \frac{1}{2} & \frac{1}{2} & \frac{1}{2} & 0 & \frac{1}{2} & 0 & 0 & 0 & 0 \\ 0 & -\frac{1}{2} & -\frac{1}{2} & -\frac{1}{2} & -\frac{1}{2} & 0 & -\frac{1}{2} & -\frac{1}{2} & -\frac{1}{2} & -\frac{1}{2} \\ 0 & 0 & 0 & 0 & 0 & \frac{1}{2} & 0 & -\frac{1}{2} & -\frac{1}{2} & -\frac{1}{2} \\ 0 & 0 & 0 & 0 & 0 & \frac{1}{2} & \frac{1}{2} & 0 & -\frac{1}{2} & -\frac{1}{2} \\ 0 & 0 & 0 & 0 & 0 & \frac{1}{2} & \frac{1}{2} & \frac{1}{2} & 0 & -\frac{1}{2} \\ 0 & 0 & 0 & 0 & 0 & \frac{1}{2} & \frac{1}{2} & \frac{1}{2} & \frac{1}{2} & 0 \end{pmatrix} \quad \Omega_{10}^{(2)} = \begin{pmatrix} 0 & 0 & 0 & 0 & 0 & 0 & 0 & 0 & 0 & 0 \\ 0 & 0 & -\frac{1}{2} & -\frac{1}{2} & -\frac{1}{2} & \frac{1}{2} & \frac{1}{2} & -\frac{1}{2} & -\frac{1}{2} & -\frac{1}{2} \\ 0 & \frac{1}{2} & 0 & -\frac{1}{2} & -\frac{1}{2} & \frac{1}{2} & \frac{1}{2} & -\frac{1}{2} & -\frac{1}{2} & -\frac{1}{2} \\ 0 & \frac{1}{2} & \frac{1}{2} & 0 & -\frac{1}{2} & \frac{1}{2} & \frac{1}{2} & -\frac{1}{2} & -\frac{1}{2} & -\frac{1}{2} \\ 0 & \frac{1}{2} & \frac{1}{2} & \frac{1}{2} & 0 & \frac{1}{2} & \frac{1}{2} & -\frac{1}{2} & -\frac{1}{2} & -\frac{1}{2} \\ 0 & -\frac{1}{2} & -\frac{1}{2} & -\frac{1}{2} & -\frac{1}{2} & 0 & -\frac{1}{2} & -\frac{1}{2} & -\frac{1}{2} & -\frac{1}{2} \\ 0 & -\frac{1}{2} & -\frac{1}{2} & -\frac{1}{2} & -\frac{1}{2} & \frac{1}{2} & 0 & -\frac{1}{2} & -\frac{1}{2} & -\frac{1}{2} \\ 0 & \frac{1}{2} & \frac{1}{2} & \frac{1}{2} & \frac{1}{2} & \frac{1}{2} & \frac{1}{2} & 0 & -\frac{1}{2} & -\frac{1}{2} \\ 0 & \frac{1}{2} & \frac{1}{2} & \frac{1}{2} & \frac{1}{2} & \frac{1}{2} & \frac{1}{2} & \frac{1}{2} & 0 & -\frac{1}{2} \\ 0 & \frac{1}{2} & \frac{1}{2} & \frac{1}{2} & \frac{1}{2} & \frac{1}{2} & \frac{1}{2} & \frac{1}{2} & \frac{1}{2} & 0 \end{pmatrix}$$

$$\Omega_{11}^{(2)} = \begin{pmatrix} 0 & 0 & 0 & 0 & 0 & 0 & 0 & 0 & 0 & 0 \\ 0 & 0 & -\frac{1}{2} & -\frac{1}{2} & -\frac{1}{2} & \frac{1}{2} & \frac{1}{2} & \frac{1}{2} & -\frac{1}{2} & -\frac{1}{2} \\ 0 & \frac{1}{2} & 0 & -\frac{1}{2} & -\frac{1}{2} & \frac{1}{2} & \frac{1}{2} & \frac{1}{2} & -\frac{1}{2} & -\frac{1}{2} \\ 0 & \frac{1}{2} & \frac{1}{2} & 0 & -\frac{1}{2} & \frac{1}{2} & \frac{1}{2} & \frac{1}{2} & -\frac{1}{2} & -\frac{1}{2} \\ 0 & \frac{1}{2} & \frac{1}{2} & \frac{1}{2} & 0 & \frac{1}{2} & \frac{1}{2} & \frac{1}{2} & -\frac{1}{2} & -\frac{1}{2} \\ 0 & -\frac{1}{2} & -\frac{1}{2} & -\frac{1}{2} & -\frac{1}{2} & 0 & -\frac{1}{2} & -\frac{1}{2} & -\frac{1}{2} & -\frac{1}{2} \\ 0 & -\frac{1}{2} & -\frac{1}{2} & -\frac{1}{2} & -\frac{1}{2} & \frac{1}{2} & 0 & -\frac{1}{2} & -\frac{1}{2} & -\frac{1}{2} \\ 0 & -\frac{1}{2} & -\frac{1}{2} & -\frac{1}{2} & -\frac{1}{2} & \frac{1}{2} & \frac{1}{2} & 0 & -\frac{1}{2} & -\frac{1}{2} \\ 0 & \frac{1}{2} & \frac{1}{2} & \frac{1}{2} & \frac{1}{2} & \frac{1}{2} & \frac{1}{2} & \frac{1}{2} & 0 & -\frac{1}{2} \\ 0 & \frac{1}{2} & \frac{1}{2} & \frac{1}{2} & \frac{1}{2} & \frac{1}{2} & \frac{1}{2} & \frac{1}{2} & \frac{1}{2} & 0 \end{pmatrix}$$

$$
\Omega_{12}^{(2)} = \begin{pmatrix}
0 & 0 & 0 & 0 & 0 & 0 & 0 & 0 & 0 & 0 & 0 & 0 & 0 \\
0 & 0 & 1 & 1 & 1 & \frac{3}{2} & \frac{3}{2} & \frac{3}{2} & \frac{3}{2} & \frac{3}{2} & \frac{3}{2} & 1 & 1 \\
0 & -1 & 0 & -\frac{1}{2} & -\frac{1}{2} & -\frac{3}{2} & -\frac{3}{2} & -\frac{3}{2} & -\frac{1}{2} & -\frac{1}{2} & -\frac{1}{2} & -\frac{1}{2} & -\frac{1}{2} \\
0 & -1 & \frac{1}{2} & 0 & -\frac{1}{2} & -\frac{1}{2} & -\frac{1}{2} & -\frac{1}{2} & \frac{1}{2} & \frac{1}{2} & \frac{1}{2} & 0 & -\frac{1}{2} \\
0 & -1 & \frac{1}{2} & \frac{1}{2} & 0 & -\frac{1}{2} & -\frac{1}{2} & -\frac{1}{2} & \frac{1}{2} & \frac{1}{2} & \frac{1}{2} & \frac{1}{2} & 0 \\
0 & -\frac{3}{2} & \frac{3}{2} & \frac{1}{2} & \frac{1}{2} & 0 & -\frac{1}{2} & -\frac{1}{2} & 2 & 2 & 2 & \frac{1}{2} & \frac{1}{2} \\
0 & -\frac{3}{2} & \frac{3}{2} & \frac{1}{2} & \frac{1}{2} & \frac{1}{2} & 0 & -\frac{1}{2} & 2 & 2 & 2 & \frac{1}{2} & \frac{1}{2} \\
0 & -\frac{3}{2} & \frac{3}{2} & \frac{1}{2} & \frac{1}{2} & \frac{1}{2} & \frac{1}{2} & 0 & 2 & 2 & 2 & \frac{1}{2} & \frac{1}{2} \\
0 & -\frac{3}{2} & \frac{1}{2} & -\frac{1}{2} & -\frac{1}{2} & -2 & -2 & -2 & 0 & -\frac{1}{2} & -\frac{1}{2} & -\frac{1}{2} & -\frac{1}{2} \\
0 & -\frac{3}{2} & \frac{1}{2} & -\frac{1}{2} & -\frac{1}{2} & -2 & -2 & -2 & \frac{1}{2} & 0 & -\frac{1}{2} & -\frac{1}{2} & -\frac{1}{2} \\
0 & -\frac{3}{2} & \frac{1}{2} & -\frac{1}{2} & -\frac{1}{2} & -2 & -2 & -2 & \frac{1}{2} & \frac{1}{2} & 0 & -\frac{1}{2} & -\frac{1}{2} \\
0 & -1 & \frac{1}{2} & 0 & -\frac{1}{2} & -\frac{1}{2} & -\frac{1}{2} & -\frac{1}{2} & \frac{1}{2} & \frac{1}{2} & \frac{1}{2} & 0 & -\frac{1}{2} \\
0 & -1 & \frac{1}{2} & \frac{1}{2} & 0 & -\frac{1}{2} & -\frac{1}{2} & -\frac{1}{2} & \frac{1}{2} & \frac{1}{2} & \frac{1}{2} & \frac{1}{2} & 0
\end{pmatrix}
\quad
\Omega_{13}^{(2)} = \begin{pmatrix}
0 & 0 & 0 & 0 & 0 & 0 & 0 & 0 & 0 & 0 \\
0 & 0 & -\frac{1}{2} & -\frac{1}{2} & -\frac{1}{2} & -\frac{1}{2} & -\frac{1}{2} & -\frac{1}{2} & -\frac{1}{2} & -\frac{1}{2} \\
0 & \frac{1}{2} & 0 & -\frac{1}{2} & -\frac{1}{2} & -\frac{1}{2} & -\frac{1}{2} & -\frac{1}{2} & -\frac{1}{2} & -\frac{1}{2} \\
0 & \frac{1}{2} & \frac{1}{2} & 0 & -\frac{1}{2} & -\frac{1}{2} & -\frac{1}{2} & -\frac{1}{2} & -\frac{1}{2} & -\frac{1}{2} \\
0 & \frac{1}{2} & \frac{1}{2} & \frac{1}{2} & 0 & -\frac{1}{2} & -\frac{1}{2} & -\frac{1}{2} & -\frac{1}{2} & -\frac{1}{2} \\
0 & \frac{1}{2} & \frac{1}{2} & \frac{1}{2} & \frac{1}{2} & 0 & -\frac{1}{2} & -\frac{1}{2} & -\frac{1}{2} & -\frac{1}{2} \\
0 & \frac{1}{2} & \frac{1}{2} & \frac{1}{2} & \frac{1}{2} & \frac{1}{2} & 0 & -\frac{1}{2} & -\frac{1}{2} & -\frac{1}{2} \\
0 & \frac{1}{2} & \frac{1}{2} & \frac{1}{2} & \frac{1}{2} & \frac{1}{2} & \frac{1}{2} & 0 & -\frac{1}{2} & -\frac{1}{2} \\
0 & \frac{1}{2} & \frac{1}{2} & \frac{1}{2} & \frac{1}{2} & \frac{1}{2} & \frac{1}{2} & \frac{1}{2} & 0 & -\frac{1}{2} \\
0 & \frac{1}{2} & \frac{1}{2} & \frac{1}{2} & \frac{1}{2} & \frac{1}{2} & \frac{1}{2} & \frac{1}{2} & \frac{1}{2} & 0
\end{pmatrix}
$$

Each matrix $\Omega_i^{(2)}$ is written in the basis B_i of polynomials shown below:

$$
\begin{aligned}
B_1 = \{ & \langle 1,2,(23)\cap(456),(234)\cap(56)\rangle, \langle 6,1,2,(23)\cap(456)\rangle, \langle (234)\cap(56),6,1,2\rangle, \\
& \langle (23)\cap(456),(234)\cap(56),6,1\rangle, \langle 2,(23)\cap(456),(234)\cap(56),6\rangle, \langle 2,3,4,5\rangle, \langle 6,2,3,4\rangle, \langle 5,6,2,3\rangle, \\
& \langle 4,5,6,2\rangle, \langle 3,4,5,6\rangle\}, \\
B_2 = \{ & \langle 1,2,(34)\cap(567),(345)\cap(67)\rangle, \langle 7,1,2,(34)\cap(567)\rangle, \langle (345)\cap(67),7,1,2\rangle, \langle (34)\cap(567), \\
& (345)\cap(67),7,1\rangle, \langle 2,(34)\cap(567),(345)\cap(67),7\rangle, \langle 3,4,5,6\rangle, \langle 7,3,4,5\rangle, \langle 6,7,3,4\rangle, \langle 5,6,7,3\rangle, \\
& \langle 4,5,6,7\rangle\}, \\
B_3 = \{ & \langle 1,2,3,(345)\cap(67)\rangle, \langle 7,1,2,3\rangle, \langle (345)\cap(67),7,1,2\rangle, \langle 3,(345)\cap(67),7,1\rangle, \langle 2,3,(345)\cap(67),7\rangle, \\
& \langle 3,4,5,6\rangle, \langle 7,3,4,5\rangle, \langle 6,7,3,4\rangle, \langle 5,6,7,3\rangle, \langle 4,5,6,7\rangle\}, \\
B_4 = \{ & \langle 1,2,3,(456)\cap(78)\rangle, \langle 8,1,2,3\rangle, \langle (456)\cap(78),8,1,2\rangle, \langle 3,(456)\cap(78),8,1\rangle, \langle 2,3,(456)\cap(78),8\rangle, \\
& \langle 4,5,6,7\rangle, \langle 8,4,5,6\rangle, \langle 7,8,4,5\rangle, \langle 6,7,8,4\rangle.\langle 5,6,7,8\rangle\}, \\
B_5 = \{ & \langle 1,2,3,4\rangle, \langle 8,1,2,3\rangle, \langle 4,8,1,2\rangle, \langle 3,4,8,1\rangle, \langle 2,3,4,8\rangle, \langle 4,5,6,7\rangle, \langle 8,4,5,6\rangle, \langle 7,8,4,5\rangle, \langle 6,7,8,4\rangle, \\
& \langle 5,6,7,8\rangle\}, \\
B_6 = \{ & \langle 1,2,3,(45)\cap(678)\rangle, \langle 8,1,2,3\rangle, \langle (45)\cap(678),8,1,2\rangle, \langle 3,(45)\cap(678),8,1\rangle, \langle 2,3,(45)\cap(678),8\rangle, \\
& \langle 4,5,6,7\rangle, \langle 8,4,5,6\rangle, \langle 7,8,4,5\rangle, \langle 6,7,8,4\rangle.\langle 5,6,7,8\rangle\},
\end{aligned}
$$

$$B_7 = \{\langle 1,2,3,(45)\cap(678)\rangle, \langle (456)\cap(78),1,2,3\rangle, \langle (45)\cap(678),(456)\cap(78),1,2\rangle,$$

$$\langle 3,(45)\cap(678),(456)\cap(78),1\rangle, \langle 2,3,(45)\cap(678),(456)\cap(78)\rangle, \langle 4,5,6,7\rangle, \langle 8,4,5,6\rangle, \langle 7,8,4,5\rangle,$$

$$\langle 6,7,8,4\rangle.\langle 5,6,7,8\rangle\},$$

$$B_8 = \{\langle 1,2,3,4\rangle, \langle (456)\cap(78),1,2,3\rangle, \langle 4,(456)\cap(78),1,2\rangle, \langle 3,4,(456)\cap(78),1\rangle, \langle 2,3,4,(456)\cap(78)\rangle,$$

$$\langle 4,5,6,7\rangle, \langle 8,4,5,6\rangle, \langle 7,8,4,5\rangle, \langle 6,7,8,4\rangle.\langle 5,6,7,8\rangle\},$$

$$B_9 = \{\langle 1,2,3,4\rangle, \langle 9,1,2,3\rangle, \langle 4,9,1,2\rangle, \langle 3,4,9,1\rangle, \langle 2,3,4,9\rangle, \langle 5,6,7,8\rangle, \langle 9,5,6,7\rangle, \langle 8,9,5,6\rangle,$$

$$\langle 7,8,9,5\rangle, \langle 6,7,8,9\rangle\},$$

$$B_{10} = \{\langle 1,2,3,4\rangle, \langle (567)\cap(89),1,2,3\rangle, \langle 4,(567)\cap(89),1,2\rangle, \langle 3,4,(567)\cap(89),1\rangle, \langle 2,3,4,(567)\cap(89)\rangle,$$

$$\langle 5,6,7,8\rangle, \langle 9,5,6,7\rangle, \langle 8,9,5,6\rangle, \langle 7,8,9,5\rangle, \langle 6,7,8,9\rangle\},$$

$$B_{11} = \{\langle 1,2,3,4\rangle, \langle (56)\cap(789),1,2,3\rangle, \langle 4,(56)\cap(789),1,2\rangle, \langle 3,4,(56)\cap(789),1\rangle, \langle 2,3,4,(56)\cap(789)\rangle,$$

$$\langle 5,6,7,8\rangle, \langle 9,5,6,7\rangle, \langle 8,9,5,6\rangle, \langle 7,8,9,5\rangle, \langle 6,7,8,9\rangle\},$$

$$B_{12} = \{\langle 1,2,3,4\rangle, \langle 4,7,8,9\rangle, \langle 5,6,(123)\cap(789)\rangle, \langle 1,2,3,(45)\cap(789)\rangle, \langle (46)\cap(789),1,2,3\rangle,$$

$$\langle (45)\cap(789),(46)\cap(789),1,2\rangle, \langle 3,(45)\cap(789),(46)\cap(789),1\rangle, \langle 2,3,(45)\cap(789),(46)\cap(789)\rangle,$$

$$\langle (45)\cap(123),(46)\cap(123),7,8\rangle, \langle 9,(45)\cap(123),(46)\cap(123),7\rangle, \langle 8,9,(45)\cap(123),(46)\cap(123)\rangle,$$

$$\langle 7,8,9(45)\cap(123)\rangle, \langle (46)\cap(123),7,8,9\rangle\},$$

$$B_{13} = \{\langle 1,2,3,4\rangle, \langle 5,1,2,3\rangle, \langle 4,5,1,2\rangle, \langle 3,4,5,1\rangle, \langle 2,3,4,5\rangle, \langle 6,7,8,9\rangle, \langle 10,6,7,8\rangle, \langle 9,10,6,7\rangle,$$

$$\langle 8,9,10,6\rangle, \langle 7,8,9,10\rangle\}.$$

Chapter 5

A Note on One-loop Cluster Adjacency in $\mathcal{N} = 4$ SYM

This chapter is based on the publication [103].

Cluster algebras [17, 18, 19] of Grassmannian type [104, 21] have been found to play a significant role in the mathematical structure of scattering amplitudes in planar maximally supersymmetric Yang-Mills theory ($\mathcal{N} = 4$ SYM) [5, 69], constraining the structure of amplitudes at the level of symbols and cobrackets [67, 69, 71, 72]. The recently introduced cluster adjacency principle [73] has opened a new line of research in this topic, shedding light on even deeper connections between amplitudes and cluster algebras. This principle applies conjecturally to various aspects of the analytic structure of amplitudes in $\mathcal{N} = 4$ SYM. The many guises of cluster adjacency, at the level of symbols [89], Yangian invariants [65, 105], and the correlation between them [81] have also been exploited to help compute new amplitudes via bootstrap [82]. These mathematical properties however are perhaps somewhat obscure, and although it is understood that cluster adjacency of a symbol implies the Steinmann relations [73], its other manifestations have less clear physical interpretations (see however [129], which establishes interesting new connections between cluster adjacency and Landau singularities). Even finer notions of cluster adjacency, that more strictly constrain pairs of adjacent symbol letters, have recently been studied in [108, 107].

In this paper we show that that the one-loop NMHV amplitudes in $\mathcal{N} = 4$ SYM theory satisfy symbol-level cluster adjacency for all n, and we check that for $n = 9$ the amplitude can be written in a form that exhibits adjacency between final symbol entries and R-invariants, supporting the conjectures of [73, 81]. The outline of this paper is as follows. In Section 2 we review the kinematics of $\mathcal{N} = 4$ SYM and the bracket test used to assess cluster adjacency. In Section 3 we review formulas for the amplitudes to which we apply the bracket test. In Section 4 we present our analysis and results as well as new cluster adjacency conjectures for Plücker coordinates and cluster variables that are quadratic in Plückers. These conjectures generalize the notion of weak separation [109, 110].

5.1 Cluster Adjacency and the Sklyanin Bracket

In $\mathcal{N} = 4$ SYM the kinematics of scattering of n massless particles is described by a collection of n *momentum twistors* [4], $Z_1^I, \ldots, Z_n^I$, each of which is a four-component ($I \in \{1, \ldots, 4\}$) homogeneous coordinate on $\mathbb{P}^3$. Thanks to dual conformal symmetry [3] the collection of momentum twistors have a $GL(4)$ redundancy and thus can be taken to represent points in

$Gr(4,n)$. By an appropriate choice of gauge we can take

$$Z = \begin{pmatrix} Z_1^1 & \cdots & Z_n^1 \\ Z_1^2 & \cdots & Z_n^2 \\ Z_1^3 & \cdots & Z_n^3 \\ Z_1^4 & \cdots & Z_n^4 \end{pmatrix} \xrightarrow[GL(4)]{} \begin{pmatrix} 1 & 0 & 0 & 0 & y^1{}_5 & \cdots & y^1{}_n \\ 0 & 1 & 0 & 0 & y^2{}_5 & \cdots & y^2{}_n \\ 0 & 0 & 1 & 0 & y^3{}_5 & \cdots & y^3{}_n \\ 0 & 0 & 0 & 1 & y^4{}_5 & \cdots & y^4{}_n \end{pmatrix}. \tag{5.1}$$

The degrees of freedom are given by $y^I{}_a = (-1)^I \langle \{1,2,3,4\} \smallsetminus \{I\}, a\rangle / \langle 1,2,3,4\rangle$ for $a = 5,6,\ldots,n$, with

$$\langle a,b,c,d\rangle \equiv \epsilon_{ijkl} Z_a^i Z_b^j Z_c^k Z_d^l \tag{5.2}$$

denoting Plücker coordinates on $\mathrm{Gr}(4,n)$. Throughout this paper we will make use of the relation between momentum twistors and dual momenta [3]

$$x_{ij}^2 = \frac{\langle i{-}1\,, i\,, j{-}1\,, j\rangle}{\langle i{-}1\, i\rangle\langle j{-}1\, j\rangle}\,, \tag{5.3}$$

where $\langle i\, j\rangle$ is the usual spinor helicity bracket (that completely drops out of our analysis due to cancellations guaranteed by dual conformal symmetry).

The fact that (5.2) are cluster variables of the $Gr(4,n)$ cluster algebra plays a constraining role in the analytic structure of amplitudes in $\mathcal{N} = 4$ SYM through the notion of cluster adjacency [73] and it is therefore of interest to test the cluster adjacency properties of amplitudes. Two cluster variables are cluster adjacent if they appear together in a common cluster of the cluster algebra (this notion is also called "cluster compatibility"). To test whether two given variables are cluster adjacent one can use the Poisson structure of the cluster algebra [104], which is related to the Sklyanin bracket [87]. We call this the *bracket test* and was first applied to amplitudes in [89]. In terms of the parameters of (5.1), the Sklyanin bracket is given by

$$\{y^I{}_a, y^J{}_b\} = \frac{1}{2}(\text{sign}(J-I) - \text{sign}(b-a))y^J{}_a y^I{}_b\,, \tag{5.4}$$

which extends to arbitrary functions as

$$\{f(y), g(y)\} = \sum_{a,b=5}^{n}\sum_{I,J=1}^{4}\frac{\partial f}{\partial y^I{}_a}\frac{\partial g}{\partial y^J{}_b}\{y^I{}_a, y^J{}_b\}\,. \tag{5.5}$$

The *bracket test* then says: two cluster variables a_i and a_j are cluster adjacent iff

$$\Omega_{ij} = \{\log a_i, \log a_j\} \in \frac{1}{2}\mathbb{Z}\,. \tag{5.6}$$

Note that whenever i, j, k, l are cyclically adjacent, $\langle i, j, k, l\rangle$ is a frozen variable and is therefore automatically adjacent with every cluster variable.

The aim of this paper is to provide evidence for two cluster adjacency conjectures for loop amplitudes of generalized polylogarithm type [73]:

Conjecture 1 "Steinmann cluster adjacency": Every pair of adjacent entries in the symbol of an amplitude is cluster adjacent.

This type of cluster adjacency implies the extended Steinmann relations at all particle multiplicities [89]. In fact it appears to be equivalent to the extended Steinmann conditions of [111] for all known integrable symbols with physical first entries (that means, of the form $\langle i, i+1, j, j+1 \rangle$).

Conjecture 2 "Final entry cluster adjacency": There exists a representation of the symbol of an amplitude in which the final symbol entry in every term is cluster adjacent to all poles of the Yangian invariant that term multiplies.

Support for these conjectures was given for NMHV amplitudes at 6- and 7-points in [82, 81] (to all loop order at which these amplitudes are currently known), and for one- and two-loop MHV amplitudes (to which only the first conjecture applies) at all multiplicities in [89].

5.2 One-loop Amplitudes

To demonstrate the cluster adjacency of NMHV amplitudes with respect to the conjectures in Section 5.1 we need to work with appropriate finite quantities after IR divergences have been subtracted. To this end we will be working with two types of regulators at one loop: BDS [112] and BDS-like [113] normalized amplitudes. In this section we review these regulators and the one-loop amplitudes relevant for our computations.

5.2.1 BDS- and BDS-like Subtracted Amplitudes

We start by reviewing the BDS normalized amplitude, which was first introduced in [112]. Consider the n-point MHV amplitude $\mathcal{A}_n^{\mathrm{MHV}}$ in planar $\mathcal{N} = 4$ SYM with gauge group $SU(N_c)$

coupling constant g_{YM}, where the tree-level amplitude has been factored out. Evaluating the amplitude in $4-2\epsilon$ dimensions regulates the IR divegences. The BDS normalization involves dividing all amplitudes by the factor

$$A_n^{\text{BDS}} = \exp\left[\sum_{L=1}^{\infty} g^{2L}\left(\frac{f^{(L)}(\epsilon)}{2}A_n^{(1)}(L\epsilon) + C^{(L)}\right)\right], \tag{5.7}$$

that encapsulates all IR divergences. Here where $g^2 = \frac{g_{\text{YM}}^2 N_c}{16\pi^2}$ is the 't Hooft coupling, the superscript (L) on any function denotes its $\mathcal{O}(g^{2L})$ term, $C^{(L)}$ is a transcendental constant and $f(\epsilon) = \frac{1}{2}\Gamma_{\text{cusp}} + \mathcal{O}(\epsilon)$, where Γ_{cusp} is the cusp anomalous dimension

$$\Gamma_{\text{cusp}} = 4g^2 + \mathcal{O}(g^4)\,. \tag{5.8}$$

The BDS-like normalization contrasts with BDS normalization by the inclusion of a dual conformally invariant function Y_n, chosen such that the BDS-like normalization only depends on two-particle Mandelstam invariants,

$$\begin{aligned} A_n^{\text{BDS-like}} &= A_n^{\text{BDS}} \exp\left[\frac{\Gamma_{\text{cusp}}}{4} Y_n\right], \quad 4 \not| \; n\,, \\ Y_n &= -F_n - 4A_{\text{BDS-like}} + \frac{n\pi^2}{4}\,, \end{aligned} \tag{5.9}$$

where F_n is (in our conventions) twice the function in Eq. (4.57) of [112] (one can use an equivalent representation from [89]) and $A_{\text{BDS-like}}$ is given on page 57 of [114]. Since $A_n^{\text{BDS-like}}$ only depends on two-particle Mandelstam invariants, which can be written entirely in terms of frozen variables of the cluster algebra, the BDS-like normalization has the nice feature of not spoiling any cluster adjacency properties. At the same time it means that BDS-like normalized amplitudes will satisfy Steinmann relations [84, 85, 86]

$$\left.\begin{aligned} \mathrm{Disc}_{x^2_{i+1,j}}\left[\mathrm{Disc}_{x^2_{i+1,i+p}}(A_n)\right] &= 0\,,\\ \mathrm{Disc}_{x^2_{i+1,i+p}}\left[\mathrm{Disc}_{x^2_{i+1,j+p+q}}(A_n)\right] &= 0\,, \end{aligned}\right\} \quad 0 < j-i \le p \quad \text{or} \quad q < i-j \le p+q\,. \tag{5.10}$$

5.2.2 NMHV Amplitudes

The one-loop n-point NMHV ratio function can be written in the dual conformally invariant form [115, 116]

$$\mathcal{P}_n = \mathcal{V}_{\text{tot}} R_{\text{tot}} + \mathcal{V}_{14n} R_{14n} + \sum_{s=5}^{n-2}\sum_{t=s+2}^{n} \mathcal{V}_{1st} R_{1st} + \text{cyclic}\,. \tag{5.11}$$

The transcendental functions $\mathcal{V}_{\text{tot}}$, $\mathcal{V}_{14n}$, and $\mathcal{V}_{1st}$ are given explicitly in Appendix 5.5. The function R_{tot} is given in terms of R-invariants [3]

$$R_{\text{tot}} = \sum_{s=3}^{n-2}\sum_{t=s+2}^{n} R_{1st}\,, \tag{5.12}$$

and R_{rst} are the five-brackets [93] written in terms of momentum supertwistors as

$$\begin{aligned} R_{rst} &= [r, s-1, s, t-1, t]\,,\\ [a,b,c,d,e] &= \frac{\delta^{(4)}(\chi_a\langle b,c,d,e\rangle + \text{cyclic})}{\langle a,b,c,d\rangle\langle b,c,d,e\rangle\langle c,d,e,a\rangle\langle d,e,a,b\rangle\langle e,a,b,c\rangle}\,. \end{aligned} \tag{5.13}$$

These are special cases of Yangian invariants [3, 11] and we will henceforth refer to them as such.

5.3 Cluster Adjacency of One-Loop NMHV Amplitudes

In this section we will describe the method we used to test the conjectures in Section 5.1 and our results.

5.3.1 The Symbol and Steinmann Cluster Adjacency

To compute the symbol of a transcendental function, we follow [12] (see also [117]). Only weight two polylogarithms appear at one loop so it is sufficient for us to use the symbols

$$\mathcal{S}(\log(R_1)\log(R_2)) = R_1 \otimes R_2 + R_2 \otimes R_1\,, \quad \mathcal{S}(\mathrm{Li}_2(R_1)) = -(1-R_1)\otimes R_1\,. \tag{5.14}$$

Once the symbol of an amplitude is computed, we expand out any cross ratios using (5.28) and (5.3), and perform the bracket test to adjacent symbol entries. It is straightforward to compute the symbol of the expressions in Appendix 5.5 using (5.14) and we find that the symbol of each of the transcendental functions of (5.11), $\mathcal{V}_{14n}$, $\mathcal{V}_{1,s,t}$, and $\mathcal{V}_{\mathrm{tot}}$, satisfy Steinmann cluster adjacency (after dropping spurious terms that cancel when expanded out), and hence satisfies *Conjecture 1*.

5.3.2 Final Entry and Yangian Invariant Cluster Adjacency

To study *Conjecture 2*, we follow [81] and start with the BDS-like normalized amplitude expanded as a linear combination of Yangian invariants times transcendental functions

$$A_{n,L}^{\text{NMHV, BDS-like}} = \sum_i \mathcal{Y}_i f_i^{(2L)}\,, \tag{5.15}$$

We seek a representation of this amplitude that satisfies *Conjecture 2*. Using the bracket test (5.6), we determine which final symbol entries are not cluster adjacent to all poles of the Yangian invariant multiplying that term. We then rewrite the non-cluster adjacent combinations of Yangian invariants and final entries by using the identities [93]

$$[a,b,c,d,e]-[a,b,c,d,f]+[a,b,c,e,f]-[a,b,d,e,f]+[a,c,d,e,f]-[b,c,d,e,f]=0\,. \tag{5.16}$$

until we are able to reach a form that satisfies final entry cluster adjacency. Note that rewriting in this manner makes the integrability of the symbol no longer manifest. The 6- and 7-point cases were studied in [81]. We checked that this conjecture is true in the 9-point case as well. To get a flavor for our 9-point calculation, consider the following term that we encounter, which does not manifestly satisfy final entry cluster adjacency:

$$\begin{aligned}&-\frac{1}{2}\big([1,2,3,4,5]+[1,2,3,5,6]+[1,2,3,6,7]-[1,2,4,5,7]-[1,2,5,6,7]\\&+[1,3,4,5,6]+[1,3,4,6,7]+[1,4,5,6,7]-[2,3,4,5,7]-[2,3,5,6,7]\big)\\&\times\left(\log\left(\frac{\langle 1,2,3,4\rangle\langle 1,7,8,9\rangle}{\langle 1,2,7,8\rangle\langle 1,3,4,9\rangle}\right)\otimes\langle 3,4,7,8\rangle\right).\end{aligned} \tag{5.17}$$

To get rid of the non-cluster adjacent combinations of Yangian invariants and final entries, we list all identities (5.16) and note that there are 14 cyclic classes of Yangian invariants at 9-points. A cyclic class is generated by taking a five-bracket and shifting all indices cyclically. This collection forms a cyclic class. Solving the identities (5.16) for 7 of the 14 cyclic classes in Mathematica (yielding $\binom{14}{7}=3432$ different solutions), we find that at least one solution, for each final entry, brings the symbol to a final entry cluster adjacent form. For the example (5.17), one of the combinations from these solutions, that is cluster adjacent, takes the form

$$\begin{aligned}&-\frac{1}{2}([1,2,3,4,8]-[1,2,3,7,8]+[1,2,4,7,8]-[1,3,4,7,8]\\&+[2,3,4,7,8]+[3,4,5,6,7])\left(\log\left(\frac{\langle 1,2,3,4\rangle\langle 1,7,8,9\rangle}{\langle 1,2,7,8\rangle\langle 1,3,4,9\rangle}\right)\otimes\langle 3,4,7,8\rangle\right).\end{aligned} \tag{5.18}$$

One can check that the complete set of Yangian invariants that are cluster adjacent to $\langle 3,4,7,8\rangle$ is given by

$$\begin{aligned}&\{[1,2,3,4,7],[1,2,3,4,8],[1,2,3,4,9],[1,2,3,7,8],[1,2,3,7,9],[1,2,3,8,9],\\&[1,2,4,7,8],[1,2,4,7,9],[1,2,4,8,9],[1,2,7,8,9],[1,3,4,7,8],[1,3,4,7,9],\\&[1,3,4,8,9],[1,3,7,8,9],[1,4,7,8,9],[2,3,4,7,8],[2,3,4,7,9],[2,3,4,8,9],\\&[2,3,7,8,9],[2,4,7,8,9],[3,4,5,6,7],[3,4,5,6,8],[3,4,5,7,8],[3,4,6,7,8],\\&[3,4,7,8,9],[3,5,6,7,8],[4,5,6,7,8]\}.\end{aligned} \tag{5.19}$$

At 10-points this method becomes much more computationally intensive as we have 26 cyclic classes. If we follow the same procedure as for 9-points, we would have to check cluster adjacency of $\binom{26}{13}=10400600$ solutions per final entry with non cluster adjacent Yangian invariants.

5.4 Cluster Adjacency and Weak Separation

In our study of one-loop NMHV amplitudes we observed some general cluster adjacency properties of symbol entries and Yangian invariants involved in the one-loop NMHV amplitude. Let us denote the various types of symbol letters by

$$a_{1;ij} = \langle i-1, i, j-1, j\rangle\,, \tag{5.20}$$

$$\begin{aligned} a_{2;ijk} &= \langle i(j\,j+1)(k\,k+1)(i-1\,i+1)\rangle \\ &= \langle i,j,j+1,i-1\rangle\langle i,k,k+1,i+1\rangle - \langle i,j,j+1,i+1\rangle\langle i,k,k+1,i-1\rangle\,, \end{aligned} \tag{5.21}$$

$$\begin{aligned} a_{3;ijkl} &= \langle i(j\,j+1)(k\,k+1)(l\,l+1)\rangle \\ &= \langle i,j,k,k+1\rangle\langle i,j+1,l,l+1\rangle - \langle i,j+1,k,k+1\rangle\langle i,j,l,l+1\rangle\,. \end{aligned} \tag{5.22}$$

In this section we summarize their cluster adjacency properties as determined by the *bracket test*.

First consider $a_{1;ij}$ and $a_{2;klm}$. We observe that these variables are adjacent if they satisfy a generalized notion of weak separation [109, 110]. In particular we find that

$$\begin{aligned} &\langle i-1,i,j-1,j\rangle \quad \text{and} \quad \langle k(l\,l+1)(m\,m+1)(k-1\,k+1)\rangle \quad \text{are cluster adjacent iff} \\ &\{i,j\} \in \{k+1,\ldots,l+1\} \vee \{l+1,\ldots,m+1\} \vee \{m+1,\ldots,k\} \quad \text{or} \\ &\{i=k, j=l+1\} \vee \{i=k, j=m+1\} \vee \{i=k+1, j=l+1\} \vee \{i=k+1, j=m+1\}\,. \end{aligned} \tag{5.23}$$

This adjacency statement can be represented by drawing a circle with labeled points $\{1,\ldots,n\}$ appearing in cyclic order, as in Figure 5.1. For the variables $a_{1;ij}$ and $a_{3;klmp}$ we observe

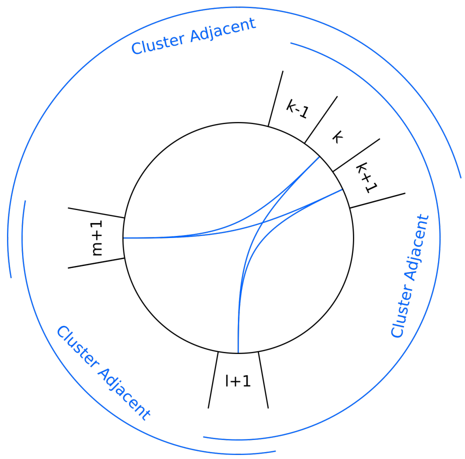

FIGURE 5.1: Weak separation graph indicating that if both i and j are within any of the green regions (or on the green chords), then $\langle i-1, i, j-1, j\rangle$ is cluster adjacent to $\langle k(l\,l+1)(m\,m+1)(k-1\,k+1)\rangle$.

$$
\begin{aligned}
&\langle i-1, i, j-1, j\rangle \quad \text{and} \quad \langle k(l\,l+1)(m\,m+1)(p\,p+1)\rangle \quad \text{are cluster adjacent iff} \\
&\{i,j\} \in \{k+1,\dots,l+1\} \vee \{l+1,\dots,m+1\} \vee \{m+1,\dots,p+1\} \vee \{p+1,\dots,k+1\} \\
&\text{or} \quad \{i=k+1, j=l+1\} \vee \{i=l+1, j=m+1\} \vee \{i=m+1, j=p+1\} \\
&\vee \{i=p+1, j=k+1\} \vee \{i=k+1, j=m+1\} \vee \{i=l+1, j=p+1\}.
\end{aligned}
\tag{5.24}
$$

This statement is represented in Figure 5.2.

For Plücker coordinate of type (5.20) and Yangian invariants (5.13), we observe

$$
\begin{aligned}
&\langle i-1, i, j-1, j\rangle \quad \text{and} \quad [a,b,c,d,e] \quad \text{are cluster adjacent iff} \\
&\{a,b,c,d,e\} \subset \binom{\{i-1, i, \dots, j-1, j\}}{5} \cup \binom{\{j-1, j, \dots, i-1, i\}}{5}.
\end{aligned}
\tag{5.25}
$$

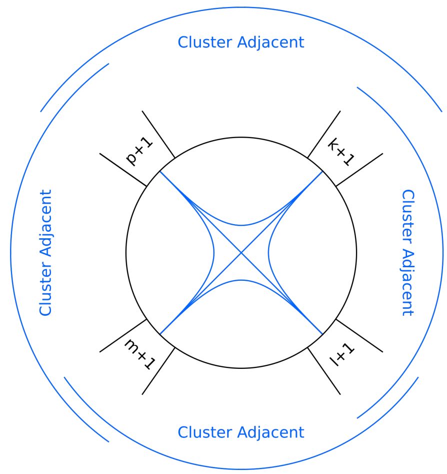

FIGURE 5.2: Weak separation graph indicating that if both i and j are within any of the green regions (or on the green chords), then $\langle i-1, i, j-1, j\rangle$ is cluster adjacent to $\langle k(l\,l+1)(m\,m+1)(p\,p+1)\rangle$.

Next up the variables (5.21) and Yangian invariants (5.13) are observed to have the adjacency condition

$$\begin{aligned}&\langle i(j\,j+1)(k\,k+1)(i-1\,i+1)\rangle \quad \text{and} \quad [a,b,c,d,e] \quad \text{are cluster adjacent iff}\\ &\{a,b,c,d,e\} \subset \{\{i,j,j+1,k,k+1\}\} \cup \binom{\{i,i+1,\ldots,j,j+1\}}{5}\\ &\cup \binom{\{j,j+1,\ldots,k,k+1\}}{5} \cup \binom{\{k,k+1,\ldots,i-1,i\}}{5}.\end{aligned} \tag{5.26}$$

Finally, for variables (5.22) and Yangian invariants (5.13), we observe adjacency when

$$\begin{aligned}&\langle i(j\,j+1)(k\,k+1)(l\,l+1)\rangle \quad \text{and} \quad [a,b,c,d,e] \quad \text{are cluster adjacent iff}\\ &\{a,b,c,d,e\} \subset \binom{\{i,\ldots,j,j+1\}}{5} \cup \binom{\{i,j,j+1,\ldots,k,k+1\}}{5}\\ &\cup \binom{\{i,k,k+1,\ldots,l,l+1\}}{5} \cup \binom{\{l,l+1,\ldots,i\}}{5}.\end{aligned} \tag{5.27}$$

The statements about cluster adjacency in this section hint at a generalization of the notion of weak separation for Plücker coordinates [109, 110]. We are only able to verify these statements "experimentally" via the bracket test. To prove such statements, we look to Theorem 1.6 of [110] which states that: given a subset $\mathcal{C}$ of $\binom{\{1,\ldots,n\}}{4}$, the set of Plücker coordinates $\{p_I\}_{I\in\mathcal{C}}$ forms a cluster in the $Gr(4,n)$ cluster algebra iff $\mathcal{C}$ is a maximally weakly separated collection. Maximally weakly separated means that if $\mathcal{C} \subseteq \binom{\{1,\ldots,n\}}{4}$ is a collection of pairwise weakly separated sets and $\mathcal{C}$ is not contained in any larger set of of pairwise weakly separated sets, then the collection $\mathcal{C}$ is maximally weakly separated. To prove the cluster adjacency statements made in this section, we would have to prove that there exists a maximally weakly separated collection containing all the weakly separated sets proposed in for each pair of coordinates/Yangian invariants considered in this section. We leave this to future work.

5.5 n-point NMHV Transcendental Functions

In this Appendix we present the transcendental functions contributing to the NMHV ratio function (5.11), from [116]. All functions are written in a dual conformally invariant form, in terms of cross ratios

$$u_{ijkl} = \frac{x_{ik}^2 x_{jl}^2}{x_{il}^2 x_{jk}^2} \tag{5.28}$$

of dual momenta (5.3). The functions $\mathcal{V}_{1,s,t}$ are given by

$$\begin{aligned}\mathcal{V}_{1,s,t} = \mathrm{Li}_2(1-u_{12t4}) - \mathrm{Li}_2(1-u_{12ts}) + \sum_{i=5}^{s}\Big[\mathrm{Li}_2(1-u_{2,i+2,i-1,i}) - \mathrm{Li}_2(1-u_{12i,i-1})\\ - \mathrm{Li}_2(1-u_{1,i+2,i-1,i}) - \frac{1}{2}\ln(u_{21i,i+2})\ln(u_{1,i+2,i-1,i}) - \frac{1}{2}\ln(u_{12ti})\ln(u_{1t,i-1,i})\\ - \frac{1}{2}\ln(u_{2,i-1,t,i+2})\ln(u_{12i,i-1})\Big], \qquad \text{for} \quad 5 \le s, t \le n-1,\end{aligned} \tag{5.29}$$

where $5 \le s \le n-2$ and $s+2 \le t \le n$, and

$$\begin{aligned}\mathcal{V}_{1,s,n} = \mathrm{Li}_2(1-u_{2sn,n-1}) + \mathrm{Li}_2(1-u_{214,n-1}) + \ln(u_{2sn,n-1})\ln(u_{21s,n-1})\\ + \sum_{i=5}^{s}\Big[\mathrm{Li}_2(1-u_{2,i+2,i-1,i}) - \mathrm{Li}_2(1-u_{12i,i-1}) - \mathrm{Li}_2(1-u_{1,i+2,i-1,i})\\ - \frac{1}{2}\ln(u_{21i,i+2})\ln(u_{1,i+2,i-1,i}) - \frac{1}{2}\ln(u_{12,n-1,i})\ln(u_{1,n-1,i-1,i})\\ - \frac{1}{2}\ln(u_{2,i-1,n-1,i+2})\ln(u_{12i,i-1})\Big] - \frac{\pi^2}{6}, \quad \text{for} \quad 4 \le s \le n-3,\end{aligned} \tag{5.30}$$

where the sum empty sum is understood to vanish for $s = 4$. The function $\mathcal{V}_{1,n-2,n}$ is given by

$$\begin{aligned}\mathcal{V}_{1,n-2,n} = \mathrm{Li}_2(1-u_{2n,n-3,n-2}) - \mathrm{Li}_2(1-u_{12,n-2,n-3}) + \mathrm{Li}_2(1-u_{2,n-3,n,n-1})\\ + \mathrm{Li}_2(1-u_{214,n-1}) - \ln(u_{n1,n-3,n-2})\ln\left(\frac{u_{12,n-2,n-1}}{u_{2,n-3,n-1,n}}\right)\\ + \ln(u_{2,n-3,n,n-1})\ln(u_{21,n-3,n-1}) + \sum_{i=5}^{n-3}\Big[\mathrm{Li}_2(1-u_{2,i+2,i-1,i})\\ - \mathrm{Li}_2(1-u_{12i,i-1}) - \mathrm{Li}_2(1-u_{1,i+2,i-1,i}) - \frac{1}{2}\ln(u_{21i,i+2})\ln(u_{1,i+2,i-1,i})\\ - \frac{1}{2}\ln(u_{12,n-1,i})\ln(u_{1,n-1,i-1,i}) - \frac{1}{2}\ln(u_{2,i-1,n-1,i+2})\ln(u_{12i,i-1})\Big] - \frac{\pi^2}{6}.\end{aligned} \tag{5.31}$$

Finally $\mathcal{V}_{\text{tot}}$ is given by two different formulas, one for $n=8$ and one for $n>8$. For $n=8$ we have

$$8\mathcal{V}_{\text{tot}}^{n=8} = -\mathrm{Li}_2(1-u_{1247}^{-1}) + \frac{1}{2}\sum_{i=4}^{6}\mathrm{Li}_2(1-u_{12i,i+1}^{-1}) + \frac{1}{4}\ln(u_{8145})\ln\left(\frac{u_{1256}u_{3478}}{u_{2367}}\right) + \text{cyclic}\,, \quad (5.32)$$

while for $n>8$ we have

$$\begin{aligned} n\mathcal{V}_{\text{tot}} = &-\mathrm{Li}_2(1-u_{124,n-1}^{-1}) + \frac{1}{2}\sum_{i=4}^{n-2}\mathrm{Li}_2(1-u_{12i,i+1}^{-1}) \\ &+\frac{1}{2}\ln(u_{n134})\ln(u_{136,n-2}) - \frac{1}{2}\ln(u_{n145})\ln(u_{236,n-2}u_{2367}) + v_n + \text{cyclic}\,, \end{aligned} \quad (5.33)$$

where

$$n\text{ odd}: \quad v_n = \sum_{i=4}^{\frac{n-1}{2}}\ln(u_{n1i,i+1})\sum_{j=1}^{i-1}\ln(u_{j,j+1,i+j,n-i+j})\,, \quad (5.34)$$

$$n\text{ even}: \quad v_n = \sum_{i=4}^{\frac{n-1}{2}}\ln(u_{n1i,i+1})\sum_{j=1}^{i-1}\ln(u_{j,j+1,i+j,n-i+j}) + \frac{1}{4}\ln(u_{n1,\frac{n}{2},\frac{n}{2}+1})\sum_{i=1}^{\frac{n-2}{2}}\ln(u_{i,i+1,i+\frac{n}{2},i+\frac{n}{2}+1})\,. \quad (5.35)$$

Chapter 6

Symbol Alphabets from Plabic Graphs

This chapter is based on the publication [118].

A central problem in studying the scattering amplitudes of planar $\mathcal{N} = 4$ super-Yang-Mills (SYM) theory is to understand their analytic structure. Certain amplitudes are known or expected to be expressible in terms of generalized polylogarithm functions. The branch points of any such amplitude are encoded in its *symbol alphabet*—a finite collection of multiplicatively independent functions on kinematic space called *symbol letters* [12]. In [5] it was observed that for $n = 6, 7$, the symbol alphabet of all (then-known) n-particle amplitudes is the set of cluster variables [17, 119] of the $\mathrm{Gr}(4, n)$ Grassmannian cluster algebra [21]. The hypothesis that this remains true to arbitrary loop order provides the bedrock underlying a bootstrap program that has enabled the computation of these amplitudes to impressively high loop order and remains supported by all available evidence (see [13] for a recent review).

For $n > 7$ the $\mathrm{Gr}(4, n)$ cluster algebra has infinitely many cluster variables [119, 21]. While it has long been known that the symbol alphabets of some $n > 7$ amplitudes (such as the two-loop MHV amplitudes [22]) are given by finite subsets of cluster variables, there was no candidate guess for a "theory" to explain why amplitudes would select the subsets that they do. At the same time, it was expected [25, 26] that the symbol alphabets of even MHV amplitudes for $n > 7$ would generically require letters that are not cluster variables—specifically, that are algebraic functions of the Plücker coordinates on $\mathrm{Gr}(4, n)$, of the type that appear in the one-loop four-mass box function [120, 121] (see Appendix 6.7). (Throughout this paper we use the adjective "algebraic" to specifically denote something that is algebraic but not rational.)

As often the case for amplitudes, guesses and expectations are valuable but explicit computations are king. Recently the two-loop eight-particle NMHV amplitude in SYM theory was computed [23], and it was found to have a 198-letter symbol alphabet that can be taken to consist of 180 cluster variables on $\mathrm{Gr}(4, 8)$ and an additional 18 algebraic letters that involve square roots of four-mass box type. (Evidence for the former was presented in [26] based on an analysis of the Landau equations; the latter are consistent with the Landau analysis but less constrained by it.) The result of [23] provided the first concrete new data on symbol alphabets in SYM theory in over eight years. We will refer to this as "the eight-particle alphabet" in this paper since (turning again to hopeful speculation) it may turn out to be the complete symbol alphabet for all eight-particle amplitudes in SYM theory at all loop order.

A few recent papers have sought to explain or postdict the eight-particle symbol alphabet and to clarify its connection to the $\mathrm{Gr}(4, 8)$ cluster algebra. In [122] polytopal realizations of certain compactifications of (the positive part of) the configuration space $\mathrm{Conf}_8(\mathbb{P}^3)$ of eight particles in SYM theory were constructed. These naturally select certain finite subsets of cluster variables, including those in the eight-particle alphabet, and the square roots of four-mass box type make a natural appearance as well. At the same time, an equivalent but dual description, involving certain fans associated to the tropical totally positive Grassmannian [123], appeared simultaneously in [124, 108]. Moreover [124] proposed a construction that precisely computes the 18 algebraic letters of the eight-particle symbol alphabet by (roughly speaking) analyzing how the simplest candidate fan is embedded within the (infinite) $\mathrm{Gr}(4,8)$ cluster fan.

In this paper we show that the algebraic letters of the eight-particle symbol alphabet are precisely reproduced by an alternate construction that only requires solving a set of simple polynomial equations associated to certain plabic graphs. This raises the possibility that symbol alphabets of SYM theory could be encoded more generally in certain plabic graphs. In Sec. 6.1 we introduce our construction with a simple example and then complete the analysis for all graphs relevant to $\mathrm{Gr}(4,6)$ in Sec. 6.2. In Sec. 6.3 we consider an example where the construction yields non-cluster variables of $\mathrm{Gr}(3,6)$ and in Sec. 6.4 we apply it to graphs that precisely reproduce the algebraic functions on $\mathrm{Gr}(4,8)$ that appear in the symbol of [23].

6.1 A Motivational Example

Motivated by [125], in this paper we consider solutions to sets of equations of the form

$$C \cdot Z = 0 \tag{6.1}$$

which are familiar from the study of several closely connected or essentially equivalent amplitude-related objects (leading singularities, Yangian invariants, on-shell forms; see for example [27, 93, 94, 28, 30]).

For the application to SYM theory that will be the focus of this paper, Z is the $n \times 4$ matrix of momentum twistors describing the kinematics of an n-particle scattering event, but it is often instructive to allow Z to be $n \times m$ for general m.

The $k \times n$ matrix $C(f_0, \ldots, f_d)$ in (6.1) parameterizes a d-dimensional cell of the totally non-negative Grassmannian $\mathrm{Gr}(k,n)_{\geq 0}$. Specifically, we always take it to be the boundary measurement of a (reduced, perfectly oriented) plabic graph expressed in terms of the face weights f_α of the graph (see [29, 30]). One could equally well use edge weights, but using face weights allows us to further restrict our attention to bipartite graphs and to eliminate some redundancy; the only residual redundancy of face weights is that they satisfy $\prod_a f_\alpha = 1$ for each graph.

For an illustrative example, consider

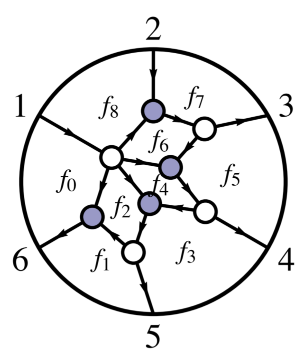

(6.2)

which affords us the opportunity to review the construction of the associated C-matrix from [29]. The graph is *perfectly oriented* because each black (white) vertex has all incident arrows but one pointing in (out). The graph has two sources $\{1,2\}$ and four sinks $\{3,4,5,6\}$ and we begin by forming a $2\times(2+4)$ matrix with the 2×2 identity matrix occupying the source columns:

$$C = \begin{pmatrix} 1 & 0 & c_{13} & c_{14} & c_{15} & c_{16} \\ 0 & 1 & c_{23} & c_{24} & c_{25} & c_{26} \end{pmatrix}. \tag{6.3}$$

The remaining entries are given by

$$c_{ij} = (-1)^s \sum_{p:i\mapsto j} \prod_{\alpha\in\widehat{p}} f_\alpha \tag{6.4}$$

where s is the number of sources strictly between i and j, the sum runs over all allowed paths p from i to j (allowed paths must traverse each edge only in the direction of its arrow) and the product runs over all faces α to the right of p, denoted by $\widehat{p}$. In this manner we find

$$\begin{aligned} c_{13} &= -f_0f_1f_2f_3f_4f_5f_6\,, & c_{23} &= f_0f_1f_2f_3f_4f_5f_6f_8\,, \\ c_{14} &= -f_0f_1f_2f_3f_4(1+f_6)\,, & c_{24} &= f_0f_1f_2f_3f_4f_6f_8\,, \\ c_{15} &= -f_0f_1f_2(1+f_4+f_4f_6)\,, & c_{25} &= f_0f_1f_2f_4f_6f_8\,, \\ c_{16} &= -f_0(1+f_2+f_2f_4+f_2f_4f_6)\,, & c_{26} &= f_0f_2f_4f_6f_8\,. \end{aligned} \tag{6.5}$$

Then for $m = 4$, (6.1) is a system of $2 \times 4 = 8$ equations for the eight independent face weights, which has the solution

$$\begin{aligned} f_0 &= -\frac{\langle 1234\rangle}{\langle 2346\rangle}\,, & f_1 &= -\frac{\langle 2346\rangle}{\langle 2345\rangle}\,, & f_2 &= \frac{\langle 2345\rangle\langle 1236\rangle}{\langle 1234\rangle\langle 2356\rangle}\,, \\ f_3 &= -\frac{\langle 2356\rangle}{\langle 2346\rangle}\,, & f_4 &= \frac{\langle 2346\rangle\langle 1256\rangle}{\langle 2456\rangle\langle 1236\rangle}\,, & f_5 &= -\frac{\langle 2456\rangle}{\langle 2356\rangle}\,, \\ f_6 &= \frac{\langle 2356\rangle\langle 1456\rangle}{\langle 3456\rangle\langle 1256\rangle}\,, & f_7 &= -\frac{\langle 3456\rangle}{\langle 2456\rangle}\,, & f_8 &= -\frac{\langle 2456\rangle}{\langle 1456\rangle}\,, \end{aligned} \tag{6.6}$$

where $\langle ijkl\rangle = \det(Z_i Z_j Z_k Z_l)$ are Plücker coordinates on $\mathrm{Gr}(4,6)$.

We pause here to point out two features evident from (6.6). First, we see that on the solution of (6.1) each face weight evaluates (up to sign) to a product of powers of $\mathrm{Gr}(4,6)$ cluster variables, i.e. to a symbol letter of six-particle amplitudes in SYM theory [12]. Moreover, the cluster variables that appear ($\langle 2346\rangle$, $\langle 2356\rangle$, $\langle 2456\rangle$, and the six frozen variables) constitute a single cluster of the $\mathrm{Gr}(4,6)$ algebra.

The fact that cluster variables of $\mathrm{Gr}(m,n)$ seem to arise, at least in this example, raises the possibility that the symbol alphabets of amplitudes in SYM theory might be given more generally by the face weights of certain plabic graphs evaluated on solutions of $C \cdot Z = 0$. A necessary condition for this to have a chance of working is that the number of independent face weights should equal the number of equations (both eight in the above example); otherwise the equations would have no solutions or continuous families of solutions. For this reason we focus exclusively on graphs for which (6.1) admits isolated solutions for the face weights as functions of generic $n \times m$ Z-matrices; in particular this requires that $d = km$. In such cases the number of isolated solutions to (6.1) is called the *intersection number* of the graph.

The possible connection between plabic graphs and symbol alphabets is especially tantalizing because it manifestly has a chance to account for both issues raised in the introduction: (1) while the number of cluster variables of $\mathrm{Gr}(4,n)$ is infinite for $n > 7$, the number of (reduced) plabic graphs is certainly finite for any fixed n, and (2) graphs with intersection number greater than 1 naturally provide candidate algebraic symbol letters. Our showcase example of (2) is presented in Sec. 6.4.

6.2 Six-Particle Cluster Variables

The problem formulated in the previous section can be considered for any k, m and n. In this section we thoroughly investigate the first case of direct relevance to the amplitudes of SYM theory: $m = 4$ and $n = 6$. Although this case is special for several reasons, it allows us to illustrate some concepts and terminology that will be used in later sections.

Modulo dihedral transformations on the six external points, there are a total of four different types of plabic graph to consider. We begin with the three graphs shown in Fig. 6.1 (a)–(c), which have $k = 2$. These all correspond to the top cell of $\mathrm{Gr}(2,6)_{\geq 0}$ and are related to each other by square moves. Specifically, performing a square move on f_2 of graph (a) yields graph (b), while performing a square move on f_4 of graph (a) yields graph (c). This contrasts with more general cases, for example those considered in the next two sections, where we are in general interested in lower-dimensional cells.

The solution for the face weights of graph (a) (the same as (6.2)) were already given in (6.6), and those of graphs (b) and (c) are derived in (6.27) and (6.29) of Appendix 6.6. The latter two can alternatively be derived from the former via the square move rule (see [29, 30]).

In particular, for graph (b) we have

$$\begin{aligned} f_0^{(b)} &= f_0^{(a)}(1+f_2^{(a)})\,, \\ f_1^{(b)} &= \frac{f_1^{(a)}}{1+1/f_2^{(a)}}\,, \end{aligned} \qquad f_2^{(b)} = \frac{1}{f_2^{(a)}}\,, \qquad \begin{aligned} f_3^{(b)} &= f_3^{(a)}(1+f_2^{(a)})\,, \\ f_4^{(b)} &= \frac{f_4^{(a)}}{1+1/f_2^{(a)}}\,, \end{aligned} \tag{6.7}$$

with f_5, f_6, f_7 and f_8 unchanged, while for graph (c) we have

$$\begin{aligned} f_2^{(c)} &= f_2^{(a)}(1+f_4^{(a)})\,, \\ f_3^{(c)} &= \frac{f_3^{(a)}}{1+1/f_4^{(a)}}\,, \end{aligned} \qquad f_4^{(c)} = \frac{1}{f_4^{(a)}}\,, \qquad \begin{aligned} f_5^{(c)} &= f_5^{(a)}(1+f_4^{(a)})\,, \\ f_6^{(c)} &= \frac{f_6^{(a)}}{1+1/f_4^{(a)}}\,, \end{aligned} \tag{6.8}$$

with f_0, f_1, f_7 and f_8 unchanged.

To every plabic graph one can naturally associate a quiver with nodes labeled by Plücker coordinates of $\mathrm{Gr}(k,n)$. In Fig. 6.1 (d)–(f) we display these quivers for the graphs under consideration, following the source-labeling convention of [126, 127] (see also [128]). Because in this case each graph corresponds to the top cell of $\mathrm{Gr}(2,6)_{\geq 0}$, each labeled quiver is a seed of the $\mathrm{Gr}(2,6)$ cluster algebra. More generally we will have graphs corresponding to lower-dimensional cells, whose labeled quivers are seeds of subalgebras of $\mathrm{Gr}(k,n)$.

Henceforth we refer to a labeled quiver associated to a plabic graph in this manner as an *input cluster*, taking the point of view that solving the equations $C \cdot Z = 0$ associates a collection of functions on $\mathrm{Gr}(m,n)$ to every such input. At the same time, there is a natural way to graphically organize the structure of each of (6.6), (6.27) and (6.29) in terms of an *output cluster*, as we now explain.

First of all we note from (6.27) and (6.29) that, like what happened for graph (a) considered in the previous section, each face weight evaluates (up to sign) to a product of powers

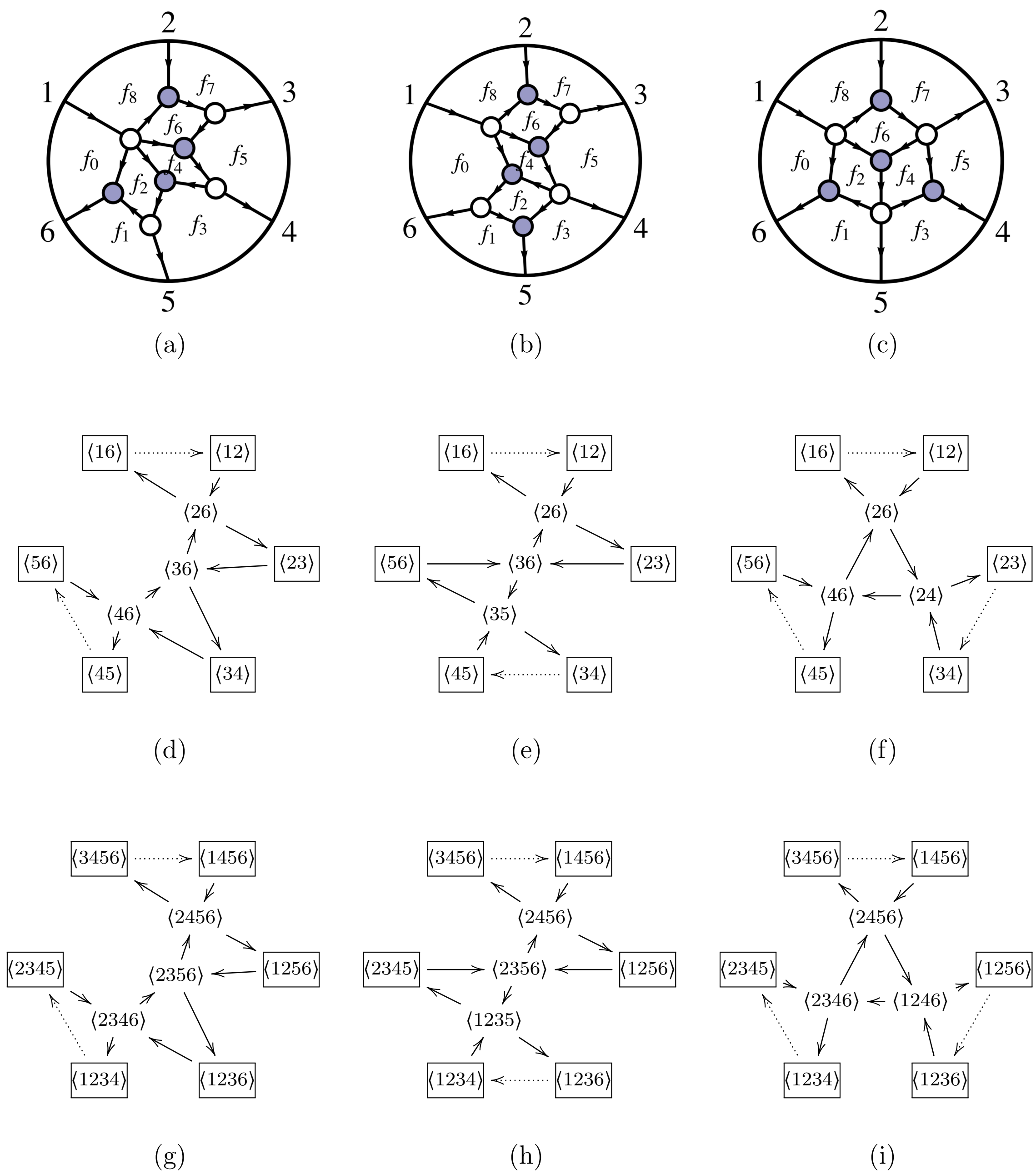

FIGURE 6.1: The three types of (reduced, perfectly orientable, bipartite) plabic graphs corresponding to km-dimensional cells of $\mathrm{Gr}(k,n)_{\geq 0}$ for $k = 2$, $m = 4$ and $n = 6$ are shown in (a)–(c). The associated input and output clusters (see text) are shown in (d)–(f) and (g)–(i) respectively. Lines connecting two frozen nodes are usually omitted, but we include in (g)–(i) the dotted lines (having "black on the right" in the dual plabic graph) that encode (6.6), (6.27) and (6.29) (up to signs).

of $\mathrm{Gr}(4,6)$ cluster variables. Second, again we see that for each graph the collection of variables that appear precisely constitutes a single cluster of $\mathrm{Gr}(4,6)$: suppressing in each case the six frozen variables, we find $\langle 2346\rangle$, $\langle 2356\rangle$ and $\langle 2456\rangle$ for graph (a); $\langle 1235\rangle$, $\langle 2356\rangle$ and $\langle 2456\rangle$ for graph (b); and $\langle 1456\rangle$, $\langle 2346\rangle$, and $\langle 2456\rangle$ for graph (c). Finally, in each case there is a unique way to label the nodes of the quiver not with cluster variables of the "input" cluster algebra $\mathrm{Gr}(2,6)$, as we have done in Fig. 6.1 (d)–(f), but with cluster variables of the "output" cluster algebra $\mathrm{Gr}(4,6)$. We show these output clusters in Fig. 6.1 (g)–(i), using the convention that the face weight (also known as the cluster $\mathcal{X}$-variable) attached to node i is $\prod_j a_j^{b_{ji}}$ where b_{ji} is the (signed) number of arrows from j to i.

For the sake of completeness, we note that there is also (modulo $\mathbb{Z}_6$ cyclic transformations) a single relevant graph with $k=1$:

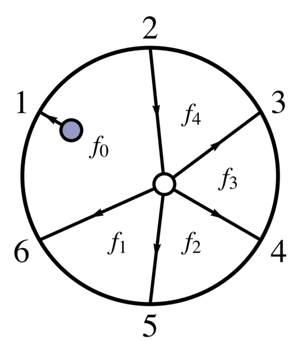

for which the boundary measurement is

$$C = \begin{pmatrix} 0 & 1 & f_0 f_1 f_2 f_3 & f_0 f_1 f_2 & f_0 f_1 & f_0 \end{pmatrix} \tag{6.9}$$

and the solution to $C \cdot Z = 0$ is given by

$$f_0 = \frac{\langle 2345\rangle}{\langle 3456\rangle}, \quad f_1 = -\frac{\langle 2346\rangle}{\langle 2345\rangle}, \quad f_2 = -\frac{\langle 2356\rangle}{\langle 2346\rangle}, \quad f_3 = -\frac{\langle 2456\rangle}{\langle 2356\rangle}, \quad f_4 = -\frac{\langle 3456\rangle}{\langle 2456\rangle}. \tag{6.10}$$

Again the face weights evaluate (up to signs) to simple ratios of $\mathrm{Gr}(4,6)$ cluster variables, though in this case both the input and output quivers are trivial. This graph is an example of the general feature that one can always uplift an n-point plabic graph relevant to our analysis to any value of $n' > n$ by inserting any number of black lollipops. (Graphs with white lollipops never admit solutions to $C{\cdot}Z = 0$ for generic Z.) In the language of symbology, this is in accord with the expectation that the symbol alphabet of an n'-particle amplitude always contains the $\mathbb{Z}_{n'}$ cyclic closure of the symbol alphabet of the corresponding n-particle amplitude.

In this section we have seen that solving $C \cdot Z = 0$ induces a map from clusters of $\mathrm{Gr}(2,6)$ (or subalgebras thereof) to clusters of $\mathrm{Gr}(4,6)$ (or subalgebras thereof). Of course, these two algebras are in any case naturally isomorphic. Although we leave a more detailed exposition for future work, we have also checked for $m = 2$ and $n \le 10$ that every appropriate plabic graph of $\mathrm{Gr}(k,n)$ maps to a cluster of $\mathrm{Gr}(2,n)$ (or a subalgebra thereof), and moreover that this map is onto (every cluster of $\mathrm{Gr}(2,n)$ is obtainable from some plabic graph of $\mathrm{Gr}(k,n)$). However for $m > 2$ the situation is more complicated, as we see in the next section.

6.3 Towards Non-Cluster Variables

Here we discuss some features of graphs for which the solution to $C \cdot Z = 0$ involves quantities that are not cluster variables of $\mathrm{Gr}(m,n)$. A simple example for $k = 2$, $m = 3$, $n = 6$ is the graph

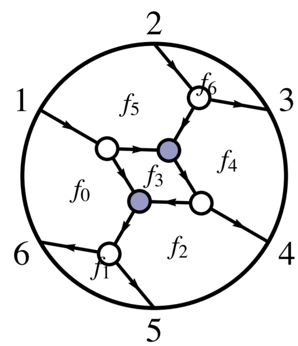

(6.11)

whose boundary measurement has the form (6.3) with

$$
\begin{aligned}
&c_{13} = -0\,, && c_{15} = -f_0 f_1(1+f_3)\,, && c_{23} = f_0 f_1 f_2 f_3 f_4 f_5\,, && c_{25} = f_0 f_1 f_3 f_5\,,\\
&c_{14} = -f_0 f_1 f_2 f_3\,, && c_{16} = -f_0(1+f_3)\,, && c_{24} = f_0 f_1 f_2 f_3 f_5\,, && c_{26} = f_0 f_3 f_5\,.
\end{aligned}
\tag{6.12}
$$

The solution to $C \cdot Z = 0$ is given by

$$
\begin{aligned}
f_0 &= \frac{\langle 123\rangle\langle 145\rangle}{\langle 1\times 4, 2\times 3, 5\times 6\rangle}\,, & f_1 &= -\frac{\langle 146\rangle}{\langle 145\rangle}\,,\\
f_2 &= \frac{\langle 1\times 4, 2\times 3, 5\times 6\rangle}{\langle 234\rangle\langle 146\rangle}\,, & f_3 &= -\frac{\langle 234\rangle\langle 156\rangle}{\langle 123\rangle\langle 456\rangle}\,,\\
f_4 &= -\frac{\langle 124\rangle\langle 456\rangle}{\langle 1\times 4, 2\times 3, 5\times 6\rangle}\,, & f_5 &= \frac{\langle 1\times 4, 2\times 3, 5\times 6\rangle}{\langle 134\rangle\langle 156\rangle}\,,\\
f_6 &= -\frac{\langle 134\rangle}{\langle 124\rangle}\,,
\end{aligned}
\tag{6.13}
$$

which involves four mutable cluster variables $\langle 124\rangle$, $\langle 134\rangle$, $\langle 145\rangle$, and $\langle 146\rangle$ which comprise a cluster of the $\mathrm{Gr}(3,6)$ algebra, together with the quantity

$$
\langle 1\times 4, 2\times 3, 5\times 6\rangle = \langle 123\rangle\langle 456\rangle - \langle 234\rangle\langle 156\rangle\,, \tag{6.14}
$$

which is not a cluster variable of $\mathrm{Gr}(3,6)$.

We can gain some insight into the origin of (6.14) by considering what happens under a square move on f_3. This transforms the face weights to

$$\begin{aligned} &f_0 = \frac{\langle 145\rangle}{\langle 456\rangle}, \quad f_1 = -\frac{\langle 146\rangle}{\langle 145\rangle}, \quad f_2 = -\frac{\langle 156\rangle}{\langle 146\rangle}, \quad f_3 = -\frac{\langle 123\rangle\langle 456\rangle}{\langle 234\rangle\langle 156\rangle}, \\ &f_4 = -\frac{\langle 124\rangle}{\langle 123\rangle}, \quad f_5 = -\frac{\langle 234\rangle}{\langle 134\rangle}, \quad f_6 = -\frac{\langle 134\rangle}{\langle 124\rangle}, \end{aligned} \tag{6.15}$$

leaving four mutable cluster variables $\langle 124\rangle$, $\langle 134\rangle$, $\langle 145\rangle$, and $\langle 146\rangle$ which comprise a cluster of the $\mathrm{Gr}(3,6)$ algebra. However, it is not possible to associate a labeled "output" quiver to (6.15) in the usual way, as we did for the examples in the previous section.

To turn this story around: had we started not with (6.11) but with its square-moved partner, we would have encountered (6.15) and then noted that performing a square move back to (6.11) would necessarily introduce the multiplicative factor

$$1 + f_3 = -\frac{\langle 1\times 4, 2\times 3, 5\times 6\rangle}{\langle 234\rangle\langle 156\rangle} \tag{6.16}$$

into four of the face weights.

The example considered in this section provides an opportunity to comment on the connection of our work to the study of cluster adjacency for Yangian invariants. In [81, 65] it was noted in several examples, and conjectured to be true in general, that the set of factors appearing in the denominator of any Yangian invariant with intersection number 1 are cluster variables of $\mathrm{Gr}(4,n)$ that appear together in a cluster. This was proven to be true for all Yangian invariants in the $m = 2$ toy model of SYM theory in [105] and for all $m = 4$ $\mathrm{N}^2\mathrm{MHV}$ Yangian invariants in [129]. We recall from [30, 130] that the Yangian invariant associated to a plabic graph (or, to use essentially equivalent language, the form associated to an on-shell diagram) is given by $d\log f_1 \wedge \cdots \wedge d\log f_d$. One of our motivations for studying the conjecture that the face weights associated to any plabic graph always evaluate on the solution of $C \cdot Z = 0$ to products of powers of cluster variables was that it would immediately imply cluster adjacency for Yangian invariants. Although the graph (6.11) violates this stronger conjecture, it does not violate cluster adjacency because on-shell forms are invariant under square moves [30]. Therefore, even though $\langle 1 \times 4, 2 \times 3, 5 \times 6 \rangle$ appears in individual face weights of (6.13), it must drop out of the associated on-shell form because it is absent from (6.15).

6.4 Algebraic Eight-Particle Symbol Letters

One reason it is obvious that the solutions of $C \cdot Z = 0$ cannot always be written in terms of cluster variables of $\mathrm{Gr}(m,n)$ is that for graphs with intersection number greater than 1 the solutions will necessarily involve algebraic functions of Plücker coordinates, whereas cluster variables are always rational.

The simplest example of this phenomenon occurs for $k = 2$, $m = 4$ and $n = 8$, for which there are four relevant plabic graphs in two cyclic classes. Let us start with

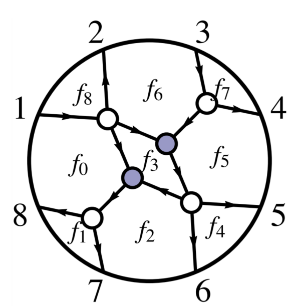

(6.17)

which has boundary measurement

$$C = \begin{pmatrix} 1 & c_{12} & 0 & c_{14} & c_{15} & c_{16} & c_{17} & c_{18} \\ 0 & c_{32} & 1 & c_{34} & c_{35} & c_{36} & c_{37} & c_{38} \end{pmatrix} \tag{6.18}$$

with

$$c_{12} = f_0 f_1 f_2 f_3 f_4 f_5 f_6 f_7\,, \qquad c_{14} = -0\,, \qquad c_{15} = -f_0 f_1 f_2 f_3 f_4\,, \tag{6.19}$$

$$c_{16} = -f_0 f_1 f_2 f_3\,, \qquad c_{17} = -f_0 f_1 (1 + f_3)\,, \qquad c_{18} = -f_0 (1 + f_3)\,, \tag{6.20}$$

$$c_{32} = 0\,, \qquad c_{34} = f_0 f_1 f_2 f_3 f_4 f_5 f_6 f_8\,, \qquad c_{35} = f_0 f_1 f_2 f_3 f_4 f_6 f_8\,, \tag{6.21}$$

$$c_{36} = f_0 f_1 f_2 f_3 f_6 f_8\,, \qquad c_{37} = f_0 f_1 f_3 f_6 f_8\,, \qquad c_{38} = f_0 f_3 f_6 f_8\,. \tag{6.22}$$

The solution to $C \cdot Z = 0$ for generic $Z \in \mathrm{Gr}(4,8)$ can be written as

$$\begin{aligned}
f_0 &= \sqrt{\frac{\langle 7(12)(34)(56)\rangle \langle 1234\rangle}{a_5 \langle 2(34)(56)(78)\rangle \langle 3478\rangle}}\,, & f_5 &= \sqrt{\frac{a_1 a_6 a_9 \langle 3(12)(56)(78)\rangle \langle 5678\rangle}{a_4 a_7 \langle 6(12)(34)(78)\rangle \langle 3478\rangle}}\,, \\
f_1 &= -\sqrt{\frac{a_7 \langle 8(12)(34)(56)\rangle}{\langle 7(12)(34)(56)\rangle}}\,, & f_6 &= -\sqrt{\frac{a_3 \langle 1(34)(56)(78)\rangle \langle 3478\rangle}{a_2 \langle 4(12)(56)(78)\rangle \langle 1278\rangle}}\,, \\
f_2 &= -\sqrt{\frac{a_4 \langle 5(12)(34)(78)\rangle \langle 3478\rangle}{a_8 \langle 8(12)(34)(56)\rangle \langle 3456\rangle}}\,, & f_7 &= -\sqrt{\frac{a_2 \langle 4(12)(56)(78)\rangle}{a_1 \langle 3(12)(56)(78)\rangle}}\,, \\
f_3 &= \sqrt{\frac{a_8 \langle 1278\rangle \langle 3456\rangle}{a_9 \langle 1234\rangle \langle 5678\rangle}}\,, & f_8 &= -\sqrt{\frac{a_5 \langle 2(34)(56)(78)\rangle}{a_3 \langle 1(34)(56)(78)\rangle}}\,, \\
f_4 &= -\sqrt{\frac{\langle 6(12)(34)(78)\rangle}{a_6 \langle 5(12)(34)(78)\rangle}}\,,
\end{aligned} \tag{6.23}$$

where

$$\langle a(bc)(de)(fg)\rangle \equiv \langle abde\rangle\langle acfg\rangle - \langle abfg\rangle\langle acde\rangle \tag{6.24}$$

and the nine a_i provide a (multiplicative) basis for the algebraic letters of the eight-particle symbol alphabet that contain the four-mass box square root $\sqrt{\Delta_{1357}}$, as reviewed in Appendix 6.7.

The nine face weights shown in (6.23) satisfy $\prod f_\alpha = 1$ so only eight are multiplicatively independent. It is easy to check that they remain multiplicatively independent if one sets all of the Plücker coordinates and brackets of the form (6.24) to one. Therefore, the f_α (multiplicatively) only span an eight-dimensional subspace of the full nine-dimensional space spanned by the nine algebraic letters. We could try building an eight-particle alphabet by taking any subset of eight of the face weights as basis elements (i.e., letters), but we would always be one letter short.

Fortunately there is a second plabic graph relevant to $\sqrt{\Delta_{1357}}$: the one obtained by performing a square move on f_3 of (6.17). As is by now familiar, performing the square move introduces one new multiplicative factor into the face weights:

$$1 + f_3 = \sqrt{\frac{\langle 1256\rangle\langle 3478\rangle}{a_9\langle 1234\rangle\langle 5678\rangle}}\,, \tag{6.25}$$

which precisely supplies the ninth, missing letter! To summarize: the union of the nine face weights associated to the graph (6.17), and the nine associated to its square-move partner, multiplicatively span the nine-dimensional space of $\sqrt{\Delta_{1357}}$-containing symbol letters in the eight-particle alphabet of [23].

The same story applies to the graphs obtained by cycling the external indices on (6.17) by one—their face weights provide all nine algebraic letters involving $\sqrt{\Delta_{2468}}$.

Of course it would be very interesting to thoroughly study the numerous plabic graphs relevant to $m = 4$, $n = 8$ that have intersection number 1. In particular it would be interesting to see if they encode all 180 of the rational (i.e., $\mathrm{Gr}(4,8)$ cluster variable) symbol letters of [23], and whether they generate additional cluster variables such as those obtained from the constructions of [124, 122, 108].

Before concluding this section let us comment briefly on "k" since one may be confused why the plabic graph (6.17), which has $k = 2$ and is therefore associated to an N^2MHV leading singularity, could be relevant for symbol alphabets of NMHV amplitudes. The symbol letters of an N^kMHV amplitude reveal all of its singularities, including multiple discontinuities that can be accessed only after a suitable analytic continuation. Physically these are computed by cuts involving lower-loop amplitudes that can have $k' > k$. Indeed the expectation that symbol letters of lower-loop higher-k amplitudes influence those of higher-loop lower-k amplitudes is manifest in the $\overline{Q}$-bar equation technology [22, 131, 132] underlying the computation of [23]. Moreover there is indirect evidence [133] that the symbol alphabet of the L-loop n-particle N^kMHV amplitude in SYM theory is independent of both k and L (beyond certain accidental shortenings that may occur for small k or L). This suggests that for the purpose of applying our construction to "*the* n-particle symbol alphabet" one should consider all relevant n-point plabic graphs regardless of k.

6.5 Discussion

The problem of "explaining" the symbol alphabets of n-particle amplitudes in SYM theory apparently requires, for $n > 7$, a mechanism for identifying finite sets of functions on $\mathrm{Gr}(4,n)$ that include some subset of the cluster variables of the associated cluster algebra, together with certain non-cluster variables that are algebraic functions of the Plücker coordinates.

In this paper we have initiated the study of one candidate mechanism that manifestly satisfies both criteria and may be of independent mathematical interest. Specifically, to every (reduced, perfectly oriented) plabic graph of $\mathrm{Gr}(k,n)_{\geq 0}$ that parameterizes a cell of dimension mk, one can naturally associate a collection of mk functions of Plücker coordinates on $\mathrm{Gr}(m,n)$.

We have seen that for some graphs the output of this procedure is naturally associated to a seed of the $\mathrm{Gr}(m,n)$ cluster algebra; for some graphs the output is a cluster's worth of cluster variables that do not correspond to a seed but rather behave "badly" under mutations (this means they transform into things which are not cluster variables under square moves on the input plabic graph); and finally for some graphs the output involves non-cluster variables including, when the intersection number is greater than 1, algebraic functions.

We leave a more thorough investigation of this problem for future work. The "smoking gun" that this procedure may be relevant to symbol alphabets in SYM theory is provided by the example discussed in Sec. 6.4, which successfully postdicts precisely the 18 multiplicatively independent algebraic letters that were recently found to appear in the two-loop eight-particle NMHV amplitude [23]. Our construction provides an alternative to the similar postdiction made recently in [124].

It is interesting to note that since for $m = 4$, $n = 8$ there are no other relevant plabic graphs having intersection number > 1, beyond those already considered Sec. 6.4, our construction has no room for any additional algebraic letters for eight-particle amplitudes. Therefore, if it is true that the face weights of plabic graphs, evaluated on the locus $C \cdot Z = 0$, provide symbol alphabets for general amplitudes, then it necessarily follows that no eight-particle amplitude, at any loop order, can have any algebraic symbol letters beyond the 18 discovered in [23].

At first glance this rigidity seems to stand in contrast to the constructions of [122, 124, 108] which each involve some amount of choice—having to do with how coarse or fine one chooses one's tropical fan, or equivalently how many factors to include in the Minkowski sum when building the dual polytope. But in fact our construction has a choice with a similar smell. When we say that we start with the C-matrix associated to a plabic graph, that automatically restricts us to very special clusters of $\mathrm{Gr}(k,n)$—those that contain only Plücker coordinates. Clusters containing more complicated, non-Plücker cluster variables are not associated to plabic graphs. One certainly could contemplate solving the $C \cdot Z = 0$ equations for C given by a "non-plabic" cluster parameterization of some cell of $\mathrm{Gr}(k,n)_{\geq 0}$ and it would be interesting to map out the landscape of possibilities.

It has been a long-standing problem to understand the precise connection between the $\mathrm{Gr}(k,n)$ cluster structure exhibited [30] at the level of integrands in SYM theory and the $\mathrm{Gr}(4,n)$ cluster structure exhibited [5] by integrated amplitudes. It was pointed out in [125] that the $C \cdot Z = 0$ equations provide a concrete link between the two, and our results shed some initial light on this intriguing but still very mysterious problem. In some sense we can think of the "input" and "output" clusters defined in Sec. 6.2 as "integrand" and "integrated" clusters with respect to the auxiliary Grassmannian space. (See the last paragraph of Sec. 6.4 for some comments on why k "disappears" upon integration.) Although we have seen that the latter are not in general clusters at all, the example of Sec. 6.4 suggests that they may be even better: exactly what is needed for the symbol alphabets of SYM theory.

Note Added: The preprint [134] appeared on arXiv shortly after and has significant overlap with the result presented in this note.

6.6 Some Six-Particle Details

Here we assemble some details of the calculation for graphs (b) and (c) of Fig. 6.1. The boundary measurement for graph (b) has the form (6.3) with

$$\begin{aligned}
c_{13} &= -f_0 f_1 f_2 f_3 f_4 f_5 f_6\,, & c_{23} &= f_0 f_1 f_2 f_3 f_4 f_5 f_6 f_8\,,\\
c_{14} &= -f_0 f_1 f_2 f_3 f_4 (1+f_6)\,, & c_{24} &= f_0 f_1 f_2 f_3 f_4 f_6 f_8\,,\\
c_{15} &= -f_0 f_1 (1+f_4+f_2 f_4+f_4 f_6+f_2 f_4 f_6)\,, & c_{25} &= f_0 f_1 f_4 f_6 f_8 (1+f_2)\,,\\
c_{16} &= -f_0 (1+f_4+f_4 f_6)\,, & c_{26} &= f_0 f_4 f_6 f_8\,,
\end{aligned} \tag{6.26}$$

and the solution to $C \cdot Z = 0$ is given by

$$\begin{aligned}
f_0^{(b)} &= -\frac{\langle 1235\rangle}{\langle 2356\rangle}\,, & f_1^{(b)} &= -\frac{\langle 1236\rangle}{\langle 1235\rangle}\,, & f_2^{(b)} &= \frac{\langle 1234\rangle\langle 2356\rangle}{\langle 2345\rangle\langle 1236\rangle}\,,\\
f_3^{(b)} &= -\frac{\langle 1235\rangle}{\langle 1234\rangle}\,, & f_4^{(b)} &= \frac{\langle 2345\rangle\langle 1256\rangle}{\langle 1235\rangle\langle 2456\rangle}\,, & f_5^{(b)} &= -\frac{\langle 2456\rangle}{\langle 2356\rangle}\,,\\
f_6^{(b)} &= \frac{\langle 2356\rangle\langle 1456\rangle}{\langle 3456\rangle\langle 1256\rangle}\,. & f_7^{(b)} &= -\frac{\langle 3456\rangle}{\langle 2456\rangle}\,, & f_8^{(b)} &= -\frac{\langle 2456\rangle}{\langle 1456\rangle}\,.
\end{aligned} \tag{6.27}$$

The boundary measurement for graph (c) has

$$\begin{aligned} c_{13} &= -f_0 f_1 f_2 f_3 f_4 f_5 f_6\,, & c_{23} &= f_0 f_1 f_2 f_3 f_4 f_5 f_6 f_8\,, \\ c_{14} &= -f_0 f_1 f_2 f_3 (1 + f_6 + f_4 f_6)\,, & c_{24} &= f_0 f_1 f_2 f_3 f_6 f_8 (1 + f_4)\,, \\ c_{15} &= -f_0 f_1 f_2 (1 + f_6)\,, & c_{25} &= f_0 f_1 f_2 f_6 f_8\,, \\ c_{16} &= -f_0 (1 + f_2 + f_2 f_6)\,, & c_{26} &= f_0 f_2 f_6 f_8\,, \end{aligned} \tag{6.28}$$

and the solution to $C \cdot Z = 0$ is

$$\begin{aligned} f_0^{(c)} &= -\frac{\langle 1234\rangle}{\langle 2346\rangle}\,, & f_1^{(c)} &= -\frac{\langle 2346\rangle}{\langle 2345\rangle}\,, & f_2^{(c)} &= \frac{\langle 2345\rangle\langle 1246\rangle}{\langle 1234\rangle\langle 2456\rangle}\,, \\ f_3^{(c)} &= -\frac{\langle 1256\rangle}{\langle 1246\rangle}\,, & f_4^{(c)} &= \frac{\langle 2456\rangle\langle 1236\rangle}{\langle 2346\rangle\langle 1256\rangle}\,, & f_5^{(c)} &= -\frac{\langle 1246\rangle}{\langle 1236\rangle}\,, \\ f_6^{(c)} &= \frac{\langle 1456\rangle\langle 2346\rangle}{\langle 3456\rangle\langle 1246\rangle}\,, & f_7^{(c)} &= -\frac{\langle 3456\rangle}{\langle 2456\rangle}\,, & f_8^{(c)} &= -\frac{\langle 2456\rangle}{\langle 1456\rangle}\,. \end{aligned} \tag{6.29}$$

6.7 Notation for Algebraic Eight-Particle Symbol Letters

Here we review some details from [23] to set the notation used in Sec. 6.4. There are two basic square roots of four-mass box type that appear in symbol letters of eight-particle amplitudes. These are $\sqrt{\Delta_{1357}}$ and $\sqrt{\Delta_{2468}}$ with

$$\Delta_{1357} = (\langle 1256\rangle\langle 3478\rangle - \langle 1278\rangle\langle 3456\rangle - \langle 1234\rangle\langle 5678\rangle)^2 - 4\langle 1234\rangle\langle 3456\rangle\langle 5678\rangle\langle 1278\rangle \tag{6.30}$$

and Δ_{2468} given by cycling every index by 1 (mod 8).

The eight-particle symbol alphabet can be written in terms of 180 $\mathrm{Gr}(4,8)$ cluster variables, plus 9 letters that are rational functions of Plücker coordinates and $\sqrt{\Delta_{1357}}$ and another 9 that are rational functions of Plücker coordinates and $\sqrt{\Delta_{2468}}$. We focus on the first 9 as the latter is a cyclic copy of the same story.

There are many different ways to write a basis for the eight-particle symbol alphabet as the various letters one can form satisfy numerous multiplicative identities among each other. For the sake of definiteness we use the basis provided in the ancillary Mathematica file attached to [23]. The choice of basis made there starts by defining

$$\begin{aligned} z &= \frac{1}{2}\left(1 + u - v + \sqrt{(1-u-v)^2 - 4uv}\right), \\ \bar{z} &= \frac{1}{2}\left(1 + u - v - \sqrt{(1-u-v)^2 - 4uv}\right) \end{aligned} \tag{6.31}$$

in terms of the familiar eight-particle cross ratios

$$u = \frac{\langle 1278\rangle\langle 3456\rangle}{\langle 1256\rangle\langle 3478\rangle}, \qquad v = \frac{\langle 1234\rangle\langle 5678\rangle}{\langle 1256\rangle\langle 3478\rangle}. \tag{6.32}$$

Note that the square root appearing in (6.31) is

$$\sqrt{(1-u-v)^2 - 4uv} = \frac{\sqrt{\Delta_{1357}}}{\langle 1256\rangle\langle 3478\rangle}. \tag{6.33}$$

Then a basis for the algebraic letters of the symbol alphabet is given by

$$\begin{aligned} a_1 &= \left.\frac{x_a - z}{x_a - \bar{z}}\right|_{i\to i+6}, & a_2 &= \left.\frac{x_b - z}{x_b - \bar{z}}\right|_{i\to i+6}, & a_3 &= -\left.\frac{x_c - z}{x_c - \bar{z}}\right|_{i\to i+6}, \\ a_4 &= -\left.\frac{x_d - z}{x_d - \bar{z}}\right|_{i\to i+4}, & a_5 &= -\left.\frac{x_d - z}{x_d - \bar{z}}\right|_{i\to i+6}, & a_6 &= \left.\frac{x_e - z}{x_e - \bar{z}}\right|_{i\to i+4}, \\ a_7 &= \left.\frac{x_e - z}{x_e - \bar{z}}\right|_{i\to i+6}, & a_8 &= \frac{z}{\bar{z}}, & a_9 &= \frac{1-z}{1-\bar{z}}, \end{aligned} \tag{6.34}$$

where the x's are defined in (13) of [23]. While the overall sign of a symbol letter is irrelevant, we have taken the liberty of putting a minus sign in front of a_3, a_4 and a_5 to ensure that each of the nine a_i, indeed each individual factor appearing in (6.23), is positive-valued for $Z \in \mathrm{Gr}(4,8)_{>0}$.

Bibliography

[1] R. P. Feynman, "Space - time approach to quantum electrodynamics," Phys. Rev. **76**, 769-789 (1949) doi:10.1103/PhysRev.76.769

[2] S. J. Parke and T. R. Taylor, "An Amplitude for n Gluon Scattering," Phys. Rev. Lett. **56**, 2459 (1986). doi:10.1103/PhysRevLett.56.2459.

[3] J. M. Drummond, J. Henn, G. P. Korchemsky and E. Sokatchev, "Dual superconformal symmetry of scattering amplitudes in N=4 super-Yang-Mills theory," Nucl. Phys. B **828**, 317-374 (2010) doi:10.1016/j.nuclphysb.2009.11.022 [arXiv:0807.1095 [hep-th]].

[4] A. Hodges, "Eliminating spurious poles from gauge-theoretic amplitudes," JHEP **1305**, 135 (2013) doi:10.1007/JHEP05(2013)135 [arXiv:0905.1473 [hep-th]].

[5] J. Golden, A. B. Goncharov, M. Spradlin, C. Vergu and A. Volovich, "Motivic Amplitudes and Cluster Coordinates," JHEP **1401**, 091 (2014) doi:10.1007/JHEP01(2014)091 [arXiv:1305.1617 [hep-th]].

[6] J. M. Maldacena, "The Large N limit of superconformal field theories and supergravity," Int. J. Theor. Phys. **38**, 1113-1133 (1999) doi:10.1023/A:1026654312961 [arXiv:hep-th/9711200 [hep-th]].

[7] J. de Boer and S. N. Solodukhin, "A Holographic reduction of Minkowski space-time," Nucl. Phys. B **665**, 545-593 (2003) doi:10.1016/S0550-3213(03)00494-2 [arXiv:hep-th/0303006 [hep-th]].

[8] S. Pasterski, S. H. Shao and A. Strominger, "Flat Space Amplitudes and Conformal Symmetry of the Celestial Sphere," arXiv:1701.00049 [hep-th].

[9] S. Pasterski and S. H. Shao, "A Conformal Basis for Flat Space Amplitudes," arXiv:1705.01027 [hep-th].

[10] R. Penrose, "The Apparent shape of a relativistically moving sphere," Proc. Cambridge Phil. Soc. **55**, 137-139 (1959) doi:10.1017/S0305004100033776

[11] J. M. Drummond, J. M. Henn and J. Plefka, "Yangian symmetry of scattering amplitudes in N=4 super Yang-Mills theory," JHEP **05**, 046 (2009) doi:10.1088/1126-6708/2009/05/046 [arXiv:0902.2987 [hep-th]].

[12] A. B. Goncharov, M. Spradlin, C. Vergu and A. Volovich, "Classical Polylogarithms for Amplitudes and Wilson Loops," Phys. Rev. Lett. **105**, 151605 (2010) doi:10.1103/PhysRevLett.105.151605 [arXiv:1006.5703 [hep-th]].

[13] S. Caron-Huot, L. J. Dixon, J. M. Drummond, F. Dulat, J. Foster, Ö. Gürdoğan, M. von Hippel, A. J. McLeod and G. Papathanasiou, "The Steinmann Cluster Bootstrap for $N = 4$ Super Yang-Mills Amplitudes," PoS **CORFU2019**, 003 (2020) doi:10.22323/1.376.0003 [arXiv:2005.06735 [hep-th]].

[14] M. Srednicki, "Quantum field theory."

[15] R. Penrose, "Twistor algebra," J. Math. Phys. **8**, 345 (1967) doi:10.1063/1.1705200

[16] R. Penrose and M. A. H. MacCallum, "Twistor theory: An Approach to the quantization of fields and space-time," Phys. Rept. **6**, 241-316 (1972) doi:10.1016/0370-1573(73)90008-2

[17] S. Fomin and A. Zelevinsky, "Cluster algebras I: Foundations," J. Am. Math. Soc. **15**, no. 2, 497 (2002) [arXiv:math/0104151].

[18] S. Fomin, L. Williams and A. Zelevinsky, "Introduction to Cluster Algebras. Chapters 1-3," arXiv:1608.05735 [math.CO].

[19] S. Fomin, L. Williams and A. Zelevinsky, "Introduction to Cluster Algebras. Chapters 4-5," arXiv:1707.07190 [math.CO].

[20] S. Fomin, L. Williams and A. Zelevinsky, "Introduction to Cluster Algebras. Chapter 6," arXiv:2008.09189 [math.AC].

[21] J. S. Scott, "Grassmannians and Cluster Algebras," Proc. Lond. Math. Soc. (3) **92**, no. 2, 345 (2006) [arXiv:math/0311149].

[22] S. Caron-Huot, "Superconformal symmetry and two-loop amplitudes in planar N=4 super Yang-Mills," JHEP **12**, 066 (2011) doi:10.1007/JHEP12(2011)066 [arXiv:1105.5606 [hep-th]].

[23] S. He, Z. Li and C. Zhang, "Two-loop Octagons, Algebraic Letters and $\bar{Q}$ Equations," Phys. Rev. D **101**, no.6, 061701 (2020) doi:10.1103/PhysRevD.101.061701 [arXiv:1911.01290 [hep-th]].

[24] S. He, Z. Li and C. Zhang, "The symbol and alphabet of two-loop NMHV amplitudes from $\bar{Q}$ equations," [arXiv:2009.11471 [hep-th]].

[25] I. Prlina, M. Spradlin, J. Stankowicz, S. Stanojevic and A. Volovich, "All-Helicity Symbol Alphabets from Unwound Amplituhedra," JHEP **05**, 159 (2018) doi:10.1007/JHEP05(2018)159 [arXiv:1711.11507 [hep-th]].

[26] I. Prlina, M. Spradlin, J. Stankowicz and S. Stanojevic, "Boundaries of Amplituhedra and NMHV Symbol Alphabets at Two Loops," JHEP **04**, 049 (2018) [arXiv:1712.08049 [hep-th]].

[27] N. Arkani-Hamed, F. Cachazo, C. Cheung and J. Kaplan, "A Duality For The S Matrix," JHEP **03**, 020 (2010) doi:10.1007/JHEP03(2010)020 [arXiv:0907.5418 [hep-th]].

[28] J. M. Drummond and L. Ferro, "The Yangian origin of the Grassmannian integral," JHEP **12**, 010 (2010) doi:10.1007/JHEP12(2010)010 [arXiv:1002.4622 [hep-th]].

[29] A. Postnikov, "Total Positivity, Grassmannians, and Networks," http://math.mit.edu/~apost/papers/tpgrass.pdf.

[30] N. Arkani-Hamed, J. L. Bourjaily, F. Cachazo, A. B. Goncharov, A. Postnikov and J. Trnka, "Grassmannian Geometry of Scattering Amplitudes," doi:10.1017/CBO9781316091548 arXiv:1212.5605 [hep-th].

[31] A. Schreiber, A. Volovich and M. Zlotnikov, "Tree-level gluon amplitudes on the celestial sphere," Phys. Lett. B **781**, 349-357 (2018) doi:10.1016/j.physletb.2018.04.010 [arXiv:1711.08435 [hep-th]].

[32] J. de Boer and S. N. Solodukhin, “A Holographic reduction of Minkowski space-time,” Nucl. Phys. B **665**, 545 (2003) doi:10.1016/S0550-3213(03)00494-2 [hep-th/0303006]. T. Banks, “The Super BMS Algebra, Scattering and Holography,” arXiv:1403.3420 [hep-th]. A. Ashtekar, “Asymptotic Quantization: Based On 1984 Naples Lectures,“ Naples, Italy: Bibliopolis,(1987). C. Cheung, A. de la Fuente and R. Sundrum, “4D scattering amplitudes and asymptotic symmetries from 2D CFT,” JHEP **1701**, 112 (2017) doi:10.1007/JHEP01(2017)112 [arXiv:1609.00732 [hep-th]]. D. Kapec, P. Mitra, A. M. Raclariu and A. Strominger, “2D Stress Tensor for 4D Gravity,” Phys. Rev. Lett. **119**, no. 12, 121601 (2017) doi:10.1103/PhysRevLett.119.121601 [arXiv:1609.00282 [hep-th]]. D. Kapec, V. Lysov, S. Pasterski and A. Strominger, “Semiclassical Virasoro symmetry of the quantum gravity $\mathcal{S}$-matrix,” JHEP **1408**, 058 (2014) doi:10.1007/JHEP08(2014)058 [arXiv:1406.3312 [hep-th]]. F. Cachazo and A. Strominger, “Evidence for a New Soft Graviton Theorem,” arXiv:1404.4091 [hep-th]. A. Strominger, “Lectures on the Infrared Structure of Gravity and Gauge Theory,” arXiv:1703.05448 [hep-th].

[33] C. Cardona and Y. t. Huang, “S-matrix singularities and CFT correlation functions,” JHEP **1708**, 133 (2017) doi:10.1007/JHEP08(2017)133 [arXiv:1702.03283 [hep-th]].

[34] S. Pasterski, S. H. Shao and A. Strominger, “Gluon Amplitudes as 2d Conformal Correlators,” arXiv:1706.03917 [hep-th].

[35] H. T. Lam and S. H. Shao, “Conformal Basis, Optical Theorem, and the Bulk Point Singularity,” arXiv:1711.06138 [hep-th].

[36] N. Banerjee, S. Banerjee, S. Atul Bhatkar and S. Jain, "Conformal Structure of Massless Scalar Amplitudes Beyond Tree level," JHEP **1804**, 039 (2018) doi:10.1007/JHEP04(2018)039 [arXiv:1711.06690 [hep-th]].

[37] F. Cachazo, S. He and E. Y. Yuan, "Scattering of Massless Particles in Arbitrary Dimensions," Phys. Rev. Lett. **113**, no. 17, 171601 (2014) doi:10.1103/PhysRevLett.113.171601 [arXiv:1307.2199 [hep-th]]. N. Arkani-Hamed, F. Cachazo, C. Cheung and J. Kaplan, "A Duality For The S Matrix," JHEP **1003**, 020 (2010) doi:10.1007/JHEP03(2010)020 [arXiv:0907.5418 [hep-th]]. R. Roiban, M. Spradlin and A. Volovich, "On the tree level S matrix of Yang-Mills theory," Phys. Rev. D **70**, 026009 (2004) doi:10.1103/PhysRevD.70.026009 [hep-th/0403190]. N. Arkani-Hamed, F. Cachazo, C. Cheung and J. Kaplan, "The S-Matrix in Twistor Space," JHEP **1003**, 110 (2010) doi:10.1007/JHEP03(2010)110 [arXiv:0903.2110 [hep-th]]. N. Arkani-Hamed, Y. Bai and T. Lam, "Positive Geometries and Canonical Forms," JHEP **1711**, 039 (2017) doi:10.1007/JHEP11(2017)039 [arXiv:1703.04541 [hep-th]].

[38] K. Aomoto, M. Kita, "Theory of Hypergeometric Functions," (Springer-Verlag, Tokyo, 2011), DOI:10.1007/978-4-431-53938-4, ISBN 9784431539384.

[39] V. G. Knizhnik and A. B. Zamolodchikov, "Current algebra and Wess-Zumino model in two dimensions", Nucl. Phys. B., 247 1 (1984), pp. 83-103, doi:10.1016/0550-3213(84)90374-2.

[40] Y. Abe, "A note on generalized hypergeometric functions, KZ solutions, and gluon amplitudes," Nucl. Phys. B **907**, 107 (2016) doi:10.1016/j.nuclphysb.2016.03.032 [arXiv:1512.06476 [hep-th]].

[41] L. Ferro, T. Lukowski and M. Staudacher, "$\mathcal{N}$ = 4 scattering amplitudes and the deformed Grassmannian," Nucl. Phys. B **889**, 192 (2014) doi:10.1016/j.nuclphysb.2014.10.012 [arXiv:1407.6736 [hep-th]].

[42] R. Britto, B. Feng, R. Roiban, M. Spradlin and A. Volovich, "All split helicity tree-level gluon amplitudes," Phys. Rev. D **71**, 105017 (2005) doi:10.1103/PhysRevD.71.105017 [hep-th/0503198].

[43] D. Oprisa and S. Stieberger, "Six gluon open superstring disk amplitude, multiple hypergeometric series and Euler-Zagier sums," hep-th/0509042.

[44] C. R. Mafra, O. Schlotterer and S. Stieberger, "Complete N-Point Superstring Disk Amplitude II. Amplitude and Hypergeometric Function Structure," Nucl. Phys. B **873**, 461 (2013) doi:10.1016/j.nuclphysb.2013.04.022 [arXiv:1106.2646 [hep-th]].

[45] I. M. Gel'fand, "General theory of hypergeometric functions", Dokl. Akad. Nauk SSSR 288 (1986), no. 1, 14-18.

[46] I. M. Gel'fand and M. M. Kapranov and A. V. Zelevinsky, "Generalized Euler integrals and A-hypergeometric functions", Adv. Math., 84 2 (1990), pp. 255-271, doi:10.1016/0001-8708(90)90048-R.

[47] D. Nandan, A. Schreiber, A. Volovich and M. Zlotnikov, "Celestial Amplitudes: Conformal Partial Waves and Soft Limits," JHEP **10**, 018 (2019) doi:10.1007/JHEP10(2019)018 [arXiv:1904.10940 [hep-th]].

[48] J. de Boer and S. N. Solodukhin, "A Holographic reduction of Minkowski spacetime," Nucl. Phys. B **665**, 545 (2003) doi:10.1016/S0550-3213(03)00494-2 [hep-th/0303006]. G. Barnich and C. Troessaert, "Symmetries of asymptotically flat 4 dimensional spacetimes at null infinity revisited," Phys. Rev. Lett. **105**, 111103 (2010) doi:10.1103/PhysRevLett.105.111103 [arXiv:0909.2617 [gr-qc]]. T. Banks, "The Super BMS Algebra, Scattering and Holography," arXiv:1403.3420 [hep-th]. A. Ashtekar, "Asymptotic Quantization: Based On 1984 Naples Lectures," Naples, Italy: Bibliopolis,(1987). A. Strominger, "Lectures on the Infrared Structure of Gravity and Gauge Theory," arXiv:1703.05448 [hep-th]. C. Cheung, A. de la Fuente and R. Sundrum, "4D scattering amplitudes and asymptotic symmetries from 2D CFT," JHEP **1701**, 112 (2017) doi:10.1007/JHEP01(2017)112 [arXiv:1609.00732 [hep-th]].

[49] H. Elvang and Y. t. Huang, "Scattering Amplitudes," [arXiv:1308.1697 [hep-th]].

[50] S. Stieberger and T. R. Taylor, "Strings on Celestial Sphere," Nucl. Phys. B **935**, 388 (2018) doi:10.1016/j.nuclphysb.2018.08.019 [arXiv:1806.05688 [hep-th]].

[51] S. Stieberger and T. R. Taylor, "Symmetries of Celestial Amplitudes," Phys. Lett. B **793**, 141 (2019) doi:10.1016/j.physletb.2019.03.063 [arXiv:1812.01080 [hep-th]].

[52] M. Pate, A. M. Raclariu and A. Strominger, "Conformally Soft Theorem in Gauge Theory," arXiv:1904.10831 [hep-th].

[53] S. Weinberg, "Infrared photons and gravitons," Phys. Rev. **140**, B516 (1965). doi:10.1103/PhysRev.140.B516

[54] L. Donnay, A. Puhm and A. Strominger, "Conformally Soft Photons and Gravitons," JHEP **1901**, 184 (2019) doi:10.1007/JHEP01(2019)184 [arXiv:1810.05219 [hep-th]].

[55] W. Fan, A. Fotopoulos and T. R. Taylor, "Soft Limits of Yang-Mills Amplitudes and Conformal Correlators," arXiv:1903.01676 [hep-th].

[56] A. Volovich, C. Wen and M. Zlotnikov, "Double Soft Theorems in Gauge and String Theories," JHEP **1507**, 095 (2015) doi:10.1007/JHEP07(2015)095 [arXiv:1504.05559 [hep-th]].

[57] T. Klose, T. McLoughlin, D. Nandan, J. Plefka and G. Travaglini, "Double-Soft Limits of Gluons and Gravitons," JHEP **1507**, 135 (2015) doi:10.1007/JHEP07(2015)135 [arXiv:1504.05558 [hep-th]].

[58] S. Caron-Huot, "Analyticity in Spin in Conformal Theories," JHEP **1709**, 078 (2017) doi:10.1007/JHEP09(2017)078 [arXiv:1703.00278 [hep-th]].

[59] D. Simmons-Duffin, D. Stanford and E. Witten, "A spacetime derivation of the Lorentzian OPE inversion formula," arXiv:1711.03816 [hep-th].

[60] J. Murugan, D. Stanford and E. Witten, "More on Supersymmetric and 2d Analogs of the SYK Model," JHEP **1708**, 146 (2017) doi:10.1007/JHEP08(2017)146 [arXiv:1706.05362 [hep-th]].

[61] F. A. Dolan and H. Osborn, "Conformal partial waves and the operator product expansion," Nucl. Phys. B **678**, 491 (2004) doi:10.1016/j.nuclphysb.2003.11.016 [hep-th/0309180].

[62] F. A. Dolan and H. Osborn, “Conformal Partial Waves: Further Mathematical Results,” arXiv:1108.6194 [hep-th].

[63] H. Osborn, “Conformal Blocks for Arbitrary Spins in Two Dimensions,” Phys. Lett. B **718**, 169 (2012) doi:10.1016/j.physletb.2012.09.045 [arXiv:1205.1941 [hep-th]].

[64] M. Hogervorst and B. C. van Rees, “Crossing symmetry in alpha space,” JHEP **1711**, 193 (2017) doi:10.1007/JHEP11(2017)193 [arXiv:1702.08471 [hep-th]].

[65] J. Mago, A. Schreiber, M. Spradlin and A. Volovich, “Yangian invariants and cluster adjacency in $\mathcal{N} = 4$ Yang-Mills,” JHEP **10**, 099 (2019) doi:10.1007/JHEP10(2019)099 [arXiv:1906.10682 [hep-th]].

[66] J. Golden and M. Spradlin, “The differential of all two-loop MHV amplitudes in $\mathcal{N} = 4$ Yang-Mills theory,” JHEP **1309**, 111 (2013) doi:10.1007/JHEP09(2013)111 [arXiv:1306.1833 [hep-th]].

[67] J. Golden and M. Spradlin, “A Cluster Bootstrap for Two-Loop MHV Amplitudes,” JHEP **1502**, 002 (2015) doi:10.1007/JHEP02(2015)002 [arXiv:1411.3289 [hep-th]].

[68] V. Del Duca, S. Druc, J. Drummond, C. Duhr, F. Dulat, R. Marzucca, G. Papathanasiou and B. Verbeek, “Multi-Regge kinematics and the moduli space of Riemann spheres with marked points,” JHEP **1608**, 152 (2016) doi:10.1007/JHEP08(2016)152 [arXiv:1606.08807 [hep-th]].

[69] J. Golden, M. F. Paulos, M. Spradlin and A. Volovich, “Cluster Polylogarithms for Scattering Amplitudes,” J. Phys. A **47**, no. 47, 474005 (2014) doi:10.1088/1751-8113/47/47/474005 [arXiv:1401.6446 [hep-th]].

[70] J. Golden and M. Spradlin, "An analytic result for the two-loop seven-point MHV amplitude in $\mathcal{N} = 4$ SYM," JHEP **1408**, 154 (2014) doi:10.1007/JHEP08(2014)154 [arXiv:1406.2055 [hep-th]].

[71] T. Harrington and M. Spradlin, "Cluster Functions and Scattering Amplitudes for Six and Seven Points," JHEP **1707**, 016 (2017) doi:10.1007/JHEP07(2017)016 [arXiv:1512.07910 [hep-th]].

[72] J. Golden and A. J. Mcleod, "Cluster Algebras and the Subalgebra Constructibility of the Seven-Particle Remainder Function," JHEP **1901**, 017 (2019) doi:10.1007/JHEP01(2019)017 [arXiv:1810.12181 [hep-th]].

[73] J. Drummond, J. Foster and Ö. Gürdoğan, "Cluster Adjacency Properties of Scattering Amplitudes in $\mathcal{N} = 4$ Supersymmetric Yang-Mills Theory," Phys. Rev. Lett. **120**, no. 16, 161601 (2018) doi:10.1103/PhysRevLett.120.161601 [arXiv:1710.10953 [hep-th]].

[74] S. Caron-Huot and S. He, "Jumpstarting the All-Loop S-Matrix of Planar $\mathcal{N} = 4$ Super Yang-Mills," JHEP **1207**, 174 (2012) doi:10.1007/JHEP07(2012)174 [arXiv:1112.1060 [hep-th]].

[75] L. J. Dixon and M. von Hippel, "Bootstrapping an NMHV amplitude through three loops," JHEP **1410**, 065 (2014) doi:10.1007/JHEP10(2014)065 [arXiv:1408.1505 [hep-th]].

[76] J. M. Drummond, G. Papathanasiou and M. Spradlin, "A Symbol of Uniqueness: The Cluster Bootstrap for the 3-Loop MHV Heptagon," JHEP **1503**, 072 (2015) doi:10.1007/JHEP03(2015)072 [arXiv:1412.3763 [hep-th]].

[77] L. J. Dixon, M. von Hippel and A. J. McLeod, "The four-loop six-gluon NMHV ratio function," JHEP **1601**, 053 (2016) doi:10.1007/JHEP01(2016)053 [arXiv:1509.08127 [hep-th]].

[78] S. Caron-Huot, L. J. Dixon, A. McLeod and M. von Hippel, "Bootstrapping a Five-Loop Amplitude Using Steinmann Relations," Phys. Rev. Lett. **117**, no. 24, 241601 (2016) doi:10.1103/PhysRevLett.117.241601 [arXiv:1609.00669 [hep-th]].

[79] L. J. Dixon, M. von Hippel, A. J. McLeod and J. Trnka, "Multi-loop positivity of the planar $\mathcal{N} = 4$ SYM six-point amplitude," JHEP **1702**, 112 (2017) doi:10.1007/JHEP02(2017)112 [arXiv:1611.08325 [hep-th]].

[80] L. J. Dixon, J. Drummond, T. Harrington, A. J. McLeod, G. Papathanasiou and M. Spradlin, "Heptagons from the Steinmann Cluster Bootstrap," JHEP **1702**, 137 (2017) doi:10.1007/JHEP02(2017)137 [arXiv:1612.08976 [hep-th]].

[81] J. Drummond, J. Foster and Ö. Gürdoğan, "Cluster adjacency beyond MHV," JHEP **1903**, 086 (2019) doi:10.1007/JHEP03(2019)086 [arXiv:1810.08149 [hep-th]].

[82] J. Drummond, J. Foster, Ö. Gürdoğan and G. Papathanasiou, "Cluster adjacency and the four-loop NMHV heptagon," JHEP **1903**, 087 (2019) doi:10.1007/JHEP03(2019)087 [arXiv:1812.04640 [hep-th]].

[83] S. Caron-Huot, L. J. Dixon, F. Dulat, M. von Hippel, A. J. McLeod and G. Papathanasiou, "Six-Gluon Amplitudes in Planar $\mathcal{N} = 4$ Super-Yang-Mills Theory at Six and Seven Loops," [arXiv:1903.10890 [hep-th]].

[84] O. Steinmann, “Über den Zusammenhang zwischen den Wightmanfunktionen und der retardierten Kommutatoren,” Helv. Phys. Acta **33**, 257 (1960).

[85] O. Steinmann, “Wightman-Funktionen und retardierten Kommutatoren II,” Helv. Phys. Acta **33**, 347 (1960).

[86] K. E. Cahill and H. P. Stapp, “Optical Theorems And Steinmann Relations,” Annals Phys. **90**, 438 (1975). doi:10.1016/0003-4916(75)90006-8

[87] E. K. Sklyanin, “Some algebraic structures connected with the Yang-Baxter equation,” Funct. Anal. Appl. **16**, 263 (1982) [Funkt. Anal. Pril. **16N4**, 27 (1982)]. doi:10.1007/BF01077848

[88] M. Gekhtman, M. Z. Shapiro and A. D. Vainshtein, “Cluster algebras and poisson geometry,” Moscow Math. J. **3**, 899 (2003) [math/0208033].

[89] J. Golden, A. J. McLeod, M. Spradlin and A. Volovich, “The Sklyanin Bracket and Cluster Adjacency at All Multiplicity,” JHEP **1903**, 195 (2019) doi:10.1007/JHEP03(2019)195 [arXiv:1902.11286 [hep-th]].

[90] S. Oh, A. Postnikov and D. E. Speyer, “Weak separation and plabic graphs,” Proc. Lond. Math. Soc. **110**, 721 (2015) [arXiv:1109.4434 [math.CO]].

[91] C. Vergu, “Polylogarithm identities, cluster algebras and the $\mathcal{N} = 4$ supersymmetric theory,” arXiv:1512.08113 [hep-th].

[92] M. F. Sohnius and P. C. West, “Conformal Invariance in $\mathcal{N} = 4$ Supersymmetric Yang-Mills Theory,” Phys. Lett. **100B**, 245 (1981). doi:10.1016/0370-2693(81)90326-9

[93] L. J. Mason and D. Skinner, "Dual Superconformal Invariance, Momentum Twistors and Grassmannians," JHEP **0911**, 045 (2009) doi:10.1088/1126-6708/2009/11/045 [arXiv:0909.0250 [hep-th]].

[94] N. Arkani-Hamed, F. Cachazo and C. Cheung, "The Grassmannian Origin Of Dual Superconformal Invariance," JHEP **1003**, 036 (2010) doi:10.1007/JHEP03(2010)036 [arXiv:0909.0483 [hep-th]].

[95] N. Arkani-Hamed, J. Bourjaily, F. Cachazo and J. Trnka, "Local Spacetime Physics from the Grassmannian," JHEP **1101**, 108 (2011) doi:10.1007/JHEP01(2011)108 [arXiv:0912.3249 [hep-th]].

[96] N. Arkani-Hamed, J. Bourjaily, F. Cachazo and J. Trnka, "Unification of Residues and Grassmannian Dualities," JHEP **1101**, 049 (2011) doi:10.1007/JHEP01(2011)049 [arXiv:0912.4912 [hep-th]].

[97] J. M. Drummond and L. Ferro, "Yangians, Grassmannians and T-duality," JHEP **1007**, 027 (2010) doi:10.1007/JHEP07(2010)027 [arXiv:1001.3348 [hep-th]].

[98] S. K. Ashok and E. Dell'Aquila, "On the Classification of Residues of the Grassmannian," JHEP **1110**, 097 (2011) doi:10.1007/JHEP10(2011)097 [arXiv:1012.5094 [hep-th]].

[99] J. L. Bourjaily, "Positroids, Plabic Graphs, and Scattering Amplitudes in Mathematica," arXiv:1212.6974 [hep-th].

[100] V. P. Nair, "A Current Algebra for Some Gauge Theory Amplitudes," Phys. Lett. B **214**, 215 (1988). doi:10.1016/0370-2693(88)91471-2.

[101] J. M. Drummond and J. M. Henn, "All tree-level amplitudes in $\mathcal{N} = 4$ SYM," JHEP **0904**, 018 (2009) doi:10.1088/1126-6708/2009/04/018 [arXiv:0808.2475 [hep-th]].

[102] L. Lippstreu, J. Mago, M. Spradlin and A. Volovich, "Weak Separation, Positivity and Extremal Yangian Invariants," JHEP **09**, 093 (2019) doi:10.1007/JHEP09(2019)093 [arXiv:1906.11034 [hep-th]].

[103] J. Mago, A. Schreiber, M. Spradlin and A. Volovich, "A Note on One-loop Cluster Adjacency in N = 4 SYM," [arXiv:2005.07177 [hep-th]].

[104] M. Gekhtman, M. Z. Shapiro and A. D. Vainshtein, Mosc. Math. J. **3**, no.3, 899 (2003) [arXiv:math/0208033 [math.QA]].

[105] T. Łukowski, M. Parisi, M. Spradlin and A. Volovich, "Cluster Adjacency for $m = 2$ Yangian Invariants," JHEP **10**, 158 (2019) doi:10.1007/JHEP10(2019)158 [arXiv:1908.07618 [hep-th]].

[106] Ö. Gürdoğan and M. Parisi, "Cluster patterns in Landau and Leading Singularities via the Amplituhedron," [arXiv:2005.07154 [hep-th]].

[107] J. Drummond, J. Foster, Ö. Gürdoğan and C. Kalousios, "Tropical fans, scattering equations and amplitudes," [arXiv:2002.04624 [hep-th]].

[108] N. Henke and G. Papathanasiou, "How tropical are seven- and eight-particle amplitudes?," [arXiv:1912.08254 [hep-th]].

[109] B. Leclerc and A. Zelevinsky, "Quasicommuting families of quantum Plücker coordinates," Adv. Math. Sci. (Kirillov's seminar), AMS Translations 181, 85 (1998).

[110] S. Oh, A. Postnikov and D. E. Speyer, "Weak separation and plabic graphs," Proc. Lond. Math. Soc. **110**, 721 (2015) [arXiv:1109.4434 [math.CO]].

[111] S. Caron-Huot, L. J. Dixon, F. Dulat, M. Von Hippel, A. J. McLeod and G. Papathanasiou, "The Cosmic Galois Group and Extended Steinmann Relations for Planar $\mathcal{N} = 4$ SYM Amplitudes," JHEP **09**, 061 (2019) doi:10.1007/JHEP09(2019)061 [arXiv:1906.07116 [hep-th]].

[112] Z. Bern, L. J. Dixon and V. A. Smirnov, "Iteration of planar amplitudes in maximally supersymmetric Yang-Mills theory at three loops and beyond," Phys. Rev. D **72**, 085001 (2005) doi:10.1103/PhysRevD.72.085001 [arXiv:hep-th/0505205 [hep-th]].

[113] L. F. Alday, D. Gaiotto and J. Maldacena, "Thermodynamic Bubble Ansatz," JHEP **09**, 032 (2011) doi:10.1007/JHEP09(2011)032 [arXiv:0911.4708 [hep-th]].

[114] L. F. Alday, J. Maldacena, A. Sever and P. Vieira, "Y-system for Scattering Amplitudes," J. Phys. A **43**, 485401 (2010) doi:10.1088/1751-8113/43/48/485401 [arXiv:1002.2459 [hep-th]].

[115] J. Drummond, J. Henn, G. Korchemsky and E. Sokatchev, "Generalized unitarity for N=4 super-amplitudes," Nucl. Phys. B **869**, 452-492 (2013) doi:10.1016/j.nuclphysb.2012.12.009 [arXiv:0808.0491 [hep-th]].

[116] H. Elvang, D. Z. Freedman and M. Kiermaier, "Dual conformal symmetry of 1-loop NMHV amplitudes in $\mathcal{N} = 4$ SYM theory," JHEP **03**, 075 (2010) doi:10.1007/JHEP03(2010)075 [arXiv:0905.4379 [hep-th]].

[117] A. B. Goncharov, "Galois symmetries of fundamental groupoids and noncommutative geometry," Duke Math. J. **128**, no.2, 209 (2005) [arXiv:math/0208144 [math.AG]]

[118] J. Mago, A. Schreiber, M. Spradlin and A. Volovich, "Symbol Alphabets from Plabic Graphs," [arXiv:2007.00646 [hep-th]].

[119] S. Fomin and A. Zelevinsky, "Cluster algebras II: Finite type classification," Invent. Math. **154**, no. 1, 63 (2003) [arXiv:math/0208229].

[120] A. Hodges, Twistor Newsletter 5, 1977; reprinted in *Advances in twistor theory*, eds. L.P. Hugston and R. S. Ward (Pitman, 1979).

[121] G. 't Hooft and M. J. G. Veltman, "Scalar One Loop Integrals," Nucl. Phys. B **153**, 365 (1979).

[122] N. Arkani-Hamed, T. Lam and M. Spradlin, "Non-perturbative geometries for planar $\mathcal{N} = 4$ SYM amplitudes," [arXiv:1912.08222 [hep-th]].

[123] D. Speyer and L. Williams, "The tropical totally positive Grassmannian," J. Algebr. Comb. **22**, no. 2, 189 (2005) [arXiv:math/0312297].

[124] J. Drummond, J. Foster, Ö. Gürdoğan and C. Kalousios, "Algebraic singularities of scattering amplitudes from tropical geometry," [arXiv:1912.08217 [hep-th]].

[125] N. Arkani-Hamed, "Positive Geometry in Kinematic Space (I): The Amplituhedron," Spacetime and Quantum Mechanics Master Class Workshop, Harvard CMSA, October 30, 2019, https://www.youtube.com/watch?v=6TYKM4a9ZAU&t=3836.

[126] G. Muller and D. Speyer, "Cluster algebras of Grassmannians are locally acyclic," Proc. Am. Math. Soc. **144**, no. 8, 3267 (2016) [arXiv:1401.5137 [math.CO]].

[127] K. Serhiyenko, M. Sherman-Bennett and L. Williams, "Combinatorics of cluster structures in Schubert varieties," arXiv:1811.02724 [math.CO].

[128] M. F. Paulos and B. U. W. Schwab, "Cluster Algebras and the Positive Grassmannian," JHEP **10**, 031 (2014) [arXiv:1406.7273 [hep-th]].

[129] Ö. Gürdoğan and M. Parisi, [arXiv:2005.07154 [hep-th]].

[130] N. Arkani-Hamed, H. Thomas and J. Trnka, "Unwinding the Amplituhedron in Binary," JHEP **01**, 016 (2018) [arXiv:1704.05069 [hep-th]].

[131] S. Caron-Huot and S. He, "Jumpstarting the All-Loop S-Matrix of Planar $\mathcal{N} = 4$ Super Yang-Mills," JHEP **07**, 174 (2012) [arXiv:1112.1060 [hep-th]].

[132] M. Bullimore and D. Skinner, "Descent Equations for Superamplitudes," [arXiv:1112.1056 [hep-th]].

[133] I. Prlina, M. Spradlin and S. Stanojevic, "All-loop singularities of scattering amplitudes in massless planar theories," Phys. Rev. Lett. **121**, no.8, 081601 (2018) [arXiv:1805.11617 [hep-th]].

[134] S. He and Z. Li, "A Note on Letters of Yangian Invariants," [arXiv:2007.01574 [hep-th]].